



# NIH Public Access

## Author Manuscript

*Chem Rev.* Author manuscript; available in PMC 2010 July 1.

Published in final edited form as:  
*Chem Rev.* 2009 July ; 109(7): 2903–2928. doi:10.1021/cr900021w.

## IMP Dehydrogenase: Structure, Mechanism and Inhibition

Lizbeth Hedstrom

Departments of Biology and Chemistry, Brandeis University, MS009, 415 South St., Waltham, MA 02454, hedstrom@brandeis.edu, Phone: 781-736-2333; Fax 781-736-2349

### 1. Introduction and scope

George Weber was among the first to recognize that extensive metabolic changes must underlie the unbridled proliferation of cancer cells<sup>1</sup>. His molecular correlation hypothesis postulated that a defined set of key “pace-maker” enzymes are stringently linked to neoplastic transformation and progression, and that inhibition of these enzymes would provide an effective strategy for chemotherapy. Weber’s subsequent discovery that inosine 5'-monophosphate dehydrogenase (IMPDH) is amplified in tumors and rapidly proliferating tissues provided the foundation for drug design targeting this enzyme<sup>2</sup>. Though yet to achieve much success in the cancer arena, IMPDH inhibitors are now widely used in immunosuppressive and antiviral chemotherapy, and IMPDH may also be a target for antimicrobial drugs.

Clinical relevance aside, IMPDH is a fascinating enzyme. It traverses several conformations while catalyzing two different chemical transformations, utilizing unusual chemical strategies to promote each reaction. Monovalent cations such as K<sup>+</sup> activate IMPDH, possibly by acting as a molecular lubricant to facilitate these conformational changes. The biology of IMPDH also displays some surprising twists. IMPDH binds nucleic acids and is associated with polyribosomes<sup>3–6</sup>, though the physiological role of this interaction also has not yet been elucidated. Perhaps most intriguing is the discovery that mutations in IMPDH are associated with hereditary retinal disease<sup>7–9</sup>. These mutations cluster to a subdomain that is not required for enzymatic activity, and the function of this subdomain is currently under debate.

This article will review recent work on the biochemistry of IMPDH, integrating structure, function and inhibition. Earlier reviews on this topic include references<sup>10–12</sup>. Several more focused reviews have addressed IMPDH as a drug target for immunosuppressive<sup>13</sup>, cancer<sup>14,15</sup>, antiviral<sup>16</sup> and antimicrobial chemotherapy<sup>17</sup>, specific classes of IMPDH inhibitors<sup>18</sup>, advances in structure and mechanism<sup>19</sup> and the role of IMPDH in retinal disease<sup>20,21</sup>. The reader is also directed to a collection of papers from the 2000 meeting, *Inosine monophosphate dehydrogenase: a major therapeutic target*<sup>22</sup>.

### 2. The biology of IMPDH

IMPDH controls the gateway to guanine nucleotides, making it an “enzyme of consequence” for virtually every organism. IMP is the product of *de novo* purine nucleotide biosynthesis and the precursor to both adenine and guanine nucleotides (Scheme 1). The IMPDH-catalyzed conversion of IMP to XMP is the first committed and rate-limiting step in guanine nucleotide biosynthesis. XMP is subsequently converted to GMP by the action of GMP synthetase

---

Correspondence to: Lizbeth Hedstrom.

Supporting Information Available: Table S1, Steady state kinetic parameters of IMPDH from various organisms and Table S2, Structures of IMPDH, are provided as supporting information. This information is available free of charge via the Internet at <http://pubs.acs.org/>.

(GMPS). With the exception of protozoan parasites such as *Giardia lamblia* and *Trichomonas vaginalis* 23-24, the IMPDH/GMPS pathway appears to be present in every organism. Moreover, many organisms contain multiple genes encoding IMPDH. Guanine nucleotides can also be produced in salvage pathways through the action of phosphoribosyltransferases and/or nucleoside phosphotransferases/kinases (Scheme 1). The relative flux through the *de novo* and salvage pathways determines the susceptibility of an organism or tissue to IMPDH inhibitors.

Rapidly growing cells have a high demand for guanine nucleotides that generally cannot be sustained by salvage pathways, which explains the importance of IMPDH in cancer and viral infection. In addition, IMPDH is a rate-determining factor in the regulation of proliferation by p53 25. Constitutive IMPDH expression prevents growth suppression while inhibition of IMPDH mimics over-expression of p53. Two IMPDH inhibitors, MPA and benzamide riboside, display cytostatic but not cytotoxic activity against the panel of 60 cancer cell lines in the National Cancer Institute screen ([http://ntp.nci.nih.gov](http://.dtp.nci.nih.gov)). Other investigations have found that IMPDH inhibitors induce differentiation and apoptosis in a variety of cell lines. The *de novo* guanine nucleotide biosynthesis pathways are also especially important in lymphocyte proliferation 26, angiogenesis 27 and axon guidance 28.

The depletion of guanine nucleotides is believed to account for the action of IMPDH inhibitors. Guanine nucleotides serve as precursors for RNA and DNA, the energy source for translation, the co-factor for G-proteins, precursors for glycosylation, the precursor for tetrahydrobiopterin synthesis as well as important allosteric regulators and signaling molecules 26. Inhibition of IMPDH both depletes guanine nucleotides and increases adenine nucleotide pools. In mammalian cells, both phosphoribosyl pyrophosphate (PRPP) synthetase and ribonucleotide reductase are stimulated by guanine nucleotides and inhibited by adenine nucleotides 29. PRPP is used in the biosynthesis of purine nucleotides via both the *de novo* and salvage pathways, and is also required in pyrimidine biosynthesis, so the imbalance between adenine and guanine nucleotides has wide-ranging repercussions. Such mis-regulation of metabolic pathways may be more consequential than the simple lack of guanine nucleotides.

## 2.1 Human IMPDH

Humans and other mammals have two IMPDH genes, encoding hIMPDH1 and hIMPDH2 30. Though hIMPDH1 predominates in the retina, spleen and resting peripheral blood mononuclear cells, most tissues express both isozymes to varying extents 31-33. hIMPDH1 knockout mice display only a mild retinopathy 34, but hIMPDH2 null mice die during embryogenesis 35. In general, hIMPDH1 is expressed constitutively at low levels, while hIMPDH2 is amplified during proliferation and transformation, though several exceptions to this rule exist. Depletion of the guanine nucleotide pool by IMPDH inhibitors increases transcription of IMPDH in at least some cell types 36. Of particular interest given the use of IMPDH inhibitors as immunosuppressive chemotherapy, both hIMPDH1 and hIMPDH2 mRNAs are amplified when lymphocytes are stimulated 31,32,37. hIMPDH2 is widely believed to be the major target for cancer chemotherapy, with the presumption that chemotherapy would be improved with specific inhibitors. This view was recently challenged by the observation that inhibition of hIMPDH1 is sufficient to block angiogenesis 27.

The “canonical” hIMPDH1 and hIMPDH2 both contain 514 residues, are 84% identical and almost indistinguishable in their kinetic properties (Table S1 in the supplemental material). hIMPDH1 also exists in two longer versions generated by alternative splicing (described in more detail in section 8)33,38. Several polymorphisms of hIMPDH1 have been identified. The H296R, D301N, G324D and G519R mutations do not appear to affect protein function while the R105W, T116M, N198K, R224P, D226N, V268I and H372Pro mutations are associated with retinal degeneration 21,39. hIMPDH2 appears to be less diverse; only the L263F

polymorphism has been identified to date; this mutation decreases the value of  $k_{cat}$  by a factor of 10<sup>40</sup>. Importantly, functional characterization has largely relied on recombinant proteins produced in *E. coli*, so the effects of post-translational modifications have largely been ignored. Perhaps more seriously, the use of recombinant proteins has limited characterization to homotetramers, while the sequence similarity and co-expression of hIMPDH1 and hIMPDH2 suggests that type 1/type 2 heterotetramers will be present in many cells. Since the NAD site is at the subunit interface and these residues do differ between isozymes, the functional properties of such heterotetramers could be significantly different than either homotetramer; this issue has not yet been addressed experimentally. Further elucidation of the roles of hIMPDH1 and hIMPDH2 awaits the development of isozyme-specific inhibitors.

Some tantalizing complexities are found in the regulation of hIMPDH1/2 (note that many of these observations do not differentiate between isozymes). Surprisingly, enzymatic activity does not appear to be controlled by allosteric effectors. The depletion of guanine nucleotides causes the aggregation of hIMPDH1/2<sup>41,42</sup>; these aggregates disassemble when the guanine nucleotide pools are restored. Insulin and oleate cause the translocation of hIMPDH1/2 to lipid vesicles<sup>43</sup>; the functional consequences of this interaction are not known. Insulin also induces the phosphorylation of IMPDH1/2, though again the functional consequences of this modification are not understood<sup>43</sup>. Protein kinase B/Akt may be responsible for this phosphorylation. An independent set of yeast two hybrid experiments show that hIMPDH2 interacts with the protein kinase B/Akt via its plekstrin homology domain; the resulting phosphorylation reduces activity<sup>44</sup>. The site of this phosphorylation was not identified and neither hIMPDH1 nor hIMPDH2 contain consensus sites for protein kinase B phosphorylation.

## 2.2. IMPDH as an antimicrobial drug target

Rapid proliferation is also a characteristic of microbial infections, so IMPDH is an attractive target for antimicrobial chemotherapy. Mammalian and microbial IMPDHs display significant structural and functional differences, which suggest that it should be possible to develop selective inhibitors<sup>45</sup>. However, the utility of IMPDH as a target for antimicrobial agents is complicated by the salvage pathways (Scheme 1). Whereas mammals can only evade a block at IMPDH by salvaging guanine and/or guanosine, many pathogens can also salvage xanthine. Indeed, deletion of IMPDH has no effect on the virulence of several bacteria<sup>46-49</sup>. Therefore it is important to demonstrate that microbial growth and/or virulence depends upon IMPDH. Unfortunately, rigorous target validation is often limited by the inability to genetically manipulate the organism in question as well as by the lack of selective inhibitors. Nevertheless, IMPDH is emerging as a promising target in several systems. The IMPDH inhibitors MPA and/or mizoribine inhibit the growth of *Tritrichomonas foetus*<sup>50</sup>, *Candida albicans*<sup>51</sup>, *Cryptosporidium parvum*<sup>52</sup>, *Leishmania donovani*<sup>53</sup>, *Trypanosoma brucei*<sup>54</sup>, *Staphylococcus aureus*<sup>55</sup>, *Eimeria tenella*<sup>56</sup> and *Plasmodium falciparum*<sup>57</sup>. As described in section 7.5, parasite-selective IMPDH inhibitors have recently been reported<sup>58</sup>.

The propensity to develop drug resistance is an important consideration in antibiotic chemotherapy. *In vitro*, many organisms develop resistance to IMPDH inhibitors by amplifying the IMPDH gene<sup>53,54,59</sup>. Drug resistant mutations in IMPDH are also observed<sup>51,59,60</sup>. The cattle parasite *T. foetus* becomes resistant to IMPDH inhibitors by rearranging its purine salvage pathways to rely on xanthine instead of hypoxanthine<sup>50</sup>. How rapidly pathogens develop resistance to IMPDH inhibitors in the clinic remains to be seen.

## 3. Purification and characterization

The IMPDH reaction was first reported in 1957 in extracts of *Aerobacter aerogenes*<sup>61</sup>. IMPDH has been isolated from mammalian<sup>62-66</sup>, bacterial<sup>67-69</sup>, parasite<sup>56,70</sup> and plant sources<sup>71,72</sup>, though the subsequent discovery that many of these organisms express multiple isozymes

calls the composition of these preparations into question. The best-characterized IMPDHs are produced as recombinant proteins in *E. coli*, and include the enzymes from *T. foetus* 73,<sup>74</sup> *C. parvum* 75 and hIMPDH2<sup>76-80</sup>. In addition, the following recombinant IMPDHs have been expressed: hIMPDH1<sup>38,79,80</sup>, Chinese hamster type 2<sup>76</sup>, *E. coli* 81, *Streptococcus pyogenes* 82, *Pneumocystis carinii* 83, *Borrelia burgdorferi* 84, *C. albicans* 51, *L. donovani* 85, *Toxoplasma gondii* 86, *P. falciparum* 87 and *Pyrococcus horikoshii* (PDB accession number 2cu0).

IMPDH monomers generally contain 400-500 residues depending on the presence of a subdomain that is not required for enzymatic activity. The tetramer is stable and monomers are not observed, though higher order aggregates have been reported<sup>41,42,69,88,89</sup>. IMPDHs are readily purified using affinity chromatography<sup>90</sup>. An IMP-resin alone can be sufficient to obtain pure enzyme if expression is high. Cibacron Blue affinity and/or cation exchange chromatography are also effective purification steps. The enzyme can be denatured with urea or guanidine hydrochloride and renatured with retention of activity<sup>68,91</sup>. Activity is optimal at pH 8. All IMPDHs are activated by K<sup>+</sup>, and thiol compounds are required to prevent oxidation of the catalytic Cys for optimal activity<sup>61</sup>. Reagents such as iodoacetamide and methylmethanethiosulphonate inactivate IMPDH. IMP protects against inactivation, which provided the first evidence that a Cys residue might be present in the active site<sup>71,92</sup>. Surprisingly given the position of IMPDH at the junction of guanine nucleotide metabolism, no allosteric regulators have been identified for IMPDH (reports that ATP is an allosteric regulator have not been confirmed<sup>5,63,79</sup>). Though negative cooperativity has been detected in isothermal titration calorimetry measurements of IMP binding<sup>93</sup>, the kinetic data are consistent with independent active sites.

## 4. The structure of IMPDH

Thirty x-ray crystal structures of IMPDH have been reported to date, of which twenty-five are deposited in the Protein Data Base (Table S2 in the supplemental material). Most IMPDH monomers contain two domains: the catalytic domain, which is a (β/α)<sub>8</sub> barrel, and the subdomain containing two CBS domains (named for the homologous domains in cystathione beta synthase; also known as Bateman domains) (Figure 1). The subdomain is not required for activity<sup>94,95</sup> and a few IMPDHs, including those from *B. burgdorferi* and *C. parvum*, do not contain the CBS subdomain. The tetramer has square planar geometry, with the sides of the barrels at the subunit interfaces (Figure 1). The CBS subdomains protrude from the corners of the tetramer. The junction between the catalytic domain and the subdomain is flexible and the relative orientation can vary by as much as 120 degrees in different crystal structures (Figure 1A)<sup>96</sup>. The CBS subdomain is disordered in many structures, and removal of the subdomain by mutagenesis facilitates crystallization.

### 4.1. The catalytic domain

Like other (β/α)<sub>8</sub> barrel proteins, the active site is found in the loops on the C-terminal ends of the β sheets. The loop containing the catalytic Cys319 (*T. foetus* IMPDH numbering will be used throughout unless otherwise noted), the C-terminal segment and the flap all display varying degrees of flexibility and disorder depending upon the complex (Table S2). This structural mobility is critical for enzymatic activity. The C-terminal segment is coupled to the Cys319 loop via a monovalent cation. How the movement of the flap coordinates with the Cys319 loop and C-terminal segment is not understood. As discussed in section 6, the various crystal x-ray crystal structures suggest that IMPDH may have a different conformation for each step of the catalytic cycle.

The catalytic Cys319 is found on the loop between β6 and α6; this loop has several different conformations and/or is disordered in many crystal structures. The Cys319 loop has essentially

identical conformations in the E-XMP\*, E•MZP and E•RVP complexes of *T. foetus*, Chinese hamster and human type 2 IMPDHs. A monovalent cation binding site is formed in these complexes, consisting of three carbonyl oxygens from the Cys319 loop and three carbonyl oxygens from a helix in the C-terminal segment (Figure 2A). A similar conformation is also observed in the *S. pyogenes* E•IMP complex, although the C-terminal helix is in a somewhat different position, and a putative water molecule is found in the monovalent cation site (Figure 2B). It is possible that this water molecule is actually an NH<sub>4</sub><sup>+</sup> (from the crystallization buffer) or another monovalent cation. Na<sup>+</sup> causes a contraction of the binding site, with adjustments of both the Cys319 loop and C-terminal segment (Figure 2C), in keeping with the smaller coordination sphere of this metal.

The Cys319 loop has alternative conformations and/or is disordered in E•IMP, E•IMP•TAD and E•XMP complexes. The Cys319 loop can move like a door on a hinge (Figure 3A)<sup>97</sup>. It can also deform in a more dramatic manner as evidenced by the adduct with 6-Cl-IMP, where the Cys319 attacks the C6-position of the purine ring instead of the 2-position as in the normal reaction (Figure 3B)<sup>96</sup>. The nucleotide occupies the same position and has the same orientation as substrates/products, but the short helix unwinds, allowing the Cys to reach C6 of the purine ring. The monovalent cation site is disrupted and the C-terminal segment disordered in both of these complexes.

The large segment between β8 and α8 forms the flap that covers the active site. Like the Cys319 loop, this flap has varying amounts of disorder depending on the ligands. Most dramatically, the distal portion of the flap moves in and out of the active site during the catalytic cycle; the open conformation is required for the dehydrogenase reaction while the closed conformation is used in the hydrolysis step<sup>19</sup>.

#### 4.2. The conservation of the active site

Key functional and structural residues are generally highly conserved, but these residues display somewhat surprising divergence in the case of IMPDH. The key catalytic residue Cys319 is indeed completely conserved, as are most of the residues that interact with IMP (Figure 4A). These residues include Ser317 and Tyr405, which form hydrogen bonds to the ribose phosphate via their hydroxyl groups, and Gly360 and Gly381, which interact with the phosphate via main chain NHs. Arg382 displays some divergence, but it also forms a hydrogen bond with the phosphate via the main chain NH, so changes at this position need not perturb this interaction. Asp358 forms hydrogen bonds to the ribose hydroxyls of IMP, and is completely conserved. Glu408, Gly409 and Glu431 interact with the purine ring of IMP via main chain hydrogen bonds. While Glu408 is often replaced with Met, Gly409 and Glu431 are completely conserved.

In contrast, and despite multiple functional constraints, the NAD site and the flap are highly divergent (Figure 4B). The carboxyl group of a conserved Asp261 forms hydrogen bonds with the ribose hydroxyls of the nicotinamide portion of NAD. The only other conserved interactions are hydrogen bonds with Gly312 and Gly314 with the carboxamide of NAD. The carboxamide can also make an alternative hydrogen bond with the side chain of Arg322, but Gln and Gly are also found at this position, so this interaction is not conserved. The hydroxyls of Ser262 and Ser263 interact with the phosphates of NAD. Neither of these residues are conserved, and, though position 262 usually contains a residue such as Thr or Cys that preserves the interaction, position 263 is often an Ala. The residues that interact with the adenine ring are varied to the extent that they are frequently difficult to identify in sequence alignments (Figure 4B). The flap is similarly variable, with only key catalytic residues Arg418 and Tyr419 completely conserved. The presence of insertions and deletions can also make it difficult to align these two residues. It has been proposed that this divergence is a response to the presence of naturally

occurring IMPDH inhibitors<sup>98</sup>. Not surprisingly, species-selective inhibitors interact with the NAD site.

#### 4.3 CBS domains

CBS domains are found in a diverse set of proteins including ClC-chloride channels, amino acid transporters and protein kinases in addition to IMPDH and cystathione beta synthase<sup>99</sup>. Mutations within CBS domains lead to a variety of hereditary diseases<sup>100</sup>. CBS domains act as adenosine nucleotide binding modules in several proteins<sup>101-106</sup>. The CBS domains of IMPDH may also function in this manner<sup>102</sup>, though several laboratories have failed to verify this observation<sup>5,63,79,107</sup>. Notably, despite their structural similarity, the CBS domains of IMPDH share little sequence identity with the other proteins<sup>108</sup>, so it would not be surprising if their function has diverged.

The CBS subdomain coordinately regulates the adenine and guanine nucleotide pool in *E. coli*<sup>107,109</sup>. Both inosine and adenosine cause growth arrest in bacteria that express a subdomain-deleted variant of IMPDH. Growth arrest is accompanied by a dramatic increase in the adenosine nucleotide pool. One deleterious effect of the amplification of the adenine nucleotide pools appears to be the allosteric inhibition of PRPP synthetase. Growth arrest is also suppressed by mutations in the enzymes that convert inosine to AMP (ADSS, ADSL and inosine-guanosine kinase; Scheme 1). The mechanism behind these intriguing observations has not yet been elucidated.

IMPDH binds nucleic acids<sup>3,4</sup>, and this function is perturbed by deletion and/or mutagenesis of the CBS subdomain<sup>4,5,9</sup>. IMPDH associates with polyribosomes in tissue culture cells and the subdomain mediates this interaction, suggesting that IMPDH has a moonlighting function in translation regulation<sup>4-6</sup>. Perhaps this function also underlies the regulation of the purine nucleotide pool in bacteria.

### 5. Substrate specificity

The substrate specificity of IMPDH is fairly typical for nucleotide-utilizing enzymes. Substitutions at the phosphate group are well tolerated: inosine 5'-phosphorothioate, 5'-mercaptop-5'deoxyinosine-5'-S-phosphate, and 5'-amino-5'-deoxyinosine-5'-N-phosphate are converted to the analogous xanthosine nucleotides with catalytic efficiencies comparable to IMP<sup>110</sup>. 2'-Deoxy-IMP and ara-IMP are also good substrates<sup>65,78,111,112</sup>, which is rather surprising given that the 2'-OH makes hydrogen bonds to the conserved Asp364 (Figure 4). The 2'-OH also forms a hydrogen bond with the carboxamide nitrogen of NAD<sup>+</sup>/TAD in some complexes, though the distance between these atoms exceeds 3.5 Å in others<sup>95,96</sup>. Modifications of the hypoxanthine ring are also tolerated: 6-thio-IMP and 8-aza-IMP are also good substrates<sup>113</sup>. IMPDH hydrolyzes 2-Cl-IMP and 2-F-IMP in the absence of NAD<sup>78,112,114</sup>, again with kinetic parameters similar to those of the normal IMPDH reaction.

IMPDH can also use a variety of dinucleotide substrates: acetylpyridine adenine dinucleotide (APAD<sup>+</sup>), thionicotinamide adenine dinucleotide (TNAD<sup>+</sup>), 3-pyridinealdehyde adenine dinucleotide, nicotinamide hypoxanthine dinucleotide (NAH) and nicotinamide guanine dinucleotide (NAG)<sup>70,75,77,79</sup>. The values of  $k_{cat}$  are similar to that of NAD<sup>+</sup>, indicating that hydride transfer is not rate-limiting. The values of  $K_m$  are generally higher than that of NAD<sup>+</sup>, which probably reflects a decrease in affinity. APAD<sup>+</sup> and TNAD<sup>+</sup> are particularly useful NAD<sup>+</sup> analogs. The redox potentials of NAD<sup>+</sup>, TNAD<sup>+</sup> and APAD<sup>+</sup> are -0.320 V, -0.285 V and -0.258 V, respectively, so that the equilibrium of the hydride transfer reaction shifts toward products with these NAD<sup>+</sup> analogs. Neither APAD<sup>+</sup> nor TNAD<sup>+</sup> displays significant substrate inhibition, again probably due to the absence of interactions with the carboxamide

group. The release of APADH is much faster than NADH, frequently simplifying kinetic analysis.

## 6. Mechanism

IMPDH catalyzes two very different chemical transformations: (1) a dehydrogenase reaction to form NADH and the covalent intermediate E-XMP\* and (2) a hydrolysis reaction which converts E-XMP\* into XMP (Scheme 2). How can a single active site accommodate two very different transition states? Aldehyde dehydrogenase catalyzes a similar two step transformation; in this case, the nicotinamide portion of NADH swings out to allow water to access the active site<sup>115</sup>. A much more profound rearrangement occurs during the IMPDH reaction: NADH departs from the enzyme and a mobile flap moves into the vacant dinucleotide site, carrying the conserved Arg418-Tyr419 dyad into the active site. Thus IMPDH has two mutually exclusive conformations, an open conformation for the redox reaction and a closed conformation for the hydrolysis of E-XMP\*<sup>19</sup>.

Hydride transfer is fast in all IMPDHs examined to date, so E-XMP\* accumulates during the catalytic cycle and can be trapped with acid<sup>73</sup>. Both the chemical and kinetic competence of E-XMP\* have been established. E-XMP\* decomposes to XMP and also reacts with NADH to form IMP and NAD<sup>+</sup><sup>74,77</sup>. More interestingly, mycophenolic acid (MPA) traps E-XMP\* and a crystal structure of the E-XMP\*•MPA complex has been solved<sup>76,116,117</sup>. In a particularly elegant experiment, Fleming and colleagues have shown that E-XMP\*•MPA also forms when IMPDH is incubated with XMP and MPA, though this reaction is very slow ( $k_{obs} = 6.5 \times 10^{-5} \text{ s}^{-1}$  versus  $k_{cat} = \sim 0.4 \text{ s}^{-1}$  for hIMPDH2<sup>116</sup>). E-XMP\*•MPA can be distinguished from free enzyme on SDS-PAGE, which provides a means to monitor drug effectiveness *in vivo*<sup>118</sup>.

### 6.1 Conformational transitions during the IMPDH reaction

The IMPDH reaction may require different protein conformations for each step of the catalytic cycle. Ten x-ray crystal structures of *T. foetus* IMPDH have been solved, so discussion will focus on this enzyme (Table S2). The flap and the Cys319 loop have different conformations and/or different degrees of disorder in each complex (Figure 5)<sup>19</sup>. While the idea that multiple conformational transitions are required during the IMPDH is very appealing, it is important to recognize that the differences between crystal structures may have more prosaic origins. The oxidation of Cys319, crystallization conditions or simply the presence of inhibitors may induce conformations that are not catalytically relevant. With such caveat asides, it appears that the active site of IMPDH is largely disordered in the absence of substrates, becomes ordered as substrates bind, and that ordering extends to docking of the C-terminal helix when K<sup>+</sup> binds.

No true apoenzyme structure is available for *T. foetus* IMPDH; the closest mimic is the E•SO<sub>4</sub><sup>-2</sup> complex, where the Cys319 loop, flap and C-terminal segment are largely disordered (Figure 5A)<sup>89</sup>. In contrast, the Cys319 loop is completely ordered in the SO<sub>4</sub><sup>-2</sup> complex of *B. burgdorferi* IMPDH. This difference may reflect different dynamical properties of the Cys319 loop arising from sequence variations. A true apoenzyme structure has been solved for hIMPDH2, and even more extensive disorder is observed in this complex, suggesting that the SO<sub>4</sub><sup>-2</sup> orders the phosphate binding portion of the Cys319 loop<sup>119</sup>.

The Cys319 loop becomes ordered when IMP binds, as do several residues of the flap (Figure 5B)<sup>120</sup>. However, this conformation of the Cys319 loop is not compatible with monovalent cation binding, so the C-terminal segment remains disordered. Here the oxidation of Cys319 is particularly problematic, because steric conflict with IMP may cause distortion of the Cys319 loop. The Cys319 loop has a structure compatible with K<sup>+</sup> binding in the *S. pyogenes* E•IMP

structure, though in this case the position of the purine ring is slightly skewed from other complexes<sup>82</sup>.

Another conformation of the Cys319 loop is observed in the E•IMP•TAD complex, which is believed to mimic E•IMP•NAD<sup>+</sup> (Figure 5C)<sup>95</sup>. This difference is most easily noted by observing the positions of Thr321 and Arg322. Thr321 points away from the Cys319, while Arg322 interacts with TAD. K<sup>+</sup> binding cannot be accommodated by this conformation, which suggests that the K<sup>+</sup> may bind, and the C-terminal helix may dock, after hydride transfer is complete.

Yet another conformation is observed in the E•RVP•MPA and E•MZP complexes, which are believed to mimic the E-XMP\*<sub>open</sub> and E-XMP\*<sub>closed</sub> complexes, respectively (Figure 5D and E). In both cases, the replacement of the purine ring with a smaller heterocycle permits the Cys319 loop to attain a conformation that can bind monovalent cation, which in turn allows docking of the C-terminal helix. Na<sup>+</sup> is bound in the E•RVP•MPA complex, which causes a contraction of the Cys319 loop and C-terminal segment relative to that of K<sup>+</sup> site in the E•MZP complex; Thr321 points away from Cys319 (also note that Cys319 is oxidized in this complex)<sup>121</sup>. Na<sup>+</sup> does activate *T. foetus* IMPDH, so it seems likely that this is a catalytically relevant conformation.

The conformation of the Cys319 loop in E•MZP closely mimics that observed in the E-XMP\*•MPA complex of Chinese hamster IMPDH<sup>76,122</sup>. Thr321 is positioned to interact with both Cys319, so that Thr321 may play an important role in activating this key catalytic residue. The nucleotide is almost completely buried in the enzyme, suggesting that a conformational change is required for release of the final product, and indeed the E•XMP complex does contain large amounts of disorder<sup>89</sup>.

## 6.2. Kinetic mechanism

Early investigations of IMPDH's from various sources concluded that the kinetic mechanism proceeded via an ordered bi-bi mechanism where IMP was the first substrate bound and XMP was the last product released. Unfortunately, these conclusions were based on product inhibition experiments that are not valid if an intermediate such as E-XMP\* accumulates. Dead-end inhibitor and equilibrium isotope exchange experiments from the Morrison laboratory suggested that IMPDH followed a random mechanism, which is closer to the truth<sup>123,124</sup>. With the discovery of the E-XMP\* intermediate, the measurement of isotope effects and the use of presteady kinetics, it is now evident that substrates bind randomly, hydride transfer is rapid and NADH release precedes the hydrolysis of E-XMP\*<sup>74,77,125,126</sup> (Scheme 3). High concentrations of NAD<sup>+</sup> trap E-XMP\*, causing substrate inhibition, confirming the ordered release of products. The values of  $K_{ii}$  for NAD<sup>+</sup> range from 0.6-3 mM, which suggests that a significant fraction of E-XMP\*•NAD<sup>+</sup> will exist under physiological conditions. Perhaps the formation of E-XMP\*•NAD<sup>+</sup> provides another mechanism of regulating guanine nucleotide biosynthesis<sup>56</sup>.

A combination of pre-steady state, steady state, isotope effect and pulse chase experiments have delineated the kinetic mechanism for IMPDH from *T. foetus*<sup>74,127</sup>. In brief, changes in intrinsic protein fluorescence monitor substrate/product binding, changes in absorbance at 340 nm measures production of both free and enzyme-bound NADH. Changes in NADH fluorescence monitor free NADH because purines are strong fluorescence quenchers, so no fluorescence is observed in the E-XMP\*•NADH complex. Lastly, incorporation of radioactivity into the protein from <sup>14</sup>C-IMP monitors E-XMP\*. These experiments permit the rate constants to be determined for each step of the reaction<sup>127</sup>.

**6.2.1. Kinetic evidence for conformational changes in the IMPDH reaction**—As expected from structural investigations, several conformational changes are evident in the kinetic mechanism. IMP binding is a two step process in the *T. foetus* enzyme<sup>74</sup>. Titration calorimetry and proteolysis experiments suggest that IMP binding also induces a conformational change in hIMPDH2<sup>93,128</sup>. Thus the IMP-induced conformational change appears to be a general feature of the IMPDH reaction.

Another conformational change occurs when NAD<sup>+</sup> binds. When E•IMP is mixed with NAD<sup>+</sup>, a burst of NADH is produced, demonstrating that the dehydrogenase reaction is fast. However, when 2-<sup>2</sup>H-IMP is used, an isotope effect of only 1.4 is observed on the burst of NADH. This observation suggests that a conformational change is also partially rate-limiting in the dehydrogenase reaction, which further suggests that the association of NAD<sup>+</sup> involves a conformational change.

Kinetic evidence for the open/closed conformational change of the flap comes from multiple inhibitor experiments. The nucleoside inhibitor tiazofurin binds in the nicotinamide portion of the dinucleotide site while ADP binds in the adenosine portion. Tiazofurin and ADP are strongly synergistic inhibitors of *T. foetus* IMPDH<sup>127,129</sup>, indicating that a conformational change occurs upon the binding of one inhibitor that increases the affinity of the second inhibitor. If the closed conformation predominates, then tiazofurin will shift the equilibrium to the open conformation, allowing ADP to bind more tightly (Figure 6; note that the order of inhibitor binding is arbitrary).

**6.2.2. Measuring the open/closed flap equilibrium with a multiple inhibitor experiment**—The equilibrium for this conformational change ( $K_c$ ) can be estimated using multiple inhibitor experiments with the assumption that the conformational change is rapid. The interaction constant  $\alpha$  is the factor that describes the decrease in the value of  $K_i$  for one inhibitor in the presence of saturating concentrations of the second inhibitor. The value of  $\alpha$  also approximates the fraction of enzyme in the open conformation ( $F_{\text{open}}$ ). This concept is best illustrated with an example: assume  $F_{\text{open}} = 0.02$ . The presence of saturating tiazofurin shifts the enzyme completely into the open conformation, i.e.,  $F_{\text{open}} = 1$ , causing ADP to bind 50 times more tightly, so that  $\alpha = 0.02 = F_{\text{open}}$ . Thus this multiple inhibitor experiment also provides an estimate the value of  $K_c$ . For *T. foetus* IMPDH,  $\alpha = 0.007$  and  $K_c = 150$ <sup>127</sup>. Note that if a mutation causes an increase in  $F_{\text{open}}$ , a corresponding decrease will be observed in the  $K_i$  of all inhibitors that bind in the dinucleotide site, providing an independent measure of the effect of a mutation on the conformational equilibrium (in the case where the residue does not directly interact with the inhibitor). The value of  $K_i$  calculated based on  $K_c$  is in good agreement with the experimentally determined values, validating the method<sup>127</sup>.

**6.2.3. Kinetic mechanisms of hIMPDH2 and *C. parvum* IMPDH**—The kinetic mechanisms of hIMPDH2 and *C. parvum* IMPDH follow the same general outline as *T. foetus* IMPDH, indicating that this mechanism is a common feature of IMPDHs<sup>126</sup>. Figure 7 displays a “kinetic alignment” of steps that contribute to  $k_{\text{cat}}$  for *T. foetus* IMPDH, *C. parvum* IMPDH and hIMPDH2. The value of  $K_c$  varies widely, as expected given the structural divergence of the flap and the dinucleotide site (Figure 4). hIMPDH2 is predominantly in the open conformation, while the *C. parvum* enzyme has a small preference for the closed conformation ( $K_c = 4$ ). Since the flap and NAD<sup>+</sup> compete for the dinucleotide site, the affinity of NAD<sup>+</sup> must be balanced against that of the flap; otherwise nonproductive complexes will accumulate. When the fraction of enzyme in the open conformation is taken into account, the “intrinsic binding affinity” of compounds that bind in the NAD site can be considerably greater than the observed binding affinity (Table 1). This principle is illustrated by *T. foetus* IMPDH, where the observed affinity of NAD<sup>+</sup> is 6.8 mM but the intrinsic affinity is 0.07 mM. Also as expected from the structural divergence, the intrinsic binding energy of NAD<sup>+</sup> distributes

differentially across the dinucleotide binding sites. Most of the affinity for TAD derives from interactions at the nicotinamide subsite in human IMPDH type 2 and *C. parvum* IMPDH while interactions with the adenosine subsite are more important in *T. foetus* IMPDH. These differences may derive from interactions with the adenine ring, which is sandwiched between His253 and Phe282 in human IMPDH type 2, Asn144 and Asn171 in *C. parvum* IMPDH and Arg241 and Trp269 in *T. foetus* IMPDH. Remarkably, the values of  $k_{HOH}$  are similar even though the dynamics of open and closed conformations are very different, suggesting that the movement of the flap simply sets the stage for the hydrolysis reaction.

With the exception of  $K_c$ , the kinetic mechanisms of *Cp*IMPDH and *Tf*IMPDH are essentially identical, in keeping with the structural similarity of the IMP and nicotinamide sites. In contrast, both chemical transformations are slower in hIMPDH2. The change in equilibrium between the E•IMP•NAD<sup>+</sup> and E-XMP\*•NADH complexes suggests that the transition state for the hydride transfer reaction has also changed. As discussed below, the substitution of Glu431 with Gln may account for the decreased catalytic power of hIMPDH2.

### 6.3. Chemical mechanism

IMPDH utilizes a plethora of catalytic strategies to solve the many challenges of the chemical transformations. IMP is bound with the glycosidic bond in the anti conformation, which places C2 away from the sugar ring, facilitating the attack of Cys319<sup>130</sup>. The reactivity of the 2-position of the purine ring is enhanced by hydrogen-bonds between the purine ring and the main chain at residues Glu408, Gly409 and Glu431 (Figure 4). The dehydrogenase reaction may proceed via a tetrahedral intermediate as shown (Scheme 2), though no experimental evidence exists on this point. Hydride is expelled to the *pro-S* face of NAD<sup>+</sup><sup>125,131,132</sup>, and E-XMP\* is formed. The hydrolysis of E-XMP\* has also several unusual features. As noted above, NADH dissociates and the flap moves into the vacant dinucleotide site. This conformational change brings the conserved Arg418-Tyr419 dyad into the space previously occupied by the nicotinamide ring. Hydrolysis of E-XMP\* requires this closed conformation<sup>122</sup>. Arg418 appears to act as a general base to activate water, as discussed in Section 6.4. As above, the hydrolysis reaction may involve an actual tetrahedral intermediate. It is quite possible that the immediate product of the hydrolysis reaction is a different tautomer of XMP than the one that predominates in solution.

Cys319 is unusually nucleophilic, yet its pK<sub>a</sub> appears to be unperturbed as measured by the pH dependence of 6-Cl-IMP inactivation (pK<sub>a</sub> = 8.4)<sup>92</sup>. Cysteine proteases and other enzymes with a catalytic Cys residue use a neighboring His to activate the thiol, but no such His is present in IMPDH. Instead, Thr321 appears to perform this function; mutation of Thr321 decreases the rate of both hydride transfer and hydrolysis by a factor of ~20<sup>133</sup>. Thr residues have recently been proposed to activate Cys residues in other enzymes<sup>134</sup>. It's worth noting that the interaction between Thr321 and Cys319 is lost during the reaction with 6-Cl-IMP (Figure 2C), so perhaps this experiment does not measure the relevant pK<sub>a</sub>.

### 6.4. Arg418 acts as a general base catalyst

All hydrolases have some mechanism to activate water, but this mechanism has been very difficult to identify in IMPDH. Surprising insights into this question were revealed by the x-ray crystal structure of E•MZP<sup>122</sup>. The affinity of MZP decreases in parallel with decreases in enzymatic activity for a series of IMPDH mutations, indicating that this compound is transition state analog (Figure 8; see Chart 1 for the structure of mizoribine)<sup>135</sup>, and the E•MZP structure does indeed display the tetrahedral disposition of nucleophile and leaving group expected in the transition-state<sup>122</sup>. Modeling purine ring in place of the imidazole of MZP, Cys319 is above C2, as expected of the leaving group and a likely catalytic water is observed below C2 (Figure 8).

Perplexingly, none of the residues usually associated with general base catalysis are positioned to activate the catalytic water. Instead, the water interacts with Thr321, Arg418 and Tyr419 ( $pK_a = 20, 12.5$ , and  $10$ , respectively)<sup>127,133</sup>. Substitution of these residues decreases the value of  $k_{cat}$  (Table 2). Loss of a general base catalyst is expected to decrease the value of  $k_{cat}$  by a factor of  $10^2$ - $10^3$  (assuming the hydrolysis step is rate-limiting); only the substitutions of Arg418 meet this criterion. Moreover, whereas mutations of Arg418 and Tyr419 decrease only the hydrolysis reaction, the mutation of Thr321 has equivalent effects on both the dehydrogenase and hydrolase reactions.

Arg418 also plays a role in stabilizing the closed conformation; therefore the effect of substitutions on the equilibrium between the open and closed conformations ( $K_c$ ) must also be evaluated. As expected, mutations of Arg418 shift  $K_c$  toward the open conformation (Table 2). However, this shift is not sufficient to explain the decrease in the value of  $k_{cat}$ . Interestingly, the Arg418Gln variant still favors the closed conformation even though Gln does not have a positive charge<sup>133</sup>. In contrast, the Arg418Lys variant favors the open conformation, showing that a positive charge is not sufficient to induce the closed conformation. The value of  $\alpha$  becomes smaller at high pH, further suggesting that neutral Arg418 favors the closed conformation. These observations are consistent with the hypothesis that Arg418 acts as a base to activate water.

Further support for this hypothesis comes from the observation that guanidine derivatives can rescue the Arg418Ala mutation<sup>136</sup>. Rescue does not restore the equilibrium between open and closed conformations. The rate of the rescue reaction increases with pH, as expected if the guanidine base is the active species, and a solvent deuterium isotope effect is observed. These observations suggest that the guanidine agents accelerate the hydrolysis of E-XMP\* by functioning as a base to activate water. The rate constant for the rescue reaction correlates with the  $pK_a$  of the rescue agent with a Bronsted coefficient of  $\sim 1$ , suggesting the proton has almost completely transferred to Arg418 in the transition state (Figure 9).

### 6.5. Two pathways to activate water

While these experimental observations strongly suggest that Arg418 may act as the general base in the hydrolysis reaction, none are conclusive. Further support for this mechanism came from combined molecular mechanics/quantum mechanics simulations<sup>137</sup>. When the starting condition is a neutral Arg418, the lowest energy path to products involves Arg418 abstracting a proton from water. Proton transfer is rate-limiting and almost complete in the transition state (Figure 10). This simulation is in remarkable agreement with experimental observations: a solvent isotope effect of 1.5 is observed in the wild-type reaction, consistent with rate-limiting proton transfer. The activity of the Arg418Ala variant can be rescued with guanidine derivatives and Bronsted analysis of the rescue reaction suggests that proton transfer is nearly complete in the transition state. The calculated barrier for the reaction is much lower than that observed experimentally. However, this can easily be explained by the starting condition of neutral Arg418; if the  $pK_a$  of Arg418 is  $\sim 12$  as is “normal”, the calculated barrier would be in good agreement with the experimental value.

When the starting condition was a positively charged Arg418, a surprising result was obtained: water was activated by a proton relay, with Thr321 abstracting a proton from water while its own proton was transferred to Glu431 (Figure 11)<sup>137</sup>. As in the case of the Arg418 pathway, proton transfer is rate-limiting. The barrier for this reaction was much higher than that observed when Arg418 acted as a general base. Nevertheless, the simulation was in good agreement with experimental values. The barrier was similar to that observed in the Arg418Ala and Arg418Gln variants. Moreover, large solvent isotope effects are observed in the reactions of the the Arg418Ala and Arg418Gln mutants, consistent with two protons moving in the transition state. More importantly, together these two simulations make a testable prediction: the Thr321

pathway should dominate at low pH when Arg418 is protonated, while the Arg418 pathway should dominate at high pH. Therefore substitution of Glu431 with Gln should shift the pH rate profile to the right. This shift is indeed observed experimentally<sup>137</sup>. Note that Glu431 is a Gln in hIMPDH2 and all eukaryotic IMPDHs. This substitution may account for the lower catalytic activity of these enzymes.

These observations indicate that *T. foetus* IMPDH has two mechanisms to activate water, which is unprecedented to the best of the author's knowledge. Why should this be so? Perhaps the Thr321 pathway is a vestige of evolution<sup>137</sup>. The most closely related enzyme, GMP reductase (GMPR), catalyzes a related redox reaction that converts GMP to IMP (Scheme 1). GMPR also contains the conserved Cys, Thr and Glu, but does not contain a structural analog to the flap with the conserved Arg418-Tyr419. Likewise, the ancestral IMPDH/GMPR probably contained the Cys, Thr and Glu, but not Arg418-Tyr419. The ancestral enzyme may have utilized the Thr321 pathway exclusively, and the Arg418-Tyr419 pathway may be a modern improvement. Interestingly, Glu431 is substituted with Gln in eukaryotic IMPDHs, showing that the Thr321 pathway is expendable.

### 6.6. Arg as a base in other enzymes

The idea that an Arg residue can act as a general base to activate water may be surprising to biochemists trained to think exclusively of Arg as a positively charged residue. Importantly, IMPDH is not alone in utilizing an Arg residue in this manner; pectate/pectin lyases, fumarate reductase, L-aspartate oxidase, lacticin 481 synthetase, myosin and photosystem II all appear to use Arg as a base<sup>138-142</sup>. Although these enzymes have several different folds and distinct evolutionary origins, a common structural motif is frequently present where the critical Arg residue is adjacent to a carboxylate group and often near a Tyr<sup>138</sup>. Arg must be deprotonated to act as a base, so either the pK<sub>a</sub> must be abnormally low or only a small fraction of the enzyme is in the active ionization state. Since a guanidine is only a strong base when the guanidinium cation can be stabilized by hydrogen bonds with water, enough deprotonated Arg may be generated by the relatively low polarity of an enzyme active site to permit efficient catalysis. As shown in Figure 12, Arg418 has significantly fewer hydrogen bonding opportunities than an Arg residue in the substrate binding pocket of trypsin; this lower polarity could generate a sufficient fraction of deprotonated Arg418 to account for catalysis.

### 6.7. Monovalent cation activation of IMPDH

All IMPDHs are activated ~100-fold by K<sup>+</sup> and similar monovalent cations. Surprisingly, the specificity of K<sup>+</sup> activation varies considerably among IMPDHs from different sources<sup>10</sup>. Ions with similar size to K<sup>+</sup>, e.g., NH<sub>4</sub><sup>+</sup> and Rb<sup>+</sup>, always activate, but smaller ions such as Na<sup>+</sup> activate some IMPDHs, inhibit some and have no effect on others (Table 3). For example, K<sup>+</sup>, NH<sub>4</sub><sup>+</sup>, Na<sup>+</sup>, Tl<sup>+</sup> and Rb<sup>+</sup> activate human IMPDH type 2, while Li<sup>+</sup> has no effect<sup>143</sup>. In contrast, both *E. coli* and *B. burgdorferi* IMPDHs are activated by K<sup>+</sup>, NH<sub>4</sub><sup>+</sup> and Cs<sup>+</sup> but inhibited by Na<sup>+</sup> and Li<sup>+</sup><sup>84</sup>. Na<sup>+</sup> has no effect on *C. parvum* IMPDH<sup>144</sup>. K<sup>+</sup> has no apparent effect on the stability of the IMPDH tetramer, though it may prevent the formation of higher order aggregates<sup>84,88,143</sup>.

Two K<sup>+</sup> sites have been identified in x-ray crystal structures of IMPDHs. Site 1 is observed in only a handful of x-ray crystal structures, i.e., E-XMP\*•MPA, E•RVP, E•RVP•MPA and E•M2P<sup>76,121,122</sup>. Here, K<sup>+</sup> interacts with six main-chain carbonyls, three in the Cys319 loop (Gly314, Gly316 and Cys319) and three in the C-terminal segment from the adjacent subunit (Glu485', Gly486' and Gly487') (Figure 2). The Cys319 loop is frequently disordered, or found in a conformation that is incompatible with K<sup>+</sup> binding, suggesting that the K<sup>+</sup> is not present throughout the catalytic cycle. A second K<sup>+</sup> site is observed in *T. foetus* IMPDH<sup>95,121</sup>, also at the interface between two monomers, involving three mainchain carbonyls (Gly20, Asn460

and Phe266'), the side chain hydroxyl of Ser22 and both oxygens of the side chain carboxyl of Asp264'. These residues are not conserved and this site is not observed in crystal structures of IMPDHs from other organisms.

A growing body of work, primarily motivated by efforts to understand channel selectivity, suggests that the specificity of a monovalent cation binding site is controlled by structural rigidity: nonspecific sites are plastic, and can adapt to the varying ligand preferences of different cations<sup>145,146</sup>. These observations suggest that the Cys319 loop and C-terminal helix will be more rigid in K<sup>+</sup>-specific IMPDHs. This expectation is borne out in the crystal structures. The Cys319 loop is well ordered in the K<sup>+</sup>-specific *B. burgdorferi* and *S. pyogenes* enzymes, but disordered in the analogous complexes of the nonspecific *T. foetus* enzyme. The structure of Na<sup>+</sup>-bound form of *T. foetus* IMPDH further corroborates these ideas (Figure 2C): the Cys 319 loop contracts and the C-terminal helix deforms, so that only 5 carbonyl oxygens interact with the Na<sup>+</sup>. Inspection of the sequences of the Cys319 loop and C-terminal helix further suggest that these structural elements are indeed more flexible in the non-specific *T. foetus* IMPDH than in the K<sup>+</sup>-specific *C. parvum* enzyme: the Cys319 loop and C-terminal segment contain more Gly residues while the C-terminal helix is less stable (Table 3). The presence of Pro at position 315 is particularly striking; this substitution seems likely to prevent this adaptation of the Cys319 loop to smaller monovalent cations.

Stabilization of the Cys319 loop and C-terminal segment provides a ready explanation for K<sup>+</sup> activation. However, this typical allosteric mechanism is not consistent with other observations. First, other structures find the Cys319 loop in conformations that cannot accommodate K<sup>+</sup> binding; if these structures reflect intermediates on the catalytic pathway, then K<sup>+</sup> must have a transient association with the enzyme<sup>19</sup>. Further, the Cys319 loop is distorted and the C-terminal segment is disordered in the structure of 6-Cl-IMP inactivated enzyme, yet K<sup>+</sup> does not protect against inactivation by 6-Cl-IMP<sup>78,147</sup>. K<sup>+</sup> does not change the affinity of IMP. Interestingly, water and salt are believed to act as molecular lubricants to increase enzyme activity in organic solvents<sup>148</sup>. Perhaps K<sup>+</sup> activates IMPDH by similarly facilitating the interchange of conformations.

## 7. Inhibitors of IMPDH

IMPDH inhibitors are used in immunosuppressive chemotherapy (MPA, mizoribine) and antiviral chemotherapy (ribavirin) (Chart 1). In addition, tiazofurin (Tiazole<sup>R</sup>) was granted orphan drug for treatment of chronic myelogenous leukemia, though neurotoxicity limits widespread use of this drug and it is not currently marketed. The efficacy of a given drug in a specific application appears to be determined by its metabolic stability and specificity. The potential of IMPDH in antimicrobial chemotherapy is beginning to be exploited with recent reports of parasite selective inhibitors.

### 7.1. Mechanisms of reversible inhibition

As described in 6.1, the kinetic mechanism of IMPDH involves random addition of IMP and NAD<sup>+</sup> (Scheme 3). IMP analogs behave as competitive inhibitors versus IMP and noncompetitive versus NAD<sup>+</sup>, as usual for this type of mechanism. However, compounds that bind in the NAD<sup>+</sup> site seldom display competitive inhibition with respect to NAD<sup>+</sup>. This behavior is a consequence of the accumulation of E-XMP\*. Uncompetitive inhibition versus both IMP and NAD<sup>+</sup> will be observed if a compound has a strong preference for E-XMP\*, that is, if  $K_{is} \gg K_{ii}$  (Scheme 3). A compound that binds to both E•IMP and E-XMP\* will be a noncompetitive/mixed inhibitor with respect to both IMP and NAD<sup>+</sup>. Competitive inhibition versus NAD<sup>+</sup> will only be observed if a compound has a strong preference for E•IMP ( $K_{ii} \gg K_{is}$ ). This situation is rarely observed.

Most inhibitor development programs have focused on hIMPDH2 since this isozyme is amplified in both proliferating T-cells and cancer. hIMPDH1 and hIMPDH2 are 84% identical, so the development of isozyme selective inhibitors is challenging. A couple of laboratories have reported success in this area, but confirmation has not been forthcoming. Unfortunately, little is known about how these inhibitors interact with hIMPDH2. While it is likely that most inhibitors trap E-XMP\* as observed with MPA, this has not been confirmed in most cases. Biochemical characterization has been generally limited to determination of IC<sub>50</sub>, and so does not provide insight into the mechanism of inhibition. When more detailed characterization is reported, the inhibitor concentrations frequently approximate the enzyme concentrations, thus invalidating steady-state analysis of mechanism.

Another complication in inhibitor evaluation arises from the relatively low values of  $k_{cat}$  for the human enzymes (Table S1). Typical assays contain an enzyme concentration of 40 nM; therefore, an inhibitor concentration of at least 20 nM will be required for 50% inhibition. Nevertheless, values of IC<sub>50</sub> less than 20 nM are frequently reported. The most likely explanation for such discrepancies is inaccuracy in the concentration of active enzyme, though it is also possible that a single inhibitor can affect more than one active site. The usual methods to determine inhibition mechanism require that inhibitor concentrations are in excess of enzyme concentration, but this too is frequently violated. These considerations should be remembered when assessing inhibitor structure-activity relationships (SAR). However, it is also important to recognize that additional information from cell proliferation and pharmacodynamics studies also inform the development of novel IMPDH inhibitors and several companies have reported promising compounds despite the limitations of the enzyme activity assays.

## 7.2. Mycophenolic acid (MPA)

Although penicillin is widely recognized as the first antibiotic, MPA was actually purified first; it was originally isolated from spoiled corn and shown to inhibit the growth of *Bacillus anthracis* in 1893 (<sup>149</sup> is an excellent review on the discovery and properties of MPA). MPA is a potent inhibitor of mammalian IMPDHs, and so was never used as an antibiotic. MPA displays antiviral and anticancer activity in cell culture models <sup>150,151</sup>. However, the efficacy of MPA *in vivo* appears to be limited by glucuronidation of the phenolic oxygen, which inactivates the drug <sup>150</sup>. Cancer cells appear to have a higher capacity for glucuronidation than normal cells, which may explain why MPA has been ineffective as an anticancer agent. MPA eventually reached the clinic as an immunosuppressive drug for the prevention of transplant rejection in the form of sodium mycophenolate (Myfortic™, Novartis) and a pro-drug, mycophenolate mofetil (CellCept™, Roche), approximately 100 years after its discovery. MPA has also been used in the treatment of psoriasis. More recently, interest in MPA as an anticancer drug has revived with the observation that it has antiangiogenic activity <sup>27</sup>. MPA also induces differentiation and/or apoptosis of several cancer cell lines, including breast <sup>152</sup>, prostate <sup>153,154</sup>, melanoma <sup>155</sup>, leukemia <sup>156,157</sup> and neuroblastoma <sup>158,159</sup>.

Multiple inhibitor experiments first demonstrated that MPA competes with tiazofurin for the nicotinamide subsite <sup>129</sup>. Modeling studies show that MPA and nicotinamide portion of NAD<sup>+</sup> have similar volumes and electronic properties <sup>160</sup>. MPA traps the E-XMP\* intermediate <sup>116,117</sup>, and x-ray crystal structure of Chinese hamster type 2 E-XMP\*•MPA complex shows that MPA stacks against the purine ring in a similar manner to the nicotinamide ring of NAD<sup>+</sup> (Figure 1376).

The strong preference for E-XMP\* makes MPA an uncompetitive inhibitor with respect to both IMP and NAD<sup>+</sup> for most IMPDHs <sup>10,56,75,79,84,86,98</sup>. Such inhibitors have a significant advantage *in vivo* because inhibition increases as substrate accumulates. This behavior contrasts with that of competitive inhibitors, which become less effective as substrate concentrations rise. This strong and selective affinity of MPA for E-XMP\* can be used to drive

the reaction backward, forming E-XMP\*•MPA from XMP with Chinese hamster IMPDH type 2<sup>116</sup>. The discrimination between E-XMP\* and other enzyme forms is not as great for bacterial IMPDHs, so, at low NAD<sup>+</sup> concentrations, MPA can also bind to E•IMP, which explains why MPA is occasionally described as a noncompetitive inhibitor. Only the noncovalent complex E•XMP•MPA appears to form with *T. foetus* IMPDH, although the oxidation of the active site Cys319 during crystallization may have prevented observation of E-XMP\*<sup>120</sup>. Given that MPA has >10<sup>3</sup>-fold higher affinity to E-XMP\* than free enzyme for mammalian IMPDHs, it is worth noting that MPA would probably never have been identified in a screen for compounds that bind to IMPDH.

**7.2.1. MPA selectivity**—Though MPA is a specific inhibitor of IMPDHs, it is approximately 10<sup>3</sup>-fold more potent against the mammalian enzymes than bacterial ones (Table S1). Mammalian IMPDHs are also slower than bacterial enzymes (see Table S1), suggesting that there is an underlying mechanistic link between catalysis and inhibitor affinity. This link can be explained by the competition between the flap and MPA for the vacant dinucleotide site. Since the closed conformation is required for the hydrolysis of E-XMP\*, hydrolysis will be faster in enzymes where the closed conformation is favored. The closed conformation also protects the enzyme from MPA, so these enzymes will also be resistant to MPA.

Likewise, the species-selectivity of MPA derives largely from the competition between MPA and the flap rather than from differences in the residues that contact MPA. For example, the value of  $K_{ii}$  for MPA is 500-fold higher for *T. foetus* IMPDH than for human hIMPDH2, corresponding to a difference in binding energy of  $\Delta\Delta G$  of 3.7 kcal/mol. However, while the human enzyme is mainly in the open conformation, *T. foetus* IMPDH favors the closed conformation ( $K_c = 150$ ,  $\Delta\Delta G = 3$  kcal/mol), so most of the selectivity comes from the difference in the equilibrium between the open and closed states.

This conclusion is confirmed by mutagenesis experiments. Two residues are different in the MPA binding site: human hIMPDH2 contains Arg322 and Gln441, while the corresponding residues are Lys310 and Glu431 in *T. foetus* IMPDH (Figure 13). *T. foetus* IMPDH does become 23-times more sensitive to MPA when these residues are “humanized”, but only ~1 kcal/mol can be attributed to binding interactions. The remaining 0.8 kcal/mol derives from destabilization of the closed conformation. Despite this destabilization, the closed conformation is still favored in the K310R/E4331Q variant.

**7.2.2. MPA derivatives**—Dose-limiting gastrointestinal toxicity and unfavorable metabolism spurred the effort to develop more potent and/or effective MPA derivatives<sup>151</sup>. However, the scaffold has proven remarkably resistant to modification. Substitutions of the phenolic hydroxyl, an obvious strategy to avoid glucuronidation, abrogate activity, as do changes in the terminal carboxylic acid<sup>161–166</sup>. Only the most modest changes are allowed in the isoprene tail, lactone, methoxy and methyl groups. The structure of the E-XMP\*•MPA complex revealed the basis for this restricted SAR<sup>76</sup>. The phenolic oxygen and the lactone carbonyl form a hydrogen bonding network that also involves Gly326, Thr333 and Gln441 and the terminal carboxylate interacts with Ser276 (hIMPDH2 numbering; the analogous residues are Gly314, Thr321 and Glu431 in *T. foetus* IMPDH), while the spatial constraints of the active site explain the low tolerance of the other positions.

The discovery that MPA bound in the nicotinamide subsite suggested that more potent and selective IMPDH inhibitors might be obtained by designing MPA derivatives that extend into the adenine binding site. Pankiewicz and colleagues have synthesized a series of such mycophenolic adenine nucleotides, known as “MAD” compounds<sup>167–169</sup>. While the initial MAD compounds were not as potent as MPA, they were resistant to glucuronidation,

suggesting that they will have improved pharmacological properties. Recent MAD derivatives approach MPA in affinity (Chart 2)<sup>168</sup>.

The efficacy of multi-drug cocktails in cancer treatment and the success of such mixtures in suppressing drug resistance have spawned efforts to create dual function inhibitors. Histone deacetylase (HDAC) inhibitors, like IMPDH inhibitors, induce differentiation and apoptosis of tumor cells, although via a different mechanism<sup>170</sup>. Thus the combination of IMPDH and HDAC inhibition is a tantalizing new strategy for anticancer drug development. MAHA, the hydroxamic acid analog of MPA, is the prototype for dual function inhibitors targeting both IMPDH and histone deacetylase (HDAC). MAHA has equivalent activity against hIMPDH2 and inhibits HDAC with an  $IC_{50} = 5 \mu\text{M}$ , presumably chelating the  $\text{Zn}^{+2}$  via the hydroxamic acid moiety<sup>171</sup>.

### 7.3. Synthetic non-nucleoside inhibitors of human IMPDH

Given the unforgiving SAR of MPA, the discovery and optimization of synthetic inhibitors has proceeded with surprising ease (reviewed in<sup>13</sup>). Some common motifs are apparent in the inhibitor structures, but SAR does not always translate from one framework to another. This observation suggests that the binding site is plastic, in keeping with disordered in the various crystal structures. To date, no structures of enzyme-inhibitor complexes are available in the PDB, and only the structure of E-XMP\*•merimepodib has been described<sup>12</sup>.

**7.3.1. Phenyl-oxazole urea inhibitors**—The phenyl-oxazole urea scaffold was discovered in a structure-based drug design effort at Vertex Pharmaceuticals (Chart 3)<sup>12</sup>. Like MPA, these compounds trap E-XMP\*; the phenyl-oxazole stacks against the purine as observed with the lactone of MPA<sup>12</sup>, with the oxazole forming a hydrogen bonding network with Gly326 and Thr333 similar to that with MPA and the methoxy group occupying the same pocket as the methyl group of MPA (Figure 14). These interactions are critical for potency<sup>172</sup>. The urea linkage forms hydrogen bonds to the Asp274, so that the remainder of the molecule extends past the methoxy substituent of MPA rather than the isoprenoid tail, entering a different groove than NAD/NADH. Merimepodib (VX-497;  $K_i$  of 7 nM) has immunosuppressive activity<sup>173</sup>. This compound also showed promise as an antiviral agent and has entered clinical trials for the treatment of hepatitis C<sup>174</sup>.

AVN944 (VX-944) is also potent inhibitor of human IMPDHs ( $K_i = 6\text{-}10 \text{ nM}$ ; curiously, it is described as a noncompetitive inhibitor in two publications, though it almost certainly traps E-XMP\* as does merimepodib; Chart 3). AVN944 induced caspase-independent apoptosis in multiple myeloma cell lines (unlike most drugs)<sup>175</sup>. AVN944 also displayed antiproliferative activity against both androgen-dependent and androgen-independent prostate cancer cell lines. The compound induced cellcycle arrest in S phase, differentiation and apoptosis via both caspase-dependent and caspase-independent pathways<sup>176</sup>. AVN944 is in clinical trials in combination with gemcitabine for the treatment of pancreatic cancer.

Potent inhibitors could also be achieved by replacing the oxazole ring with a cyano group (VX-148,  $K_i = 14$  and 6 nM for hIMPDH1 and hIMPDH2, respectively)<sup>177</sup>. Unfortunately, the structure of an enzyme complex with VX-148 has not been reported, so how the cyano group replaces the interactions of the oxazole ring is not known. VX-148 displays promising immunosuppressive activity<sup>177</sup>.

Many other potent inhibitors of human hIMPDH2 have been reported, though none have reached clinical trials. Metabolism of the aniline groups of merimepodib is a point of concern, so strategies have been developed to find isosteres of the urea linker. Several heterocyclic rings have proven useful in this regard<sup>178,179</sup>. BMS developed 2-aminooxazoles, yielding potent inhibitors such as Compound 1 (Chart 4) that also display immunosuppressive activity in

arthritis model<sup>180</sup>. Cyano-guanidine and indole groups are also useful replacements (Compounds **2** and **3**)<sup>181,182</sup>, while triazines (Compound **4**)<sup>183</sup> and diamide (Compound **5**)<sup>184</sup> linkers yielded good inhibitors that were ineffective in T cell proliferation assays. Compound **5** is reported to be an uncompetitive inhibitor with respect to NAD<sup>+</sup> ( $K_{ii} = 23$  nM)<sup>184</sup>, but this experiment was performed under tight-binding conditions, whereas the analysis used assumes that inhibitor concentrations are in excess of enzyme concentration. Therefore the actual value of  $K_i$  is lower and the uncompetitive mechanism, though likely, remains to be confirmed.

Amide linkers could also replace the urea group, although in this case equivalent potency was not achieved and again immunosuppressive activity was not observed (Compound **6**)<sup>185</sup>. Note that because the enzyme assays used in this work contained 40 nM hIMPDH2, the lowest value of IC<sub>50</sub> that should be observed is 20 nM. Therefore, the report of IC<sub>50</sub> values of 5 nM or less, as with the case of quinolone based linkers (Compound **7**)<sup>186,187</sup>, must be viewed with suspicion. Intriguingly, compound **7** was reported to have 30-fold higher affinity for hIMPDH2 than hIMPDH1, but this must also be called into question given the uncertainties in the enzyme assay. The quinazolinethione framework provides another alternative to the urea linker, as exemplified by compound **8**<sup>179</sup>. Further elaboration of this structure (e.g., compound **9**) did not substantially improve either potency or biological immunosuppressive activity<sup>188</sup>. Unfortunately, no x-ray crystal structures have been reported for these compounds, so whether these frameworks interact with Asp274 as designed has not been confirmed.

As noted above, MPA and merimepodib display common binding interactions: both the lactone of MPA and the oxazole of merimepodib form hydrogen bonds with Gly326 and Thr333 while the adjacent aromatic rings stack against the purine ring of E-XMP\* and the methoxy group binds in a pocket. 3-(Oxazolyl-5-yl) indoles were designed to provide similar interactions, and potent inhibitors such as compound **10** have been reported by the BMS group (Chart 5)<sup>189</sup>.

With the exception of VX-148, replacement of the oxazole ring has not been as successful. Cyanoindole and pyridylindole frameworks have so far yielded weaker inhibitors (e.g., compounds **11** and **12**, Chart 5) with weak immunosuppressive activity<sup>190,191</sup>. The SAR of these inhibitors differs significantly from their oxazole and urea analogs, which suggests that these inhibitors may have a different binding mode. Unfortunately, neither the mechanisms of inhibition nor protein crystal structures of enzyme-inhibitor complexes have been reported, so whether these inhibitors trap E-XMP\* as supposed is not known.

**7.3.2. Novel frameworks**—High throughput screening has yielded several novel frameworks which presumably stack against the purine ring of E-XMP\* (Chart 6). Zeneca reported the first compounds discovered in this way: pyridazines. However, attempts to improve the lead compound (**13**) could only improve potency by approximately a factor of 2 (compound **14**)<sup>192</sup>. The BMS group improved weak acridone and isoquinoline lead compounds (Compounds **15** and **17**) with the modification of linkers and additional aromatic and hydrophobic groups (Chart 6)<sup>193,194</sup>. The resulting inhibitors have nanomolar affinities (compounds **16** and **18**; although, as noted above, the values of IC<sub>50</sub> cannot be less than 20 nM). Compound **16** was reported to be a reversible uncompetitive inhibitor with  $K_{ii} = 20$  nM<sup>186</sup>, but these experiments were also performed under tight-binding conditions and are therefore unreliable.

**7.3.3. 1,5-Diazabicyclo[3.1.0]hexane-2,4-diones**—Compounds such as **19** are reported to be specific inhibitors of hIMPDH2, and not of hIMPDH1 (Chart 7)<sup>195</sup>. Curiously, these compounds were reported to be competitive inhibitors with respect to IMP, though the data were not very convincing; given that the IMP binding site is conserved, the structural basis of this selectivity is not clear. The SAR around these compounds is also puzzling: the mechanism

of very similar diones can vary from competitive versus IMP to competitive versus NAD<sup>+</sup> 196. The high values of  $K_i$ , which require high concentrations of compound for inhibition, coupled with the broad nmr peaks <sup>197</sup>, suggests that the active component may be a polymer or aggregate. These compounds display antineoplastic activity, which is reversed upon addition of guanosine, as commonly observed for IMPDH activity <sup>198</sup>. However, this cytotoxicity is often more potent than IMPDH inhibition <sup>196</sup>. The categorization of these compounds as IMPDH inhibitors awaits further confirmation.

#### 7.4. Other Non-nucleoside Natural Product Inhibitors

The allure of IMPDH as a cancer target has lead several laboratories to search for natural product inhibitors by screening directly for enzyme inhibition rather than cytotoxicity (Chart 8). The compounds uncovered in these efforts have had no clinical impact as yet. Several compounds appear to nonspecifically modify the catalytic Cys. Sesquiterpene lactones such as helenalin seem likely to function in this manner <sup>199</sup>, as do the bastadins <sup>200</sup>. Isolation of an IMPDH inhibitor (**20**) from tunicate extracts yielded a disulfide containing alkaloid with an IC<sub>50</sub> = 0.015 µg/ml; inhibition was relieved by dithiothreitol, suggesting that this compound formed a disulfide with the catalytic Cys <sup>201</sup>. Halicyclamine A of IMPDH was originally discovered in a screen for hIMPDH2 inhibitors <sup>202</sup> and was recently re-discovered in a screen for anti-tuberculosis activity <sup>203</sup>. However, the anti-tuberculosis activity does not result from inhibition of IMPDH <sup>203</sup>. Daphnane-type diterpene esters such as 3-hydrogenkwadaphnin (3-HG) (Chart 8) are also reported to inhibit IMPDH<sup>204,205</sup>. This compound displays potent antileukemic activity and appears to decrease IMPDH activity in cells. Guanosine protects against cytotoxic effects, which is usually diagnostic for drugs that target IMPDH. Curiously, 3-HG does not inhibit IMPDH activity in crude lysates, suggesting that it is not an inhibitor of IMPDH <sup>204</sup>. Another screen for hIMPDH2 inhibitors in 5000 fungal strains identified two compounds in one extract, 2264A and 2264B <sup>206</sup>. 2264A has an IC<sub>50</sub> = 70 µM, but looks to be a nonspecific alkylator. The structure of 2264B is more promising, though the IC<sub>50</sub> = 12 µM is also high. Both compounds inhibit lymphocyte proliferation.

Two natural product screening efforts have identified unsaturated fatty acids as inhibitors of mammalian hIMPDH2s. Pellynic acid (IC<sub>50</sub> = 1 µM) was isolated from extracts of marine sponge <sup>207</sup>. Linoleic acid (C18:2) was identified as the IMPDH inhibitor in a basidiomycete extract, and lead to the subsequent discovery that eicosadenoic acid is a competitive inhibitor versus IMPDH with  $K_i$  = 3 µM <sup>208</sup>. The concentrations of fatty acid in these experiments are well above the critical micelle concentration, which suggests that the actual inhibitor in these experiments is a micelle or aggregate.

#### 7.5. Parasite-selective IMPDH inhibitors

Thus far, specific inhibitors have only been reported for *Cryptosporidium* IMPDH. *Cryptosporidium* is a major cause of diarrhea and malnutrition and a potential bio-warfare agent. The parasite has a very streamlined purine salvage pathway that requires IMPDH to produce guanine nucleotides. Intriguingly, *Cryptosporidium* IMPDH was obtained from a bacteria via lateral gene transfer <sup>52,209</sup>, and therefore differs greatly from the host enzyme <sup>75</sup>. Ten selective inhibitors of *Cryptosporidium* IMPDH were discovered in a high throughput screen designed to target the NAD<sup>+</sup>/NADH site (Chart 9)<sup>58</sup>. These compounds were either noncompetitive or uncompetitive inhibitors with respect to both IMP and NAD<sup>+</sup>, as expected for compounds that bind in the dinucleotide site. Multiple inhibitor experiments show that all of the compounds compete with tiazofurin for the nicotinamide subsite. Surprisingly, while some of the inhibitors also antagonize ADP binding, others have a different binding mode. The best inhibitors display antiparasitic activity in a cell culture model of infection <sup>58</sup>.

## 7.6. Reversible Nucleoside inhibitors

Many nucleotide monophosphates inhibit IMPDH with micromolar to millimolar affinities (Chart 10). Most such compounds are competitive inhibitors with respect to IMP. The exception is AMP, which binds preferentially to the adenosine portion of the dinucleotide site (it is likely that AMP also has low affinity for the IMP site). Nucleosides are very poor inhibitors. As noted above, IMPDH crystallizes with phosphate and sulfate occupying the site of the 5'-phosphate of IMP, suggesting that these interactions are very important for binding. Virtually every monophosphate will bind to IMPDH to some extent; indeed, IMP analogs containing phenyl substituents at the 2 and 8 positions are nevertheless micromolar inhibitors<sup>210,211</sup>. This fact, coupled with the general enthusiasm for IMPDH as a potential drug target, can lead to mis-assignment of mechanism of action. For example, triciribine phosphate has been reported to be a millimolar IMPDH inhibitor<sup>212</sup>, but with such low affinity, inhibition of IMPDH seems unlikely to account for its potent antineoplastic activity; more recently, cytotoxicity has been associated with the inhibition of serine/threonine Akt/PKB protein kinases<sup>213</sup>.

IMPDHs generally have similar affinity for GMP and IMP (Table S1). The physiological concentrations of both IMP and GMP are ~60 μM<sup>214</sup>, which enables GMP to act as a feedback regulator. Other GMP analogs are also potent inhibitors. Oxanosine has antimicrobial and antitumor activity (Chart 10)<sup>215</sup>; this activity is reversed by guanosine, suggesting that oxanosine acts by inhibiting guanine nucleotide biosynthesis. Oxanosine monophosphate inhibits IMPDH with  $K_i = 1 \mu\text{M}$ , but not GMPS<sup>216</sup>. Oxanosine was originally isolated from *Actinomycetes*, but more recently has been shown to be a product of nitrosative deamination of guanosine, and thus may be responsible for the mutagenic effects of HNO<sub>2</sub><sup>217</sup>. Deoxyoxanosine-modified nucleic acids crosslink proteins<sup>104</sup>, which suggests that oxanosine-IMP will react with IMPDH to covalently modify the enzyme (Scheme 4).

Several nucleosides display biological effects that have been attributed to inhibition of IMPDH, though *in vitro* confirmation is not always available. For example, 3-deazaguanosine has antiviral activity and inhibits guanine nucleotide biosynthesis in Erlich ascites tumor cells presumably by forming the monophosphate<sup>218</sup>. Similarly, 1-amino-guanosine, inhibits both cell growth and production of guanine nucleotides (Chart 10)<sup>219</sup> (note that the report that 1-aminoguanosine is a potent inhibitor of IMPDH in reference<sup>220</sup> is incorrect).

**7.6.1. Mizoribine**—Mizoribine (Bredinin™) is another natural product inhibitor of IMPDH that is currently used as an immunosuppressive agent in Japan<sup>221</sup>. Mizoribine is an imidazole nucleoside; it is activated to the 5'-monophosphate (MZP) by adenosine kinase. MZP is a potent inhibitor of IMPDHs with values of  $K_i$  values ranging from 0.5 nM (*E. coli*) - 8 nM (hIMPDH1) depending on the enzyme source (Table S1). MZP is also a potent inhibitor of GMPR (C. Swales and L. Hedstrom, personal communication), as well as a weak inhibitor of GMP synthase ( $K_i = 10 \mu\text{M}$ )<sup>221</sup>. Interestingly, AICARMP, the purine nucleotide precursor where an amine replaces the O5, does not inhibit IMPDH. As noted above, the E•MZP complex resembles the transition state for the hydrolysis reaction.

**7.6.2. Ribavirin**—Ribavirin is a synthetic nucleoside<sup>222</sup> and is sold under a variety of names and formulations, including Copegus, Rebetol, Ribasphere, Vilona and Virazole. Like mizoribine, it is activated to the 5'-monophosphate (RVP) by adenosine kinase, but its subsequent interactions are more promiscuous<sup>223</sup>. RVP is a potent inhibitor of IMPDHs (Table S1), binding in the IMP site. Inhibition of IMPDH may be sufficient to account for antiviral activity<sup>224</sup>. However, ribavirin undergoes further transformation to the triphosphate, which inhibits RNA capping enzymes<sup>225</sup>. Ribavirin triphosphate can also inhibit polymerases<sup>226</sup> and is incorporated into RNA, where it induces lethal mutations<sup>227</sup>. Ribavirin also acts as an

immunomodulator, enhancing the T-cell response, though the molecular mechanism of this effect is not understood<sup>228</sup>. While the origin of the antiviral activity of ribavirin is currently under debate, it seems likely that all of these mechanisms may contribute, though one or another may dominate for a given virus<sup>229,230</sup>.

Surprisingly, although the hIMPDH2 prefers the open conformation and the *T. foetus* enzyme prefers the closed, x-ray crystal structures of E•RVP find the hIMPDH2 in the closed conformation<sup>12</sup> and the *T. foetus* enzyme in the open conformation<sup>121</sup>. This result might be chalked up to the capriciousness of protein crystallization, or might also be the consequence of oxidation of the catalytic Cys319 in the *T. foetus* enzyme. In either case, these results point to the danger of assuming that the crystal structure represents the lowest energy conformation in solution. Ternary complexes of E•RVP and MPA (*T. foetus* IMPDH) and MAD (hIMPDH2) have also been solved. Importantly, as in MZP, the absence of the C2 carbon allows the active site loop to assume the same conformation as in the E-XMP\* complex.

**7.6.3. Tiazofurin**—Tiazofurin and selenazofurin, its selenium analog, are also synthetic nucleosides which display potent antiviral and antitumor activities (reviewed in<sup>231</sup>). Tiazofurin was approved for treatment of chronic myelogenous leukemia. Dose-limiting toxicity includes headache, somnolence and nausea.

Despite their close resemblance to ribavirin, the active metabolites of tiazofurin and selenazofurin are not the monophosphates. Instead, these compounds are converted into adenine dinucleotides, TAD and SAD<sup>232,233</sup>. TAD and SAD can bind to free enzyme, E•IMP and E-XMP\*, and so generally act as noncompetitive inhibitors with respect to both IMP and NAD<sup>+</sup> (note that uncompetitive inhibition can also be observed depending on assay conditions). These dinucleotides are reasonably specific inhibitors of IMPDH, which is rather surprising given their close resemblance to NAD<sup>+</sup>/NADH<sup>234</sup>. This selectivity is attributed to the unusual conformation of the thiazole nucleoside<sup>235</sup>. Small molecule x-ray crystal structure reveals that the conformation of the inhibitor is locked by an electrostatic interaction between the sulfur of the thiazole ring and the furanose oxygen of the ribose moiety so that the C-glycosidic torsion angle is 24 degrees<sup>236</sup>. This conformation is recognized by IMPDH<sup>95</sup>, but cannot be accommodated by other dehydrogenases<sup>237</sup>. Similar interactions are proposed for the selenium and furanose oxygen<sup>96</sup>. SAD is approximately 8-20-times more potent inhibitor of hIMPDH1 and hIMPDH2 than TAD (Table 4)<sup>220</sup>. In contrast, oxazofurin, the oxygen analog of tiazofurin, does not display cytotoxicity; oxygen-oxygen repulsion causes a C-glycosidic torsion angle of 70 degrees, which is believed to account for the lack of inhibition<sup>238</sup>. Substitution of N with CH has little effect on the potency of TAD but decreases the potency of SAD by approximately a factor of 20. The molecular basis of this SAR is not understood. The furan analog is 100-fold less potent, again demonstrating the importance of the S-O and Se-O interactions (Table 4).

The accumulation of TAD determines the efficacy of tiazofurin. Tiazofurin is first phosphorylated to the monophosphate by adenosine kinase, nicotinamide riboside kinase and/or 5'-nucleotidase<sup>239,240</sup>, then converted to TAD by the action of NMN adenyltransferase (also known as NAD-pyrophosphorylase; this enzyme does not process RVP). TAD is degraded by a phosphodiesterase, so that the sensitivity of a given cell line to tiazofurin is determined by the ratio of pyrophosphorylase to phosphodiesterase. Tiazofurin resistance can result from decreases in uptake and/or NMN adenyltransferase as well as by increases in the amount of phosphodiesterase. These observations prompted the development of non-hydrolyzable analogs of TAD<sup>241,242</sup>. Beta-methylene TAD inhibits hIMPDH2 with equivalent potency to TAD, while the potency of beta-difluoromethylene-TAD is decreased by a factor of 3. Intriguingly, beta-methylene-TAD displays decreases the guanine nucleotide pools of P388 cells and displays cytotoxicity<sup>241</sup>, which indicates that this compound enters cells.

Methylenebis(sulfonamide) derivatives were also designed to resist hydrolysis, but these compounds were relatively poor inhibitors and failed to display antiproliferation activity<sup>243</sup>.

**7.6.4. Benzamide riboside**—Benzamide riboside (BR) was originally synthesized as an inhibitor of poly(ADP-ribose) polymerase (PARP) (Chart 10)<sup>244</sup>. Though BR failed to inhibit PARP, it did display a cytotoxicity profile very similar to tiazofurin and selenazofurin, which suggested that BR acted as an IMPDH inhibitor<sup>245</sup>. Like tiazofurin, BR is converted to a dinucleotide, BAD, via phosphorylation followed by adenylation. BAD is a potent inhibitor of IMPDH with  $K_i \sim 100$  nM, but a poor inhibitor of other dehydrogenases<sup>246</sup>. Guanine nucleotide pools are depleted when cells are treated with BR, further demonstrating that IMPDH is the cellular target. However, BR induces more apoptosis than would be expected from depletion of the guanine nucleotide pool<sup>247,248</sup>. BR displays skeletal muscle toxicity in preclinical trials, which limits its utility<sup>249</sup>. These observations suggest that BR may have additional cellular targets.

**7.6.5. “Fat base” nucleotide**—The “fat base” nucleotide imidazo[4,5-e][1,4]diazepine is another potential transition state analog of the IMPDH reaction (Scheme 5)<sup>250</sup>. The fat base nucleotide is a time-dependent inhibitor of IMPDH with  $K_i$  values of 1 nM (hIMPDH2) - 50 nM (*E. coli*) depending on the enzyme source. IMP, but not NAD<sup>+</sup>, protects against inhibition. The enzyme-inhibitor complex is stable to dialysis but activity is recovered when the enzyme is denatured and refolded. Carbinolamines such as the fat base exist primarily in the hydrated form in aqueous solution, but are in rapid equilibrium with the dehydro form. Therefore it is likely that the dehydro form reacts with Cys331 to form an adduct which resembles the transition state. Similar strategies have been used in the inhibition of cysteine proteases by aldehydes and adenosine deaminase by coformycin<sup>251</sup>. No cytotoxicity has been reported for the fat base nucleoside, which probably reflects a failure in uptake and/or phosphorylation.

## 7.7. Mechanism-based inactivators

IMPDH contains a catalytic Cys319 residue, which is an unusual feature for a nucleotide metabolic enzyme, shared only by GMPR. The catalytic Cys is both a bane and a blessing: as noted above, nonspecific alkylation can complicate screening efforts. However, the catalytic Cys can also provide specificity. Several analogs of IMP have been designed to form covalent adducts with this residue, including 6-Cl-IMP, EICARMP, 2-Cl-methyl-IMP, 6-thio-IMP and 2-vinyl-IMP, 2-F-vinyl-IMP (Chart 11)<sup>92,113,252-256</sup>. All of these compounds are time-dependent irreversible inactivators of IMPDH. 6-Cl-IMP and EICARMP also inactive GMPR, and it seems likely that the other compounds will also inactivate this enzyme.

**7.7.1. 6-Cl-IMP**—The reaction of 6-Cl-IMP is the best characterized of the covalent inactivators (Chart 11)<sup>92,257</sup>. IMP protects against inactivation, but neither NAD<sup>+</sup> nor K<sup>+</sup> affect inactivation<sup>147,258</sup>. Modification of the catalytic Cys has been verified<sup>73,258</sup>, and X-ray crystal structures of the hIMPDH2 complex show that the nucleotide occupies the same position as IMP, but the catalytic Cys has moved to attack the 6 position, deforming the active site loop and disrupting the K<sup>+</sup> site<sup>96</sup>. This observation suggests that the plasticity of the loop may control the rate of inactivation. The inactivation of IMPDH by 6-Cl-IMP is much slower than its reaction with EICARMP as described below, though as in the catalytic reaction, bacterial enzymes react faster than mammalian (*A. aerogenes*,  $k_{inact} = 0.12$  s<sup>-1</sup>,  $K_i = 260$  μM,  $k_{inact}/K_i = 460$  M<sup>-1</sup>s<sup>-1</sup><sup>252</sup>; hIMPDH2,  $k_{inact} = 3.5 \times 10^{-3}$  s<sup>-1</sup>,  $K_i = 78$  μM,  $k_{inact}/K_i = 44$  M<sup>-1</sup>s<sup>-1</sup><sup>258</sup>).

**7.7.2. EICAR**—EICAR was designed as a mechanism-based inactivator of IMPDH (Chart 11)<sup>259</sup>. EICAR displays both antileukemic and antiviral activity. It is activated to mono-, di- and tri-phosphates and also to the dinucleotide, EAD<sup>260</sup>. Guanosine protects against the action of EICAR, suggesting that the antiviral and cytotoxic effects of EICAR indeed result from

inhibition of IMPDH<sup>259</sup>. EICARMP is a potent inhibitor of IMPDH (for *E. coli* IMPDH,  $K_i > 2 \mu\text{M}$ ,  $k_{inact}/K_i = 2.3 \times 10^4 \text{ M}^{-1}\text{s}^{-1}$ ; for hIMPDH2,  $K_i = 16 \mu\text{M}$ ,  $k_{inact} = 2.7 \times 10^{-2} \text{ s}^{-1}$ ,  $k_{inact}/K_i = 1.7 \times 10^3 \text{ M}^{-1}\text{s}^{-1}$ )<sup>91</sup>. IMP protects against inactivation, but NAD<sup>+</sup> has no effect. EICARMP modifies the catalytic Cys319 as expected<sup>91</sup>. EAD also inactivates IMPDH, although it is a poor inactivator relative to EICARMP (for *E. coli* IMPDH,  $k_{inact}/K_i = 0.66 \text{ M}^{-1}\text{s}^{-1}$ ,  $K_i \gg 27 \mu\text{M}$  (W. Wang, N. Minakawa, A. Matsuda and L. Hedstrom, unpublished observations)). Activity is not recovered upon denaturation and refolding, indicating that a covalent bond forms. IMP, but not NAD<sup>+</sup>, protects against inactivation, suggesting that EAD acts as a nonspecific alkylating agent. EICARMP is also a potent inactivator of GMPR (C. Swales and L. Hedstrom, unpublished observations).

**7.7.3. Other inactivators**—2-Cl-methyl-IMP, 2-F-methyl-IMP and 2-vinyl-IMP are also time-dependent inactivators of IMPDH that have been shown to modify the catalytic Cys (Chart 11)<sup>254</sup>. 2-[2-(Z)-Fluorovinyl]-IMP is a time dependent inactivator of comparable potency to EICARMP (for *E. coli* IMPDH,  $K_i = 1 \mu\text{M}$  and  $k_{inact} = 0.027 \text{ s}^{-1}$ ,  $k_{inact}/K_i = 2.7 \times 10^4 \text{ M}^{-1}\text{s}^{-1}$ ), though modification of the catalytic Cys has not been explicitly demonstrated<sup>256</sup>. 2-Formyl-IMP is at least 300-times more potent than 2-hydroxymethyl-IMP; this compound may form a thiohemiacetal with the catalytic Cys<sup>254</sup>. 6-thio-IMP and 6-thio-GMP are also time-dependent inactivators of IMPDH<sup>113</sup>. Glutathione protects against inactivation, suggesting that these compounds also modify the active site Cys, perhaps by forming a disulfide bond. As expected, these compounds also inactivate GMPR<sup>257</sup>. 8-(2-Cl-4-O<sub>2</sub>N-PhCH<sub>2</sub>S)-IMP is also a time dependent inactivator of IMPDH and may also modify the catalytic Cys, though this reaction has not been characterized<sup>210</sup>.

## 8. Moonlighting functions: hIMPDH1 and retinal disease

The biological consequences of the IMPDH inhibitors are attributed to depletion of the guanine nucleotide pools, but the presence of the CBS subdomain suggests that the cellular role of IMPDH extends beyond its enzymatic activity. As described in 4.3, the CBS subdomain coordinately regulates the adenine and guanine nucleotide pools and associates with polyribosomes. IMPDH also associates with lipid vesicles and is phosphorylated<sup>43</sup>. IMPDH has been reported to associate with many proteins, including: protein kinase B<sup>44</sup>; a translation factor, a transcription factor and glutamate dehydrogenase<sup>261</sup>; and proteins involved in transcription regulation, splicing and rRNA processing in yeast<sup>262-265</sup>. Several observations suggest that the function of the tumor suppressor p53 is linked to IMPDH<sup>25,266</sup>. At present there is no model to account for these disparate observations. Perhaps the most curious observation in this regard is that IMPDH binds single stranded nucleic acids with nanomolar affinity, and this interaction is mediated by the subdomain<sup>3,4</sup>. IMPDH associates with polyribosomes, suggesting that this enzyme has a previously unappreciated role in translation regulation<sup>6</sup>.

The physiological importance of the interaction of IMPDH with polyribosomes is underscored by the discovery that mutations in the CBS subdomain of hIMPDH1 account for 2-3% of autosomal dominant retinitis pigmentosa (adRP)<sup>7,8,267</sup>. At present, nine alleles of hIMPDH1 are associated with retinal disease. Arg224Pro, Asp226Asn and Arg231Pro clearly cause adRP while Thr116Met, Val268Ile, His372Pro are very likely to be pathogenic<sup>7-9,268</sup>. The Asp226Asn mutation alone accounts for 1% of adRP cases. Lys238Glu has been found in adRP patients but not in controls<sup>267</sup>. Two hIMPDH1 mutations, Arg105Trp and Asn198Lys, are associated with Leber congenital amaurosis (LCA), a more severe hereditary blindness<sup>9</sup>. These mutations do not affect enzymatic activity, as expected given their location in or near the CBS subdomain (Figure 15)<sup>5,9,34,38</sup>. The tissue specificity of disease is somewhat surprising given the widespread expression of hIMPDH1. hIMPDH1 predominates in the adult retina<sup>42</sup>, and mammalian photoreceptors contain novel hIMPDH1 mRNAs derived from alternative splicing

which encode two variants of hIMPDH1, hIMPDH1(546) and hIMPDH1(595) (Figure 15; 33,26<sup>9</sup>). These novel isoforms may account for the tissue specificity of disease. Both retinal isoforms contain a 32 residue C-terminal extension while hIMPDH1(595) has an additional 49 residues on the N-terminus. These extensions do not display significant similarity to other proteins in a BLAST search. hIMPDH1(546) is the major isozyme in the human retina while hIMPDH1(595) is the more abundant protein in the mouse<sup>33</sup>. Like the subdomain, the N- and C-terminal extensions are likely to confer novel functions on hIMPDH1. The enzymatic activity of the retinal isoforms is indistinguishable from the canonical hIMPDH1<sup>38</sup>. However, the Asp226Asn mutation decreases the association of the retinal isoforms with polyribosomes<sup>6</sup>. Importantly, retinal hIMPDH1 associates with polyribosomes translating rhodopsin mRNA<sup>6</sup>. Virtually any perturbation of rhodopsin expression triggers apoptosis of photoreceptor cells, so this observation provides an attractive mechanism for hIMPDH1-linked retinal disease.

How these moonlighting functions are affected by IMPDH inhibitors is a crucial question as illustrated by thymidylate synthase, a key enzyme in pyrimidine biosynthesis. Thymidylate synthase serves as its own translational regulator, binding to its cognate mRNA and repressing translation<sup>270</sup>. Substrates cause thymidylate synthase to release mRNA and translation resumes. Importantly, the efficacy of thymidylate synthase inhibitors in malaria treatment is due to differences in this translational regulation<sup>271</sup>. Inhibitors also release translational repression in mammalian cells, producing more enzyme. However, neither substrates nor inhibitors relieve translational repression in malaria parasites, so enzyme levels remain at basal levels. Malaria parasites are more sensitive to the thymidylate synthase inhibitors because they do not over-produce the enzyme in response to drug treatment. Although we do not yet understand the moonlighting functions of IMPDH, the lessons of thymidylate synthase suggest that these functions could be a critical determinant of the clinical efficacy of IMPDH inhibitors. In the case of adRP, such IMPDH-targeted drugs could well ameliorate or exacerbate disease.

## 9. Conclusions

IMPDH combines a fascinating catalytic mechanism with profound biological significance. While enzymes such as chymotrypsin may be adequately described (at least to a first approximation) as rigid transition state templates, IMPDH undergoes an array of conformational changes in the course of a complicated catalytic cycle that involves two different chemical transformations. Monovalent cations may act to promote these conformational changes. A novel strategy to activate water provides a clue to the evolutionary origins of this “enzyme of consequence” for virtually every organism. IMPDH controls the guanine nucleotide pool, which in turn controls proliferation and many other physiological processes, making IMPDH an important target for immunosuppressive, cancer and antiviral chemotherapy. Intense efforts to develop better inhibitors for these applications, as well as for antimicrobial chemotherapy, continue. Lastly, uncharacterized moonlighting functions await discovery.

## Supplementary Material

Refer to Web version on PubMed Central for supplementary material.

## Acknowledgments

Supported by NIH GM54403 (L.H.). Molecular graphics images were produced using the UCSF Chimera package from the Resource for Biocomputing, Visualization, and Informatics at the University of California, San Francisco (supported by NIH P41 RR-01081). The author thanks Marc Jacobs of Vertex Pharmaceuticals, Inc. for providing the coordinates of the merimepodib complex (Figure 14), Clemens Lakner for the alignment used in Figure 4, and Helen Josephine, Gregory Patton and Steven Karel for comments on the manuscript.

## References

1. Weber G. *Cancer Res* 1983;43:3466. [PubMed: 6305486]
2. Jackson R, Weber G, Morris HP. *Nature* 1975;256:331. [PubMed: 167289]
3. Cornuel JF, Moraillon A, Gueron M. *Biochimie* 2002;84:279. [PubMed: 12106905]
4. McLean JE, Hamaguchi N, Belenky P, Mortimer SE, Stanton M, Hedstrom L. *Biochem J* 2004;379:243. [PubMed: 14766016]
5. Mortimer SE, Hedstrom L. *Biochem J* 2005;390:41. [PubMed: 15882147]
6. Mortimer SE, Xu D, McGrew D, Hamaguchi N, Lim HC, Bowne SJ, Daiger SP, Hedstrom L. *J Biol Chem* 2008;283:36354. [PubMed: 18974094]
7. Bowne SJ, Sullivan LS, Blanton SH, Cepko CL, Blackshaw S, Birch DG, Hughbanks-Wheaton D, Heckenlively JR, Daiger SP. *Hum Mol Genet* 2002;11:559. [PubMed: 11875050]
8. Kennan A, Aherne A, Palfi A, Humphries M, McKee A, Stitt A, Simpson DA, Demtroder K, Orntoft T, Ayuso C, Kenna PF, Farrar GJ, Humphries P. *Hum Mol Genet* 2002;11:547. [PubMed: 11875049]
9. Bowne SJ, Sullivan LS, Mortimer SE, Hedstrom L, Zhu J, Spellicy CJ, Gire AI, Hughbanks-Wheaton D, Birch DG, Lewis RA, Heckenlively JR, Daiger SP. *Invest Ophthalmol Vis Sci* 2006;47:34. [PubMed: 16384941]
10. Hedstrom L. *Curr Med Chem* 1999;6:545. [PubMed: 10390600]
11. Saunders JO, Raybuck SA. *Ann Rep Med Chem* 2000;35:201.
12. Sintchak MD, Nimmesgern E. *Immunopharmacology* 2000;47:163. [PubMed: 10878288]
13. Ratcliffe AJ. *Curr Opin Drug Discov Devel* 2006;9:595.
14. Chen L, Pankiewicz KW. *Curr Opin Drug Discov Devel* 2007;10:403.
15. Olah E, Kokeny S, Papp J, Bozsik A, Keszei M. *Adv Enzyme Regul* 2006;46:176. [PubMed: 16857242]
16. Nair V, Shu Q. *Antivir Chem Chemother* 2007;18:245. [PubMed: 18046958]
17. Shu Q, Nair V. *Med Res Rev* 2008;28:219. [PubMed: 17480004]
18. Chen L, Petrelli R, Felczak K, Gao G, Bonnac L, Yu JS, Bennett EM, Pankiewicz KW. *Curr Med Chem* 2008;15:650. [PubMed: 18336280]
19. Hedstrom L, Gan L. *Curr Opin Chem Biol* 2006;10:520. [PubMed: 16919497]
20. Daiger SP, Sullivan LS, Bowne SJ, Kennan A, Humphries P, Birch DG, Heckenlively JR. *Adv Exp Med Biol* 2003;533:1. [PubMed: 15180241]
21. Hedstrom L. *Nucleos Nucleot Nucl* 2008;27:839.
22. Pankiewicz, KW.; Goldstein, BM., editors. Inosine monophosphate dehydrogenase: a major therapeutic target. Oxford University Press; Washington DC: 2003.
23. Morrison HG, McArthur AG, Gillin FD, Aley SB, Adam RD, Olsen GJ, Best AA, Cande WZ, Chen F, Cipriano MJ, Davids BJ, Dawson SC, Elmendorf HG, Hehl AB, Holder ME, Huse SM, Kim UU, Lasek-Nesselquist E, Manning G, Nigam A, Nixon JE, Palm D, Passamanek NE, Prabhu A, Reich CI, Reiner DS, Samuelson J, Svard SG, Sogin ML. *Science* 2007;317:1921. [PubMed: 17901334]
24. Carlton JM, Hirt RP, Silva JC, Delcher AL, Schatz M, Zhao Q, Wortman JR, Bidwell SL, Alsmark UC, Besteiro S, Sicheritz-Ponten T, Noel CJ, Dacks JB, Foster PG, Simillion C, Van de Peer Y, Miranda-Saavedra D, Barton GJ, Westrop GD, Muller S, Dessi D, Fiori PL, Ren Q, Paulsen I, Zhang H, Bastida-Corcuera FD, Simoes-Barbosa A, Brown MT, Hayes RD, Mukherjee M, Okumura CY, Schneider R, Smith AJ, Vanacova S, Villalvazo M, Haas BJ, Pertea M, Feldblyum TV, Utterback TR, Shu CL, Osoegawa K, de Jong PJ, Hrdy I, Horvathova L, Zubacova Z, Dolezal P, Malik SB, Logsdon JM Jr, Henze K, Gupta A, Wang CC, Dunne RL, Upcroft JA, Upcroft P, White O, Salzberg SL, Tang P, Chiu CH, Lee YS, Embley TM, Coombs GH, Mottram JC, Tachezy J, Fraser-Liggett CM, Johnson PJ. *Science* 2007;315:207. [PubMed: 17218520]
25. Liu Y, Bohn SA, Sherley JL. *Mol Biol Cell* 1998;9:15. [PubMed: 9436988]
26. Allison AC, Eugui EM. *Immunopharmacology* 2000;47:85. [PubMed: 10878285]
27. Chong CR, Qian DZ, Pan F, Wei Y, Pili R, Sullivan DJ Jr, Liu JO. *J Med Chem* 2006;49:2677. [PubMed: 16640327]
28. Long H, Cameron S, Yu L, Rao Y. *Genetics* 2006;172:1633. [PubMed: 16322525]

29. Allison AC, Kowalski WJ, Muller CD, Eugui EM. Ann NY Acad Sci 1993;696:63. [PubMed: 7906496]
30. Natsumeda Y, Ohno S, Kawasaki H, Konno Y, Weber G, Suzuki K. J Biol Chem 1990;265:5292. [PubMed: 1969416]
31. Jain J, Almquist SJ, Ford PJ, Shlyakhter D, Wang Y, Nimmessern E, Germann UA. Biochem Pharmacol 2004;67:767. [PubMed: 14757177]
32. Senda M, Natsumeda Y. Life Sci 1994;54:1917. [PubMed: 7910933]
33. Bowne SJ, Liu Q, Sullivan LS, Zhu J, Spellicy CJ, Rickman CB, Pierce EA, Daiger SP. Invest Ophthalmol Vis Sci 2006;47:3754. [PubMed: 16936083]
34. Aherne A, Kennan A, Kenna PF, McNally N, Lloyd DG, Alberts IL, Kiang AS, Humphries MM, Ayuso C, Engel PC, Gu JJ, Mitchell BS, Farrar GJ, Humphries P. Hum Mol Genet 2004;13:641. [PubMed: 14981049]
35. Gu JJ, Tolin AK, Jain J, Huang H, Santiago L, Mitchell BS. Mol Cell Biol 2003;23:6702. [PubMed: 12944494]
36. Glesne DA, Collart FR, Huberman E. Mol Cell Biol 1991;11:5417. [PubMed: 1717828]
37. Dayton JS, Lindsten T, Thompson CB, Mitchell BS. J Immunol 1994;152:984. [PubMed: 7905505]
38. Xu D, Cobb GC, Spellicy CJ, Bowne SJ, Daiger SP, Hedstrom L. Arch Biochem Biophys 2008;472:100. [PubMed: 18295591]
39. Wang J, Yang JW, Zeevi A, Webber SA, Girnita DM, Selby R, Fu J, Shah T, Pravica V, Hutchinson IV, Burkart GJ. Clin Pharmacol Ther 2008;83:711. [PubMed: 17851563]
40. Wang J, Zeevi A, Webber S, Girnita DM, Addonizio L, Selby R, Hutchinson IV, Burkart GJ. Pharmacogenet Genomics 2007;17:283. [PubMed: 17496727]
41. Ji Y, Gu J, Makhov AM, Griffith JD, Mitchell BS. J Biol Chem 2006;281:206. [PubMed: 16243838]
42. Gunter JH, Thomas EC, Lengefeld N, Kruger SJ, Worton L, Gardiner EM, Jones A, Barnett NL, Whitehead JP. Int J Biochem Cell Biol 2008;40:1716. [PubMed: 18295529]
43. Whitehead JP, Simpson F, Hill MM, Thomas EC, Connolly LM, Collart F, Simpson RJ, James DE. Traffic 2004;5:739. [PubMed: 15355510]
44. Ingle E, Hemmings BA. FEBS Lett 2000;478:253. [PubMed: 10930578]
45. Zhang R, E G, Rotella F, Westbrook E, Huberman E, Joachimiak A, Collart FR. Curr Med Chem 1999;6:537. [PubMed: 10390599]
46. Ivanovics G, Marjai E, Dobozy A. J Gen Microbiol 1968;53:147. [PubMed: 4976582]
47. McFarland WC, Stocker BA. Microb Pathog 1987;3:129. [PubMed: 2849016]
48. Noreiga FR, Losonsky G, Lauderbaugh C, Liao FM, Wang JY, Levine MM. Infect Immun 1996;64:3055. [PubMed: 8757833]
49. Straley SC, Harmon PA. Infect Immun 1984;45:649. [PubMed: 6469351]
50. Hedstrom L, Cheung K, Wang CC. Biochem Pharm 1990;39:151. [PubMed: 1967525]
51. Kohler GA, White TC, Agabian N. J Bact 1997;179:2331. [PubMed: 9079920]
52. Striepen B, Pruijssers AJ, Huang J, Li C, Gubbels MJ, Umejiego NN, Hedstrom L, Kissinger JC. Proc Natl Acad Sci USA 2004;101:3154. [PubMed: 14973196]
53. Wilson K, Collart F, Huberman E, Stringer J, Ullman B. J Biol Chem 1991;266:1665. [PubMed: 1671039]
54. Wilson K, Berens RL, Sifri CD, Ullman B. J Biol Chem 1994;269:28979. [PubMed: 7961861]
55. Abraham EP. Biochem J 1945;39:398. [PubMed: 16747929]
56. Hupe D, Azzolina B, Behrens N. J Biol Chem 1986;261:8363. [PubMed: 2873141]
57. Webster HK, Whaun JM. J Clin Invest 1982;70:461. [PubMed: 7047569]
58. Umejiego NN, Gollapalli D, Sharling L, Voltsun A, Lu J, Benjamin NN, Stroupe AH, Riera TV, Striepen B, Hedstrom L. Chem Biol 2008;15:70. [PubMed: 18215774]
59. Lightfoot T, Snyder FF. Biochim Biophys Acta 1994;1217:156. [PubMed: 7906545]
60. Farazi T, Leichman J, Harris T, Cahoon M, Hedstrom L. J Biol Chem 1997;272:961. [PubMed: 8995388]
61. Magasanik B, Moyed HS, Gehring LB. J Biol Chem 1957;226:339. [PubMed: 13428767]

62. Anderson J, Sartorelli A. *J Biol Chem* 1968;243:4762. [PubMed: 4301223]
63. Holmes E, Pehlke D, Kelley W. *Biochim Biophys Acta* 1974;364:209. [PubMed: 4371273]
64. Jackson R, Morris H, Weber G. *Biochem J* 1977;166:1. [PubMed: 197916]
65. Miller R, Adamczyk D. *Biochem Pharm* 1976;25:883. [PubMed: 944580]
66. Pugh ME, Skibo EB. *Comp Biochem Physiol B* 1993;105:381. [PubMed: 8102965]
67. Wu T, Scrimgeour K. *Can J Biochem* 1973;51:1380. [PubMed: 4356246]
68. Krishnaiah K. *Arch Biochem Biophys* 1975;170:567. [PubMed: 1103737]
69. Gilbert H, Lowe C, Drabble W. *Biochem J* 1979;183:481. [PubMed: 44191]
70. Verham R, Meek TD, Hedstrom L, Wang CC. *Mol Biochem Parasit* 1987;24:1.
71. Turner JF, King JE. *Biochem J* 1961;79:147. [PubMed: 13778733]
72. Atkins C, Shelp B, Storer P. *Arch Biochem Biophys* 1985;236:807. [PubMed: 2857550]
73. Huete-Perez JA, Wu JC, Witby FG, Wang CC. *Biochemistry* 1995;34:13889. [PubMed: 7577983]
74. Digits JA, Hedstrom L. *Biochemistry* 1999;38:2295. [PubMed: 10029522]
75. Umejiego NN, Li C, Riera T, Hedstrom L, Striepen B. *J Biol Chem* 2004;279:40320. [PubMed: 15269207]
76. Sintchak MD, Fleming MA, Futer O, Raybuck SA, Chambers SP, Caron PR, Murcko M, Wilson KP. *Cell* 1996;85:921. [PubMed: 8681386]
77. Wang W, Hedstrom L. *Biochemistry* 1997;36:8479. [PubMed: 9214292]
78. Markham GD, Bock CL, Schalk-Hihi C. *Biochemistry* 1999;38:4433. [PubMed: 10194364]
79. Carr SF, Papp E, Wu JC, Natsumeda Y. *J Biol Chem* 1993;268:27286. [PubMed: 7903306]
80. Hager PW, Collart FR, Huberman E, Mitchell BS. *Biochem Pharm* 1995;49:1323. [PubMed: 7763314]
81. Kerr, K., Brandeis University, 1998.
82. Zhang RG, Evans G, Rotella FJ, Westbrook EM, Beno D, Huberman E, Joachimiak A, Collart FR. *Biochemistry* 1999;38:4691. [PubMed: 10200156]
83. O'Gara MJ, Lee CH, Weinberg GA, Nott JM, Queener SF. *Antimicrob Agents Chemother* 1997;41:40. [PubMed: 8980752]
84. Zhou X, Cahoon M, Rosa P, Hedstrom L. *J Biol Chem* 1997;272:21977. [PubMed: 9268334]
85. Dobie F, Berg A, Boitz JM, Jardim A. *Mol Biochem Parasitol* 2007;152:11. [PubMed: 17173987]
86. Sullivan WJ Jr, Dixon SE, Li C, Striepen B, Queener SF. *Antimicrob Agents Chemother* 2005;49:2172. [PubMed: 15917510]
87. Hariharan J, Rane R, Ayyanathan K, Philomena, Kumar VP, Prahlad D, Datta S. *J Biomol Screen* 1999;4:187. [PubMed: 10838438]
88. Heyde E, Morrison J. *Biochim Biophys Acta* 1976;429:635. [PubMed: 1268228]
89. Whitby FG, Luecke H, Kuhn P, Somoza JR, Huete-Perez JA, Philips JD, Hill CP, Fletterick RJ, Wang CC. *Biochemistry* 1997;36:10666. [PubMed: 9271497]
90. Ikegami T, Natsumeda Y, Weber G. *Life Sciences* 1987;40:2277. [PubMed: 2884545]
91. Wang W, Papov VV, Minakawa N, Matsuda A, Biemann K, Hedstrom L. *Biochemistry* 1996;35:95. [PubMed: 8555204]
92. Gilbert H, Drabble W. *Biochem J* 1980;191:533. [PubMed: 6112982]
93. Bruzzese FJ, Connelly PR. *Biochemistry* 1997;36:10428. [PubMed: 9265623]
94. Nimmessern E, Black J, Futer O, Fulghum JR, Chambers SP, Brummel CL, Raybuck SA, Sintchak MD. *Protein Express Purif* 1999;17:282.
95. Gan L, Petsko GA, Hedstrom L. *Biochemistry* 2002;41:13309. [PubMed: 12403633]
96. Colby TD, Vanderveen K, Strickler MD, Markham GD, Goldstein BM. *Proc Natl Acad Sci, USA* 1999;96:3531. [PubMed: 10097070]
97. McMillan FM, Cahoon M, White A, Hedstrom L, Petsko GA, Ringe D. *Biochemistry* 2000;39:4533. [PubMed: 10758003]
98. Kohler GA, Gong X, Bentink S, Theiss S, Pagani GM, Agabian N, Hedstrom L. *J Biol Chem* 2005;280:11295. [PubMed: 15665003]
99. Bateman A. *Trends Biochem Sci* 1997;22:12. [PubMed: 9020585]

100. Kemp BE. *J Clin Invest* 2004;113:182. [PubMed: 14722609]
101. Janosik M, Kery V, Gaustadnes M, Maclean KN, Kraus JP. *Biochemistry* 2001;40:10625. [PubMed: 11524006]
102. Scott JW, Hawley SA, Green KA, Anis M, Stewart G, Scullion GA, Norman DG, Hardie DG. *J Clin Invest* 2004;113:274. [PubMed: 14722619]
103. Meyer S, Savaresi S, Forster IC, Dutzler R. *Nat Struct Mol Biol* 2007;14:60. [PubMed: 17195847]
104. Chen HJ, Chiu WL, Lin WP, Yang SS. *Chembiochem* 2008;9:1074. [PubMed: 18351683]
105. Jamsen J, Tuomunen H, Salminen A, Belogurov GA, Magretova NN, Baykov AA, Lahti R. *Biochem J* 2007;408:327. [PubMed: 17714078]
106. Bennetts B, Rychkov GY, Ng HL, Morton CJ, Stapleton D, Parker MW, Cromer BA. *J Biol Chem* 2005;280:32452. [PubMed: 16027167]
107. Pimkin M, Markham GD. *Mol Microbiol* 2008;69:342. [PubMed: 18312263]
108. Bateman, AG. The CBS domain web page. <http://www.sanger.ac.uk/Users/agb/CBS/CBS.html>
109. Pimkin M, Pimkina J, Markham GD. *J Biol Chem*. 2009
110. Hampton A, Brox L, Bayer M. *Biochemistry* 1969;8:2303. [PubMed: 4307993]
111. Bouhss A, Sakamoto H, Palibroda N, Chiriac M, Sarfati R, Smith JM, Craescu CT, Barzu O. *Anal Biochem* 1995;225
112. Kerr KM, Digits JA, Kuperwasser N, Hedstrom L. *Biochemistry* 2000;39:9804. [PubMed: 10933797]
113. Hampton A. *J Biol Chem* 1963;238:3068. [PubMed: 14081926]
114. Antonino LC, Wu JC. *Biochemistry* 1994;33:1753. [PubMed: 7906542]
115. Perez-Miller SJ, Hurley TD. *Biochemistry* 2003;42:7100. [PubMed: 12795606]
116. Fleming MA, Chambers SP, Connelly PR, Nimmessern E, Fox T, Bruzzese FJ, Hoe ST, Fulghum JR, Livingston DJ, Stuver CM, Sintchak MD, Wilson KP, Thomson JA. *Biochemistry* 1996;35:6990. [PubMed: 8679523]
117. Link JO, Straub K. *J Am Chem Soc* 1996;118:2091.
118. McPhillips CC, Hyle JW, Reines D. *Proc Natl Acad Sci USA* 2004;101:12171. [PubMed: 15292516]
119. Bryson, S. Ph D thesis. University of Toronto; Toronto: 2001. Structure determination of the apo-form of human inosine 5'-monophosphate dehydrogenase type II.
120. Prosise GL, Luecke H. *J Mol Biol* 2003;326:517. [PubMed: 12559919]
121. Prosise GL, Wu JZ, Luecke H. *J Biol Chem* 2002;277:50654. [PubMed: 12235158]
122. Gan L, Seyedsayamost MR, Shuto S, Matsuda A, Petsko GA, Hedstrom L. *Biochemistry* 2003;42:857. [PubMed: 12549902]
123. Heyde E, Morrison J. *Biochim Biophys Acta* 1976;429:661. [PubMed: 5138]
124. Heyde E, Nagabhushanam A, Vonarx M, Morrison J. *Biochim Biophys Acta* 1976;429:645. [PubMed: 178371]
125. Xiang B, Markham GD. *Arch Biochem Biophys* 1997;348:378. [PubMed: 9434751]
126. Riera TV, Wang W, Josephine HR, Hedstrom L. *Biochemistry* 2008;47:8689. [PubMed: 18642884]
127. Guillén Schlippe YV, Riera TV, Seyedsayamost MR, Hedstrom L. *Biochemistry* 2004;43:4511. [PubMed: 15078097]
128. Nimmessern E, Fox T, Fleming MA, Thomson JA. *J Biol Chem* 1996;271:19421. [PubMed: 8702630]
129. Hedstrom L, Wang CC. *Biochemistry* 1990;849. [PubMed: 1971185]
130. Xiang B, Markham GD. *J Biol Chem* 1996;271:27531. [PubMed: 8910338]
131. You K. *CRC Crit Rev Biochem* 1985;17:313. [PubMed: 3157549]
132. Cooney D, Hamel E, Cohen M, Kang GJ, Dalal M, Marquez V. *Biochim Biophys Acta* 1987;916:89. [PubMed: 2889473]
133. Guillén Schlippe YV, Hedstrom L. *Biochemistry* 2005;44:11700. [PubMed: 16128570]
134. Salsbury FR Jr, Knutson ST, Poole LB, Fetrow JS. *Protein Sci* 2008;17:299. [PubMed: 18227433]
135. Kerr KM, Hedstrom L. *Biochemistry* 1997;36:13365. [PubMed: 9341229]
136. Guillén Schlippe YV, Hedstrom L. *Biochemistry* 2005;44:16695. [PubMed: 16342959]

137. Min D, Josephine HR, Li H, Lakner C, MacPherson IS, Naylor GJ, Swofford D, Hedstrom L, Yang W. PLoS Biol 2008;6:e206. [PubMed: 18752347]
138. Guillén Schlippe YV, Hedstrom L. Arch Biochem Biophys 2005;433:266. [PubMed: 15581582]
139. Huang LS, Sun G, Cobessi D, Wang AC, Shen JT, Tung EY, Anderson VE, Berry EA. J Biol Chem 2006;281:5965. [PubMed: 16371358]
140. You YO, van der Donk WA. Biochemistry 2007;46:5991. [PubMed: 17455908]
141. McEvoy JP, Brudvig GW. Phys Chem Chem Phys 2004;6:4754.
142. Onishi H, Mochizuki N, Morales MF. Biochemistry 2004;43:3757. [PubMed: 15049682]
143. Xiang B, Taylor JC, Markham GD. J Biol Chem 1996;271:1435. [PubMed: 8576135]
144. Riera, TV. Ph D thesis. Brandeis University; Waltham MA: 2008. Thermodynamic and kinetic consequences of conformational changes in IMP dehydrogenase catalysis: characterization of flap mutants and potassium activation.
145. Varma S, Rempe SB. Biophys Chem 2006;124:192. [PubMed: 16875774]
146. Varma S, Rempe SB. Sandia Technical Report. 2006SAND2006-6207J
147. Kerr KM, Cahoon MC, Bosco DA, Hedstrom L. Arch Biochem Biophys 2000;375:131. [PubMed: 10683258]
148. Eppler RK, Komor RS, Huynh J, Dordick JS, Reimer JA, Clark DS. Proc Natl Acad Sci USA 2006;103:5706. [PubMed: 16585507]
149. Bentley R. Chem Rev 2000;100:3801. [PubMed: 11749328]
150. Franklin TJ, Jacobs V, Jones G, Ple P, Bruneau P. Cancer Res 1996;56:984. [PubMed: 8640790]
151. Papageorgiou C. Mini-Rev Med Chem 2001;1:71. [PubMed: 12369992]
152. Bacus SS, Kiguchi K, Chin D, King CR, Huberman E. Mol Carcinog 1990;3:350. [PubMed: 1980588]
153. Floryk D, Huberman E. Cancer Lett 2006;231:20. [PubMed: 16356827]
154. Floryk D, Tollaksen SL, Giometti CS, Huberman E. Cancer Res 2004;64:9049. [PubMed: 15604271]
155. Kiguchi K, Collart FR, Henning-Chubb C, Huberman E. Cell Growth Differ 1990;1:259. [PubMed: 1980599]
156. Kiguchi K, Collart FR, Henning-Chubb C, Huberman E. Exp Cell Res 1990;187:47. [PubMed: 1967583]
157. Collart FR, Huberman E. Blood 1990;75:570. [PubMed: 1967537]
158. Messina E, Gazzaniga P, Micheli V, Barile L, Lupi F, Agliano AM, Giacomello A. Int J Cancer 2004;112:352. [PubMed: 15352052]
159. Messina E, Micheli V, Giacomello A. Neurosci Lett 2005;375:97. [PubMed: 15670649]
160. Makara GM, Kesseru GM, Kajtar-Peredy M, Anderson WK. J Med Chem 1996;39:1236. [PubMed: 8632430]
161. Anderson WK, Boehm TL, Makara GM, Swann RT. J Med Chem 1996;39:46. [PubMed: 8568826]
162. Nelson P, Eugui E, Wang C, Allison A. J Med Chem 1990;33:833. [PubMed: 1967654]
163. Nelson PH, Carr SF, Devens BH, Eugui EM, Franco F, Gonzalez C, Hawley RC, Loughhead DG, Milan DJ, Papp E, Patterson JW, Rouhafza S, Sjogren EB, Smith DB, Stephenson RA, Talamas FX, Waltos AM, Weikert RJ, Wu JC. J Med Chem 1996;39:4181. [PubMed: 8863796]
164. Beisler J, Hillery S. J Pharm Sci 1975;64:84. [PubMed: 1133712]
165. Jones D, Mills S. J Med Chem 1971;14:305. [PubMed: 5553742]
166. Franklin TJ, Jacobs VN, Jones G, Ple P. Drug Met Disp 1997;25:367.
167. Lesiak K, Watanabe KA, Majumdar A, Powell J, Seidman M, Vanderveen K, Goldstein BM, Pankiewicz KW. J Med Chem 1998;41:618. [PubMed: 9484510]
168. Rejman D, Olesiak M, Chen L, Patterson SE, Wilson D, Jayaram HN, Hedstrom L, Pankiewicz KW. J Med Chem 2006;49:5018. [PubMed: 16884314]
169. Chen L, Petrelli R, Olesiak M, Wilson DJ, Labello NP, Pankiewicz KW. Bioorg Med Chem 2008;16:7462. [PubMed: 18583139]
170. Mei S, Ho AD, Mahlknecht U. Int J Oncol 2004;25:1509. [PubMed: 15547685]
171. Chen L, Wilson D, Jayaram HN, Pankiewicz KW. J Med Chem 2007;50:6685. [PubMed: 18038969]

172. Iwanowicz EJ, Watterson SH, Guo J, Pitts WJ, Murali Dhar TG, Shen Z, Chen P, Gu HH, Fleener CA, Rouleau KA, Cheney DL, Townsend RM, Hollenbaugh DL. *Bioorg Med Chem Lett* 2003;13:2059. [PubMed: 12781195]
173. Jain J, Almquist SJ, Shlyakhter D, Harding MW. *J Pharm Sci* 2001;90:625. [PubMed: 11288107]
174. Markland W, McQuaid TJ, Jain J, Kwong AD. *Antimicrob Agents Chemother* 2000;44:859. [PubMed: 10722482]
175. Ishitsuka K, Hidemitsu T, Hamasaki M, Raje N, Kumar S, Podar K, Le Gouill S, Shiraishi N, Yasui H, Roccaro AM, Tai YZ, Chauhan D, Fram R, Tamura K, Jain J, Anderson KC. *Oncogene* 2005;24:5888. [PubMed: 15940263]
176. Floryk D, Thompson TC. *Int J Cancer* 2008;123:2294. [PubMed: 18712736]
177. Jain J, Almquist SJ, Heiser AD, Shlyakhter D, Leon E, Memmott C, Moody CS, Nimmesgern E, Decker C. *J Pharmacol Exp Ther* 2002;302:1272. [PubMed: 12183689]
178. Dhar TG, Liu C, Pitts WJ, Guo J, Watterson SH, Gu H, Fleener CA, Rouleau K, Sherbina NZ, Barrish JC, Hollenbaugh D, Iwanowicz EJ. *Bioorg Med Chem Lett* 2002;12:3125. [PubMed: 12372516]
179. Buckley GM, Davies N, Dyke HJ, Gilbert PJ, Hannah DR, Haughan AF, Hunt CA, Pitt WR, Profit RH, Ray NC, Richard MD, Sharpe A, Taylor AJ, Whitworth JM, Williams SC. *Bioorg Med Chem Lett* 2005;15:751. [PubMed: 15664851]
180. Dhar TG, Shen Z, Guo J, Liu C, Watterson SH, Gu HH, Pitts WJ, Fleener CA, Rouleau KA, Sherbina NZ, McIntyre KW, Shuster DJ, Witmer MR, Tredup JA, Chen BC, Zhao R, Bednarz MS, Cheney DL, MacMaster JF, Miller LM, Berry KK, Harper TW, Barrish JC, Hollenbaugh DL, Iwanowicz EJ. *J Med Chem* 2002;45:2127. [PubMed: 12014950]
181. Iwanowicz EJ, Watterson SH, Liu C, Gu HH, Mitt T, Leftheris K, Barrish JC, Fleener CA, Rouleau K, Sherbina NZ, Hollenbaugh DL. *Bioorg Med Chem Lett* 2002;12:2931. [PubMed: 12270177]
182. Watterson SH, Dhar TG, Ballentine SK, Shen Z, Barrish JC, Cheney D, Fleener CA, Rouleau KA, Townsend R, Hollenbaugh DL, Iwanowicz EJ. *Bioorg Med Chem Lett* 2003;13:1273. [PubMed: 12657262]
183. Pitts WJ, Guo J, Dhar TG, Shen Z, Gu HH, Watterson SH, Bednarz MS, Chen BC, Barrish JC, Bassolino D, Cheney D, Fleener CA, Rouleau KA, Hollenbaugh DL, Iwanowicz EJ. *Bioorg Med Chem Lett* 2002;12:2137. [PubMed: 12127522]
184. Gu HH, Iwanowicz EJ, Guo J, Watterson SH, Shen Z, Pitts WJ, Dhar TG, Fleener CA, Rouleau K, Sherbina NZ, Witmer M, Tredup J, Hollenbaugh D. *Bioorg Med Chem Lett* 2002;12:1323. [PubMed: 11965381]
185. Watterson SH, Liu C, Dhar TG, Gu HH, Pitts WJ, Barrish JC, Fleener CA, Rouleau K, Sherbina NZ, Hollenbaugh DL, Iwanowicz EJ. *Bioorg Med Chem Lett* 2002;12:2879. [PubMed: 12270168]
186. Watterson SH, Carlsen M, Dhar TG, Shen Z, Pitts WJ, Guo J, Gu HH, Norris D, Chorba J, Chen P, Cheney D, Witmer M, Fleener CA, Rouleau K, Townsend R, Hollenbaugh DL, Iwanowicz EJ. *Bioorg Med Chem Lett* 2003;13:543. [PubMed: 12565968]
187. Dhar TG, Watterson SH, Chen P, Shen Z, Gu HH, Norris D, Carlsen M, Haslow KD, Pitts WJ, Guo J, Chorba J, Fleener CA, Rouleau KA, Townsend R, Hollenbaugh D, Iwanowicz EJ. *Bioorg Med Chem Lett* 2003;13:547. [PubMed: 12565969]
188. Birch HL, Buckley GM, Davies N, Dyke HJ, Frost EJ, Gilbert PJ, Hannah DR, Haughan AF, Madigan MJ, Morgan T, Pitt WR, Ratcliffe AJ, Ray NC, Richard MD, Sharpe A, Taylor AJ, Whitworth JM, Williams SC. *Bioorg Med Chem Lett* 2005;15:5335. [PubMed: 16202581]
189. Dhar TG, Shen Z, Fleener CA, Rouleau KA, Barrish JC, Hollenbaugh DL, Iwanowicz EJ. *Bioorg Med Chem Lett* 2002;12:3305. [PubMed: 12392738]
190. Dhar TG, Shen Z, Gu HH, Chen P, Norris D, Watterson SH, Ballantine SK, Fleener CA, Rouleau KA, Barrish JC, Townsend R, Hollenbaugh DL, Iwanowicz EJ. *Bioorg Med Chem Lett* 2003;13:3557. [PubMed: 14505670]
191. Beavers RE, Buckley GM, Davies N, Fraser JL, Galvin FC, Hannah DR, Haughan AF, Jenkins K, Mack SR, Pitt WR, Ratcliffe AJ, Richard MD, Sabin V, Sharpe A, Williams SC. *Bioorg Med Chem Lett* 2006;16:2539. [PubMed: 16483773]
192. Franklin TJ, Morris WP, Jacobs VN, Culbert EJ, Heys CA, Ward WH, Cook PN, Jung F, Ple P. *Biochem Pharmacol* 1999;58:867. [PubMed: 10449198]

193. Watterson SH, Chen P, Zhao Y, Gu HH, Dhar TG, Xiao Z, Ballentine SK, Shen Z, Fleener CA, Rouleau KA, Obermeier M, Yang Z, McIntyre KW, Shuster DJ, Witmer M, Dambach D, Chao S, Mathur A, Chen BC, Barrish JC, Robl JA, Townsend R, Iwanowicz EJ. *J Med Chem* 2007;50:3730. [PubMed: 17585753]
194. Chen P, Norris D, Haslow KD, Murali Dhar TG, Pitts WJ, Watterson SH, Cheney DL, Bassolino DA, Fleener CA, Rouleau KA, Hollenbaugh DL, Townsend RM, Barrish JC, Iwanowicz EJ. *Bioorg Med Chem Lett* 2003;13:1345. [PubMed: 12657279]
195. Barnes BJ, Eakin AE, Izzydore RA, Hall IH. *Biochemistry* 2000;39:13641. [PubMed: 11076502]
196. Hall IH, Barnes BJ, Ward ES, Wheaton JR, Warren AE, Izzydore RA. *Arch Pharm (Weinheim)* 2001;334:109. [PubMed: 11382145]
197. Izzydore RA, Chapman JJ, Mitchell JA, Cummings R, Jones GT, McIver CD. *J Chem Soc Perkin Trans II* 1988:1415.
198. Barnes BJ, Eakin AE, Izzydore RA, Hall IH. *Biochem Pharmacol* 2001;62:91. [PubMed: 11377400]
199. Page JD, Chaney SG, Hall IH, Lee KH, Holbrook DJ. *Biochim Biophys Acta* 1987;926:186. [PubMed: 2889474]
200. Jaspars M, Rali T, Laney M, Schatzman RC, Diaz MC, Schmitz FJ, Pordesimo EO, Crews P. *Tetrahedron* 1994;50:7367.
201. Abas SA, Hossain B, van der Helm D, Schmitz FJ. *J Org Chem* 1996;61:2709. [PubMed: 11667102]
202. Jaspars M, Pasupathy V, Crews P. *J Org Chem* 1994;59:3253.
203. Arai M, Sobou M, Vilchez C, Baughn A, Hashizume H, Prusakorn P, Ishida S, Matsumoto M, Jacobs WR Jr, Kobayashi M. *Bioorg Med Chem* 2008;16:6732. [PubMed: 18556206]
204. Moosavi MA, Yazdanparast R, Sanati MH, Nejad AS. *Int J Biochem Cell Biol* 2005;37:2366. [PubMed: 16084123]
205. Hall IH, Liou YF, Oswald CB, Lee KH. *Eur J Cancer Clin Oncol* 1986;22:45. [PubMed: 3754212]
206. Lin J, Ke A, Zhang X, Zheng Z, Zhu J, Lu X, Li Y, Cui X, Shi Y, Zhang H, He J. *Chinese J Antibiotics* 2008;33:463.
207. Fu X, Abbas SA, Schmitz FJ, Vidasky I, Gross ML, Laney M, Schatzman RC, Cabuslay RD. *Tetrahedron* 1997;53:799.
208. Mizushina Y, Dairaku I, Yanaka N, Takeuchi T, Ishimaru C, Sugawara F, Yoshida H, Kato N. *Biochimie* 2007;89:581. [PubMed: 17383068]
209. Striepen B, White MW, Li C, Guerini MN, Malik SB, Logsdon JM Jr, Liu C, Abrahamsen MS. *Proc Natl Acad Sci USA* 2002;99:6304. [PubMed: 11959921]
210. Skibo E, Meyer R. *J Med Chem* 1981;24:1155. [PubMed: 6120232]
211. Wong C, Meyer R. *J Med Chem* 1984;27:429. [PubMed: 6142953]
212. Moore EC, Hurlbert RB, Boss GR, Massia SP. *Biochem Pharmacol* 1989;38:4045. [PubMed: 2480792]
213. Yang L, Dan HC, Sun M, Liu Q, Sun XM, Feldman RI, Hamilton AD, Polokoff M, Nicosia SV, Herlyn M, Sefti SM, Cheng JQ. *Cancer Res* 2004;64:4394. [PubMed: 15231645]
214. Traut TW. *Mol Cell Biochem* 1994;140:1. [PubMed: 7877593]
215. Shimada N, Yagisawa N, Naganawa H, Takita T, Hamada M, Takeuchi T, Umezawa H. *J Antibiot* 1981;34:1216. [PubMed: 7328060]
216. Uehara Y, Hasegawa M, Hori M, Umezawa H. *Cancer Res* 1985;45:5230. [PubMed: 2413989]
217. Suzuki T, Yamaoka R, Nishi M, Ide H, Makino K. *J Am Chem Soc* 1996;118:2515.
218. Streeter D, Koyama H. *Biochem Pharm* 1976;25:2413. [PubMed: 1033766]
219. Smith C, Fontenelle L, Muzik H, Paterson A, Unger H, Brox L, Henderson J. *Biochem Pharm* 1974;23:2727. [PubMed: 4472552]
220. Franchetti P, Grifantini M. *Curr Med Chem* 1999;6:599. [PubMed: 10390603]
221. Ishikawa H. *Curr Med Chem* 1999;6:575. [PubMed: 10390602]
222. Witkowski JT, Robins RK, Sidwell RW, Bauer RJ. *J Med Chem* 1972;15:1150. [PubMed: 4347550]
223. Gish RG. *J Antimicrob Chemother* 2006;57:8. [PubMed: 16293677]
224. Leyssen P, Balzarini J, De Clercq E, Neyts J. *J Virol* 2005;79:1943. [PubMed: 15650220]

225. Smith, RA.; Kirkpatrick, W. *Developments in Antiviral Therapy*. Collier, LH.; Oxford, T., editors. Academic Press; London: 1980.
226. Eriksson B, Helgstrand E, Johansson NG, Larsson A, Misiorny A, Noren JO, Philipson L, Stenberg K, Stening G, Stridh S, Oberg B. *Antimicrob Agents Chemother* 1977;11:946. [PubMed: 879760]
227. Crotty S, Cameron CE, Andino R. *Proc Natl Acad Sci USA* 2001;98:6895. [PubMed: 11371613]
228. Hultgren C, Milich DR, Weiland O, Sallberg M. *J Gen Virol* 1998;79(Pt 10):2381. [PubMed: 9780043]
229. Parker WB. *Virus Res* 2005;107:165. [PubMed: 15649562]
230. Graci JD, Cameron CE. *Rev Med Virol* 2006;16:37. [PubMed: 16287208]
231. Pankiewicz KW, Patterson SE, Black PL, Jayaram HN, Risal D, Goldstein BM, Stuyver LJ, Schinazi RF. *Curr Med Chem* 2004;11:887. [PubMed: 15083807]
232. Cooney D, Jayaram H, Gebeyehu G, Betts C, Kelley J, Marquez V, Johns D. *Biochem Pharm* 1982;31:2133. [PubMed: 6126195]
233. Kuttan R, Robins R, Saunders P. *Biochem Biophys Res Commun* 1982;107:862. [PubMed: 6127996]
234. Goldstein B, Bell J, Marquez V. *J Med Chem* 1990;33:1123. [PubMed: 1969483]
235. Goldstein BM, Colby TD. *Current Med Chem* 1999;6:519.
236. Goldstein BM, Takusagawa F, Berman HM, Srivastava PC, Robins RK. *J Am Chem Soc* 1983;105:7416.
237. Li H, Hallows WH, Punzi JS, Marquez VE, Carrell HL, Pankiewicz KW, Watanabe KA, Goldstein BM. *Biochemistry* 1994;33:23. [PubMed: 8286346]
238. Goldstein BM, Li H, Hallows WH, Langs DA, Franchetti P, Cappellacci L, Grifantini M. *J Med Chem* 1994;37:1684. [PubMed: 8201602]
239. Saunders PP, Spindler CD, Tan MT, Alvarez E, Robins RK. *Cancer Res* 1990;50:5269. [PubMed: 2143686]
240. Fridland A, Connelly MC, Robbins TJ. *Cancer Res* 1986;46:532. [PubMed: 3000575]
241. Marquez V, Tseng CKH, Gebeyehu G, Cooney DA, Ahluwalia GS, Kelley JA, Dalal M, Fuller RW, Wilson YA, Johns DG. *J Med Chem* 1986;29:1726. [PubMed: 2875185]
242. Lesiak K, Watanabe KA, Majumdar A, Seidman M, Vanderveen K, Goldstein BM, Pankiewicz KW. *J Med Chem* 1997;40:2533. [PubMed: 9258359]
243. Chen L, Gao G, Bonnac L, Wilson DJ, Bennett EM, Jayaram HN, Pankiewicz KW. *Bioorg Med Chem Lett* 2007;17:3152. [PubMed: 17395461]
244. Gharehbaghi K, Grunberger W, Jayaram HN. *Curr Med Chem* 2002;9:743. [PubMed: 11966437]
245. Jayaram HN, Gharehbaghi K, Jayaram NH, Rieser J, Krohn K, Paull KD. *Biochem Biophys Res Commun* 1992;186:1600. [PubMed: 1354960]
246. Gharehbaghi K, Sreenath A, Hao Z, Paull KD, Szekeres T, Cooney DA, Krohn K, Jayaram HN. *Biochem Pharmacol* 1994;48:1413. [PubMed: 7945441]
247. Polgar D, Gfatter S, Uhl M, Kassie F, Leisser C, Krupitza G, Grusch M. *Curr Med Chem* 2002;9:765. [PubMed: 11966440]
248. Novotny L, Rauko P, Yalowitz JA, Szekeres T. *Curr Med Chem* 2002;9:773. [PubMed: 11966441]
249. Jayaram HN, Yalowitz JA, Arguello F, Greene JF Jr. *Curr Med Chem* 2002;9:787. [PubMed: 11966443]
250. Wang W, Hedstrom L. *Biochemistry* 1998;37:11949. [PubMed: 9718319]
251. Wolfenden R. *Ann Rev Biochem Bioengin* 1976;5:271.
252. Brox L, Hampton A. *Biochemistry* 1968;7:2589. [PubMed: 4298224]
253. Matsuda A, Minakawa N, Sasaki T, Ueda T. *Chem Pharm Bull* 1988;36:2730. [PubMed: 3272143]
254. Zhang HZ, Rao K, Carr SF, Papp E, Straub K, Wu J, Fried J. *J Med Chem* 1997;40:4. [PubMed: 9016322]
255. Pal S, Bera B, Nair V. *Bioorg Med Chem* 2002;10:3615. [PubMed: 12213477]
256. Nair V, Kamboj RC. *Bioorg Med Chem Lett* 2003;13:645. [PubMed: 12639549]
257. Brox LW, Hampton A. *Biochemistry* 1968;7:398. [PubMed: 4394751]

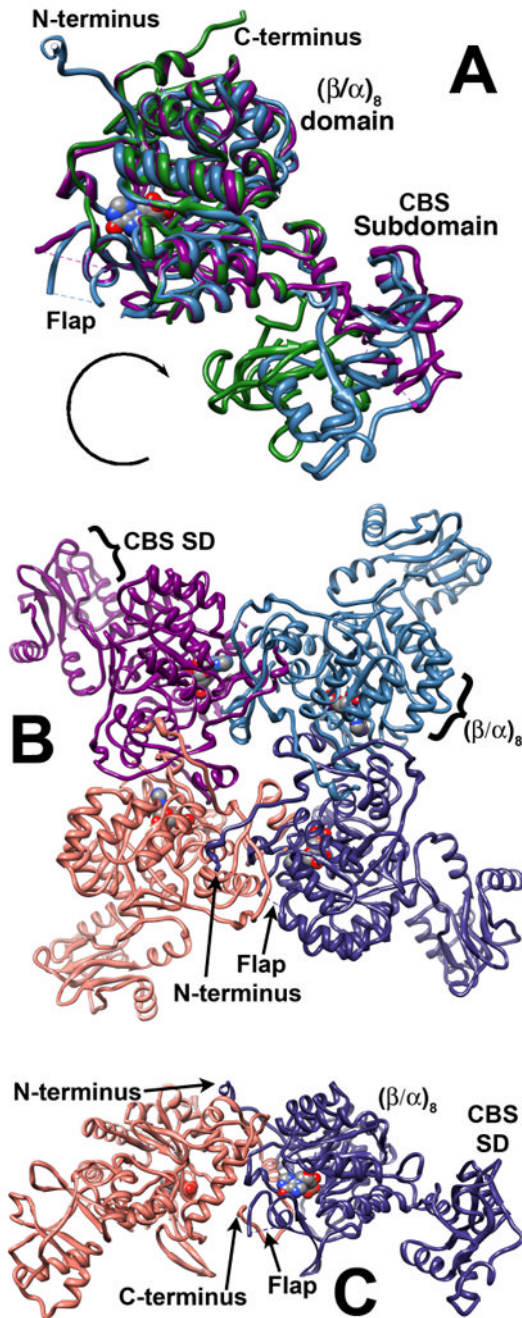
258. Antonino LC, Straub K, Wu JC. Biochemistry 1994;33:1760. [PubMed: 7906543]
259. Minakawa N, Matsuda A. Curr Med Chem 1999;6:615. [PubMed: 10390604]
260. Balzarini J, Stet L, Matsuda A, Wiebe L, Knauss E, De Clercq E. Adv Exp Med Biol 1998;431:723. [PubMed: 9598159]
261. Uetz P, Giot L, Cagney G, Mansfield TA, Judson RS, Knight JR, Lockshon D, Narayan V, Srinivasan M, Pochart P, Qureshi-Emili A, Li Y, Godwin B, Conover D, Kalbfleisch T, Vijayadamodar G, Yang M, Johnston M, Fields S, Rothberg JM. Nature 2000;403:623. [PubMed: 10688190]
262. Lindstrom DL, Squazzo SL, Muster N, Burckin TA, Wachter KC, Emigh CA, McCleery JA, Yates JR 3rd, Hartzog GA. Mol Cell Biol 2003;23:1368. [PubMed: 12556496]
263. Ho Y, Gruhler A, Hellbut A, Bader GD, Moore L, Adams SL, Millar A, Taylor P, Bennett K, Boutilier K, Yang L, Wolting C, Donaldson I, Scchandorff S, Shewnarane J, Vo M, Taggart J, Goudreault M, Muskat B, Alfarano C, Dewar D, Lin Z, Michalickova K, Willemans AR, Sasl H, Nielsen PA, Rasmussen KJ, Andersen JR, Johansen LE, Hansens LK, Jespersen H, Podtelejnikov A, Neilsen E, Crawford J, Poulsens V, Sorensen BD, Matthiesen J, Hendrickson RC, Gleeson F, Pawson T, Moran MF, Durocher D, Mann M, Hogue CWV, Figgeys D, Tyers M. Nature 2002;415:180. [PubMed: 11805837]
264. Krogan NJ, Peng WT, Cagney G, Robinson MD, Haw R, Zhong G, Guo X, Zhang X, Canadien V, Richards DP, Beattie BK, Lalev A, Zhang W, Davierwala AP, Mnaimneh S, Starostine A, Tikuisis AP, Grigull J, Datta N, Bray JE, Hughes TR, Emili A, Greenblatt JF. Mol Cell 2004;13:225. [PubMed: 14759368]
265. Stevens SW, Ryan DE, Ge HY, Moore RE, Young MK, Lee TD, Abelson J. Mol Cell 2002;9:31. [PubMed: 11804584]
266. Sherley JL. J Biol Chem 1991;266:24815. [PubMed: 1761576]
267. Wada Y, Sandberg MA, McGee TL, Stillberger MA, Berson EL, Dryja TP. Invest Ophthalmol Vis Sci 2005;46:1735. [PubMed: 15851576]
268. Grover S, Fishman GA, Stone EM. Ophthalmology 2004;111:1910. [PubMed: 15465556]
269. Spellicy CJ, Daiger SP, Sullivan LS, Zhu J, Liu Q, Pierce EA, Bowne SJ. Mol Vis 2007;13:1866. [PubMed: 17960124]
270. Chu E, Allegra CJ. Adv Enzyme Regul 1996;36:143. [PubMed: 8869745]
271. Zhang K, Rathod PK. Science 2002;296:545. [PubMed: 11964483]
272. Digits JA, Hedstrom L. Biochemistry 2000;39:1771. [PubMed: 10677226]
273. Kuzmic P. Anal Biochem 1996;237:260. [PubMed: 8660575]
274. Munoz V, Serrano L. J Mol Biol 1995;245:275. [PubMed: 7844817]
275. Pettersen EF, Goddard TD, Huang CC, Couch GS, Greenblatt DM, Meng EC, Ferrin TE. J Comp Chem 2004;25:1605. [PubMed: 15264254]

## Biography



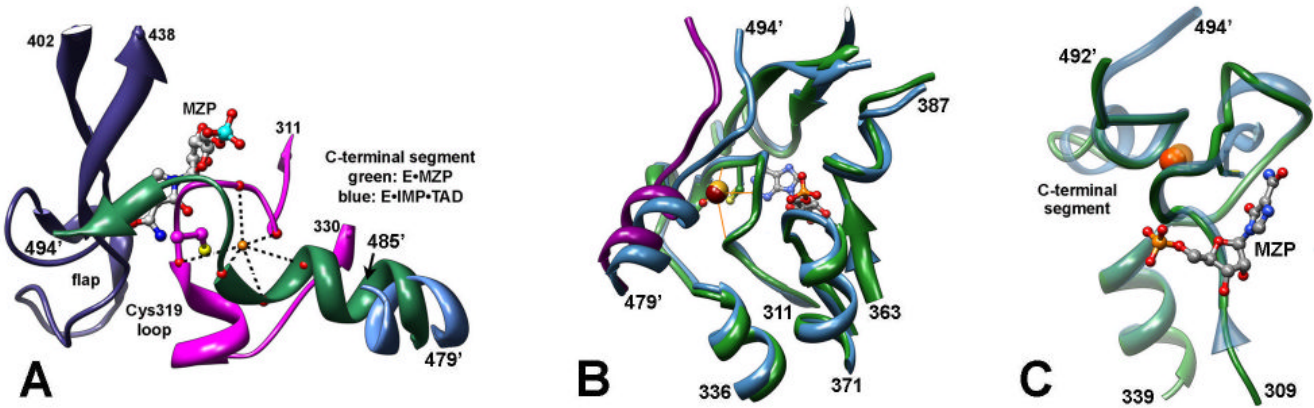
Lizbeth Hedstrom received a B.S. in Chemistry from University of Virginia in 1980. She earned a Ph.D. in Biochemistry from Brandeis University under the direction of Prof. Robert Abeles, where she developed mechanism-based inactivators of serine proteases. She completed her postdoctoral training at UCSF, first in the laboratory of Prof. C.C. Wang, where she investigated purine nucleotide biosynthesis in protozoan parasites, and later in the laboratory

of Prof. William Rutter, where she re-engineered the substrate specificity of trypsin to resemble that of chymotrypsin. She returned to Brandeis in 1992, where she is now the Markey Professor of Biology and Chemistry. Her laboratory investigates proteases and enzymes involved in nucleotide metabolism.

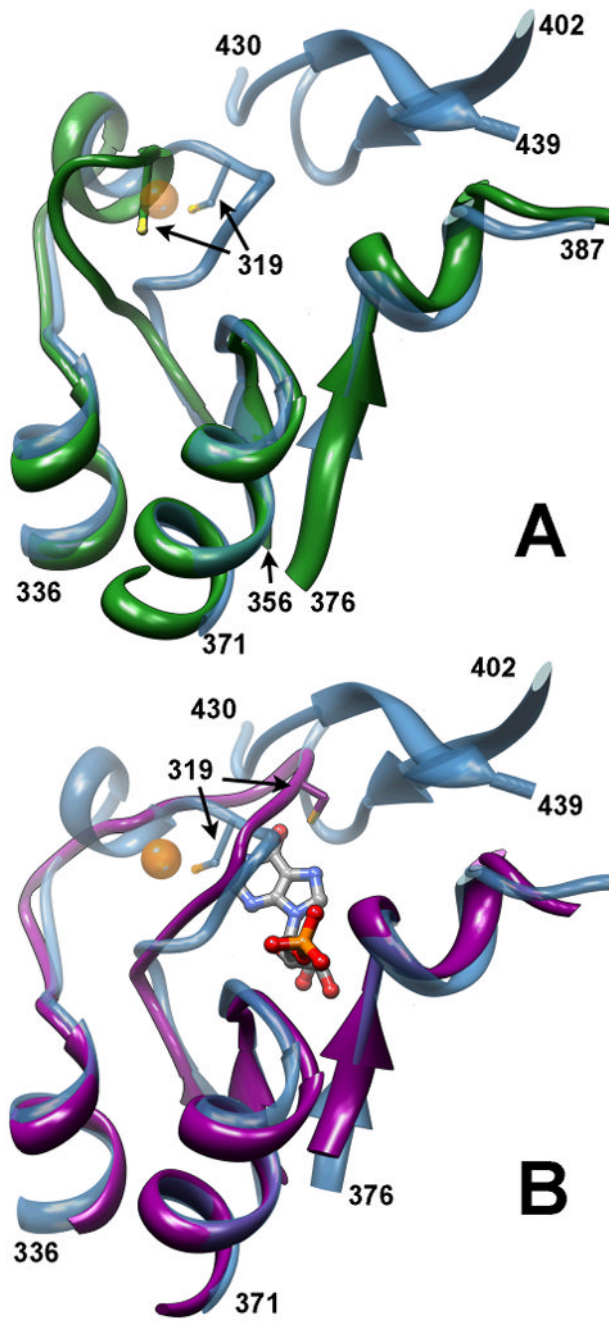


**Figure 1. The structure of IMPDH**

A. The CBS subdomain rotates relative to the barrel domain. IMP is shown in spacefill. The CBS subdomain is completely ordered in the crystal structure of *S. pyogenes* IMPDH (blue, 1zfj); only part of the CBS subdomain is visible in the structures of Chinese hamster IMPDH (magenta, 1jr1) and hIMPDH2 (green, 1b3o). The flap is disordered in all structures, as are portions of the N- and C-termini. B. The tetramer structure of *S. pyogenes* IMPDH showing square planar geometry. SD, subdomain; C. Side view of B, showing dimer interactions. All molecular graphics images were created using the UCSF Chimera package from the Resource for Biocomputing, Visualization, and Informatics at the University of California, San Francisco (supported by NIH P41 RR-01081)<sup>275</sup>.

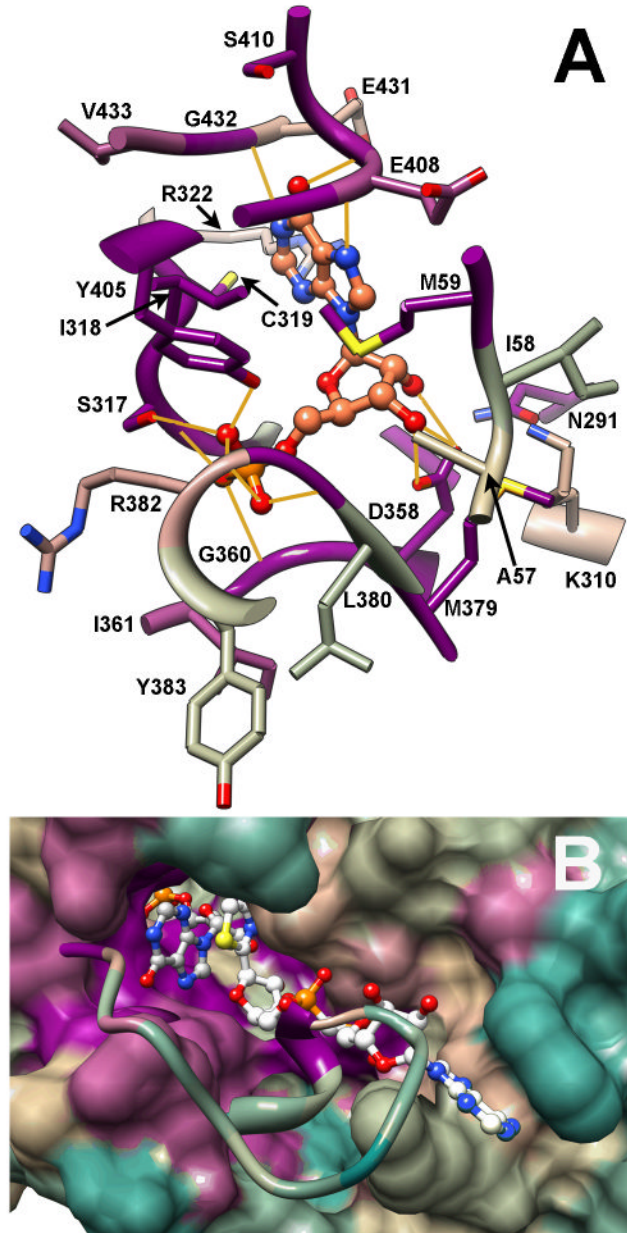
**Figure 2. The conserved K<sup>+</sup> site**

A. *T. foetus* IMPDH. magenta, Cys319 loop; slate blue, flap; green, C-terminal segment in E•MZP (1pvn); blue, C-terminal segment in E•IMP•TAD (the rest is disordered). Interactions between K<sup>+</sup> (orange) and the carbonyl oxygens of Gly314, Gly316, Cys319, Glu485, Gly486 and Gly487 are shown. (') designates residues from the adjacent subunit. B. *S. pyogenes* E•IMP (1ZFJ); the C-terminal segment is magenta, the Cys319 loop and its subunit are green and the putative NH<sub>4</sub><sup>+</sup> is firebrick; one of the ligands is a water (red). The K<sup>+</sup> site of *T. foetus* E•MZP (blue, 1PVN) is shown for comparison in both panels, K<sup>+</sup> in orange. C. Comparison of K<sup>+</sup> and Na<sup>+</sup> binding in *T. foetus* IMPDH. K<sup>+</sup> site, blue (1PVN). Na<sup>+</sup> site, green. Na<sup>+</sup>, gold. (1ME7). Note how the Cys319 loop and C-terminal segment contract.



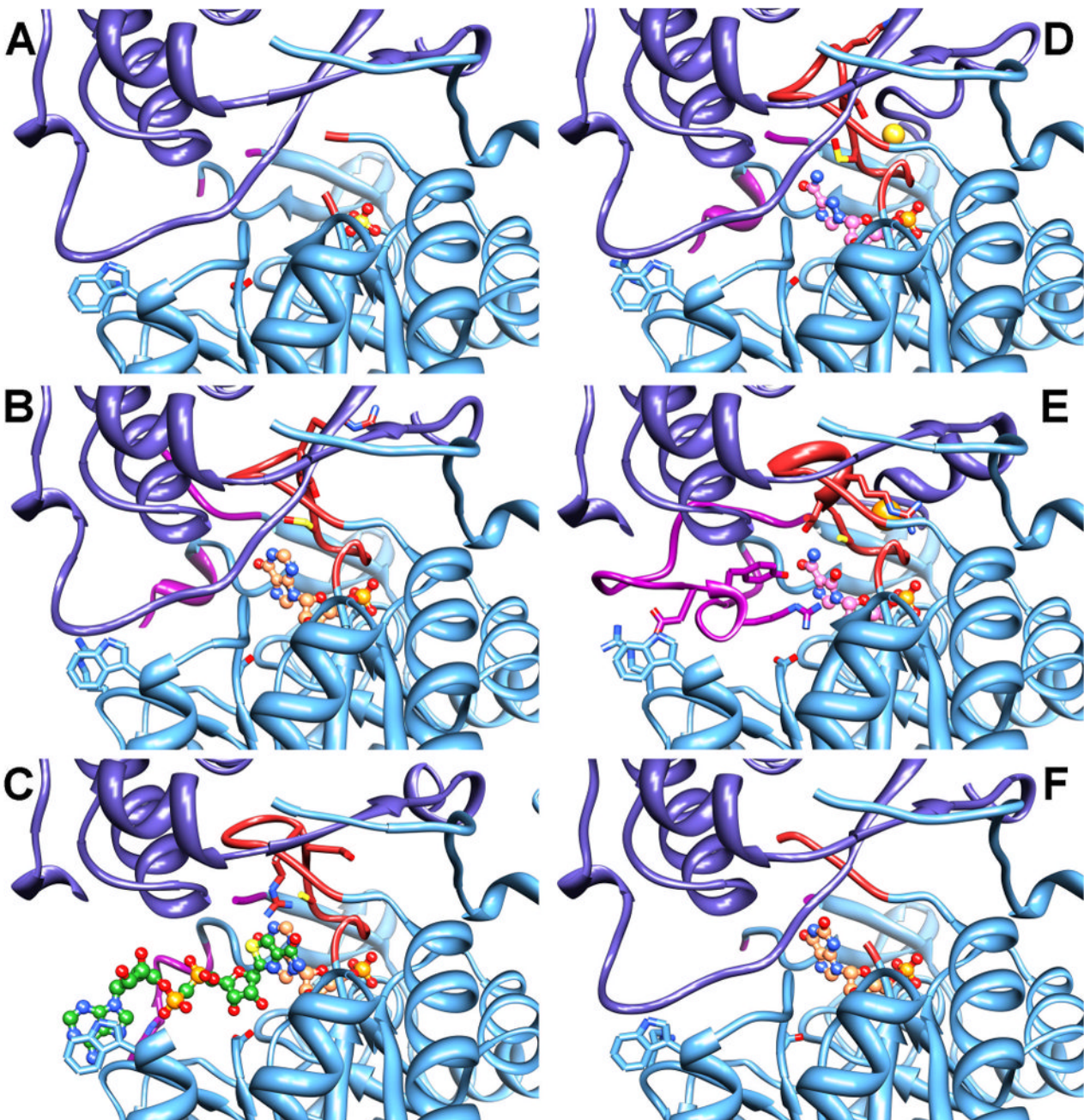
**Figure 3. Conformations of the Cys319 loop**

The structure of *T. foetus* E•MZP (1pvn) is shown in blue with the  $\text{K}^+$  in orange for comparison. A. The Cys319 loop can move like a hinge. The structure of *B. burgdorferi* E•P<sub>1</sub> (1EEP) is shown in green. Note that this conformation is incompatible with  $\text{K}^+$  binding. B. The Cys319 loop can adopt other conformations. The structure of the 6-Cl-IMP adduct of IMPDH2 (1jcn) is shown in magenta. Note that both the flap (residues 402-439) and the  $\text{K}^+$  site are disrupted.



**Figure 4. IMP and NAD sites**

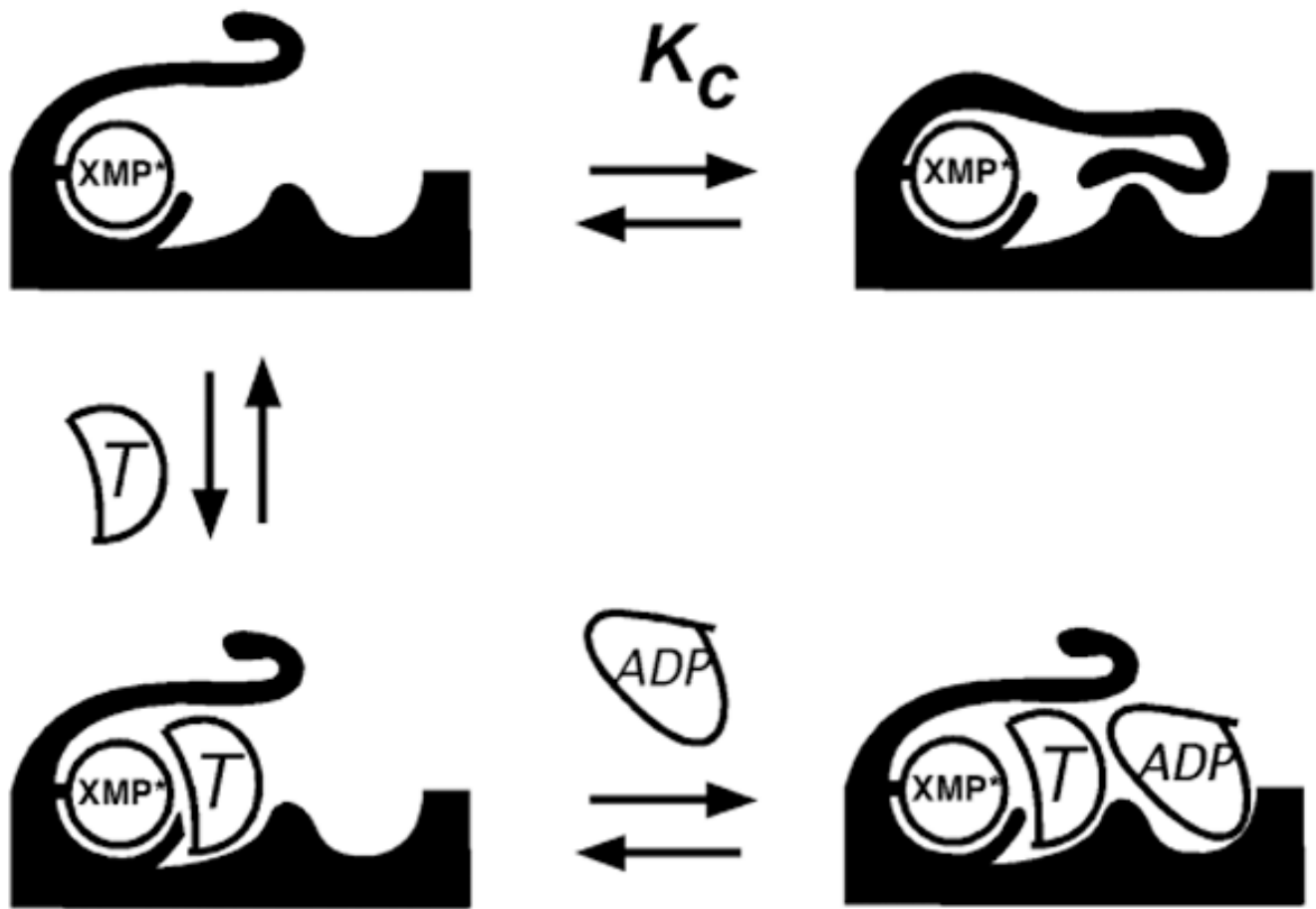
A. The IMP site of *T. foetus* IMPDH from the E•IMP•TAD complex (1lrt). Residues within 5 Å of IMP are shown, with hydrogen bonds depicted in gold. IMP is shown in coral. Residues are colored by percent conservation of most common residue: cyan, 9%; tan, 55%; magenta, 100%. The alignment includes sequences of 444 IMPDHs<sup>137</sup>. B. The IMP and NAD sites of *T. foetus* IMPDH from the E•IMP•TAD complex (1lrt) is shown in surface rendering while the flap from the closed conformation (1pvn) is shown in ribbon. Residues 409, 431, 432 and the side chains of 319 and 414 (*T. foetus* numbering) have been removed so that IMP can be seen. Note that the flap binds in the same site as the dinucleotide. In contrast to the IMP site, and despite these multiple functional constraints, both the flap and the dinucleotide site are highly diverged. Panel B is modified from reference<sup>126</sup> with permission.



**Figure 5. Conformational transitions in the catalytic cycle of IMPDH**

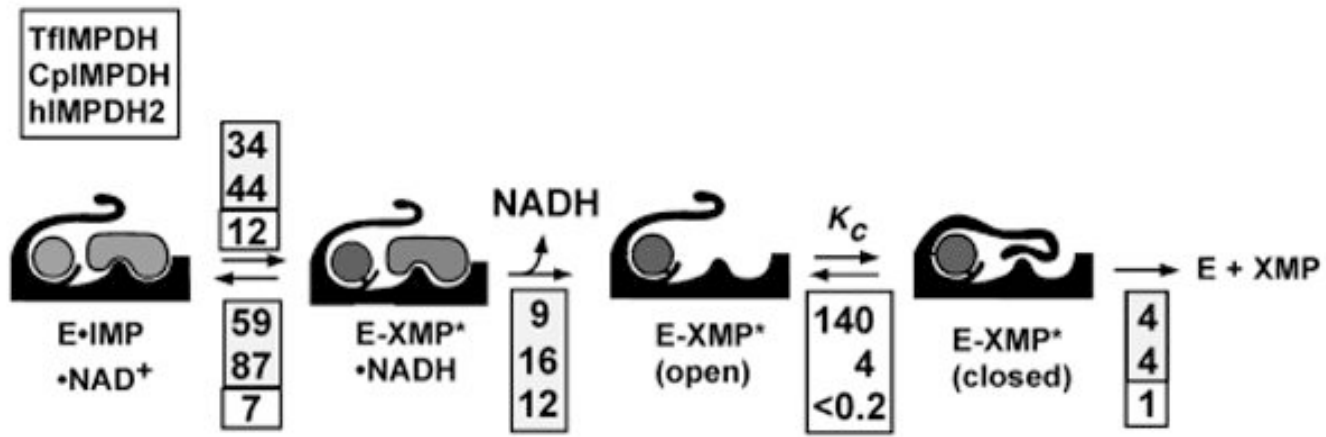
The following complexes of *T. foetus* IMPDH are shown: A. E•SO<sub>4</sub><sup>-2</sup> (PDB accession number 1ak5), model for apoenzyme<sup>89</sup>. B. E•IMP (1me9)<sup>120</sup>. C. E•IMP•TAD (1lrt), model for E•IMP•NAD<sup>+</sup><sup>95</sup>. D. E•RVP•Na<sup>+</sup> (1ME8), model for E-XMP\*<sub>open</sub> 121. F. E•MZP•K<sup>+</sup> (1pvn), model for E-XMP\*<sub>closed</sub> 122. G. E•XMP<sup>89</sup>. Color key: monomer with active site, blue; adjacent monomer, dark blue; Cys319 loop (residues 313-328), firebrick; flap (residues 412-432), dark magenta; IMP, coral; TAD, green; RVP, pink; MZP, pink; XMP, coral; K<sup>+</sup>, orange sphere; Na<sup>+</sup>, gold sphere. Residues 262-268 have been omitted from panels D and G to permit a view of Asp261. In addition, residues 14-27(adjacent monomer) were omitted in

panels D, F and G for better visualization of the adenosine subsite. A second K<sup>+</sup>, unique to *T. foetus* IMPDH, was also omitted from all panels.



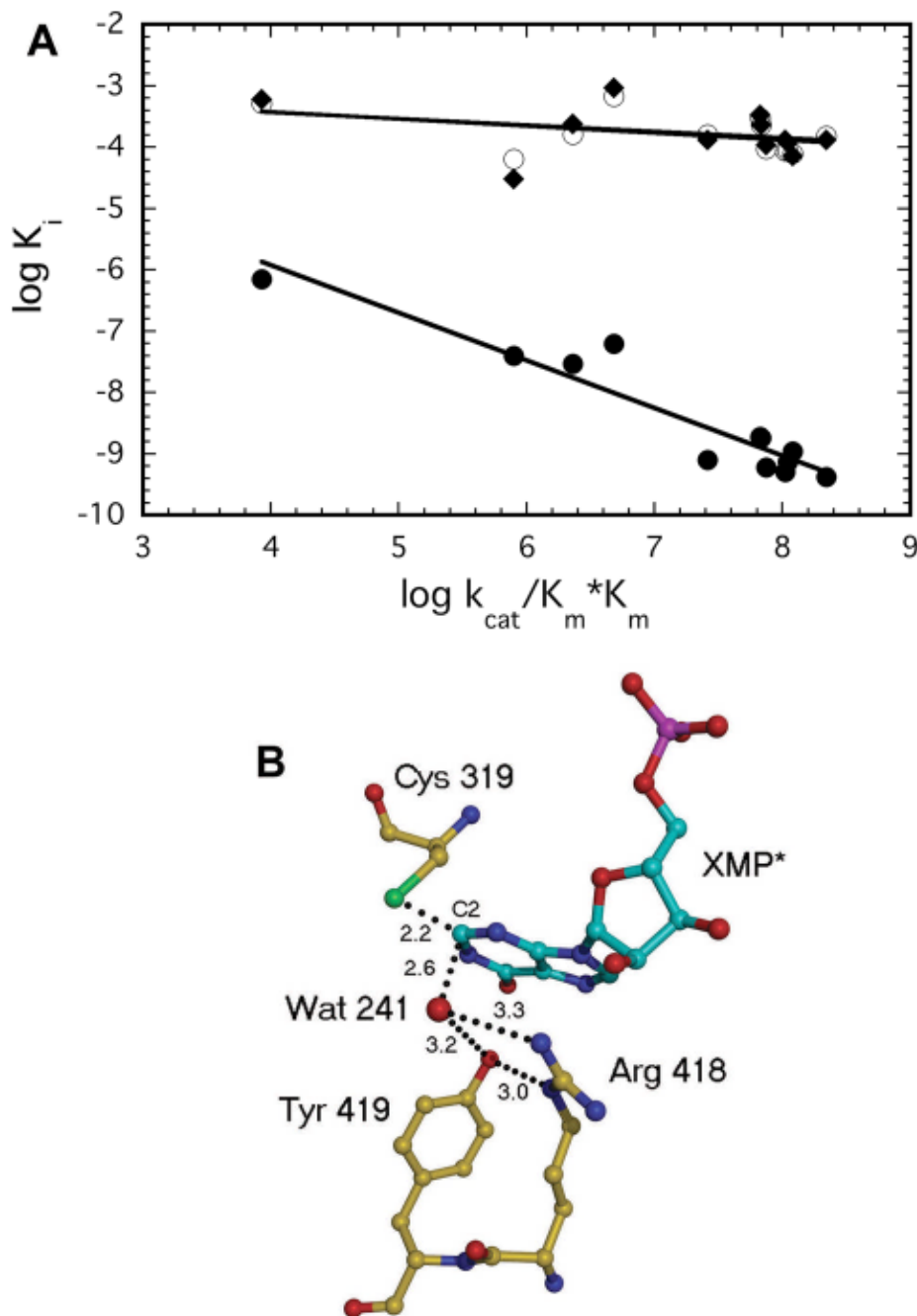
**Figure 6. The multiple inhibitor experiment**

If the closed conformation is favored, the first inhibitor ( $T$  = tiazofurin) shifts the equilibrium to the open conformation, allowing the second inhibitor (ADP) to bind more tightly.

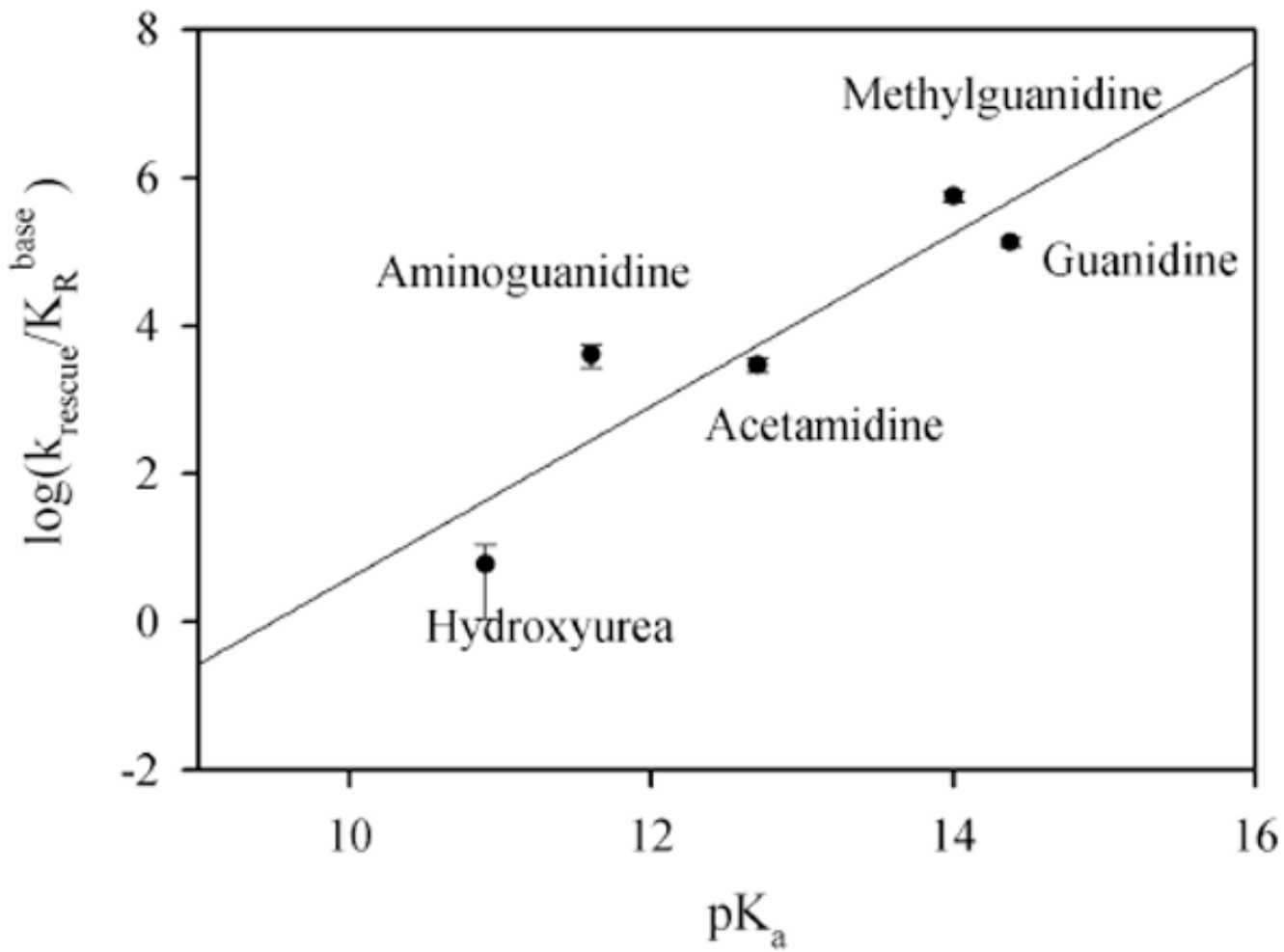


**Figure 7. Kinetic alignment of IMPDHs from *T. foetus* (TfIMPDH), *C. parvum* (CpIMPDH) and human (hIMPDH2)**

The units for the rate constants are  $s^{-1}$ . Reprinted from reference <sup>126</sup> with permission.

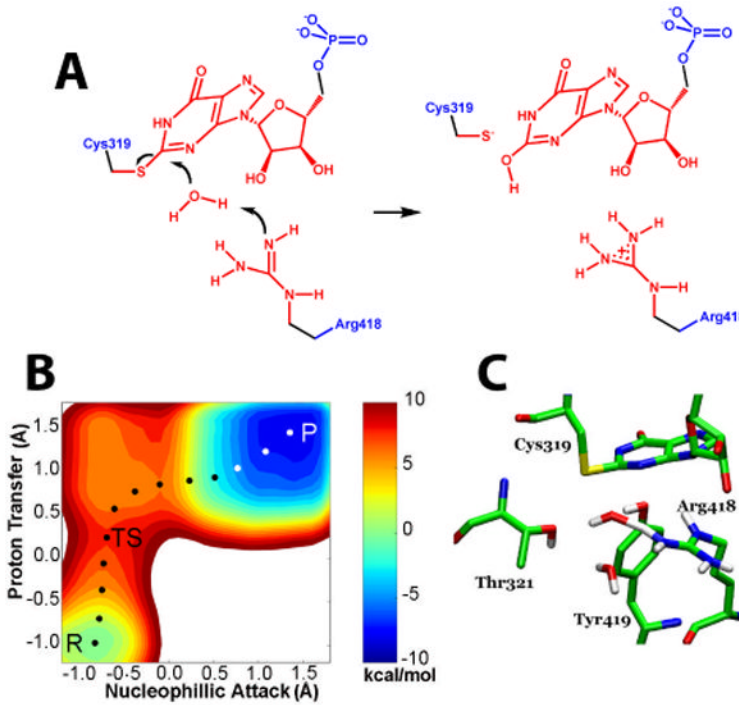


**Figure 8. The transition state analogy of MZP**  
 A. Correlation of  $K_i$  and  $k_{\text{cat}} / K_m * K_m$ .  $K_i$  is GMP ( $\circ$ ),  $K_i$  is XMP ( $\diamond$ ),  $K_i$  MMP ( $\bullet$ ). Reprinted from reference <sup>135</sup> with permission. B. E-XMP\* modeled into the E•MZP structure (1pvn). Reprinted from reference <sup>122</sup> with permission.



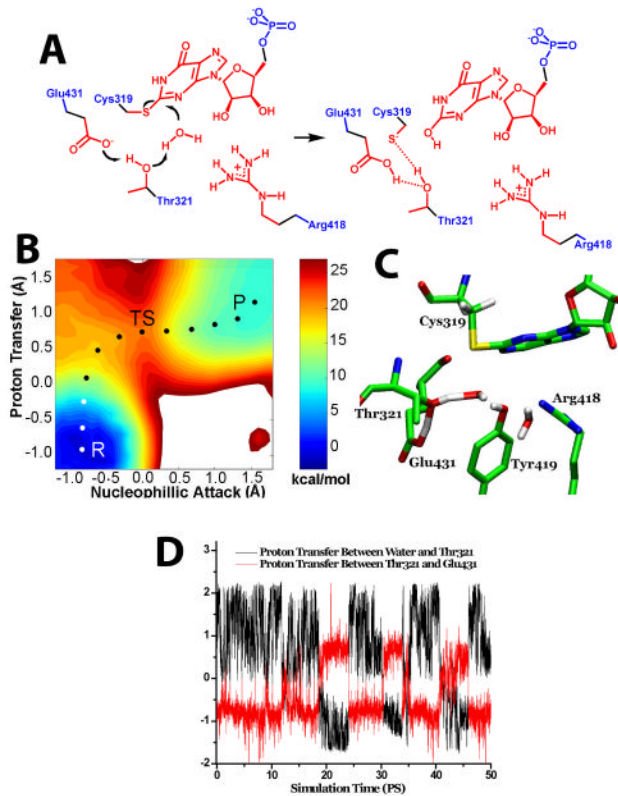
**Figure 9. Guanidine derivatives rescue Arg418Ala IMPDH<sup>136</sup>**

The Bronsted  $\beta$  values are  $1.1 \pm 0.3$ ;  $R=0.9$ , including the hydroxyurea and  $0.7 \pm 0.3$ ;  $R=0.85$ , without hydroxyurea (not shown). Similar  $\beta$  values are obtained when the values of  $pK_a$  are normalized for the number of equivalent protons. Reprinted from reference<sup>136</sup> with permission.



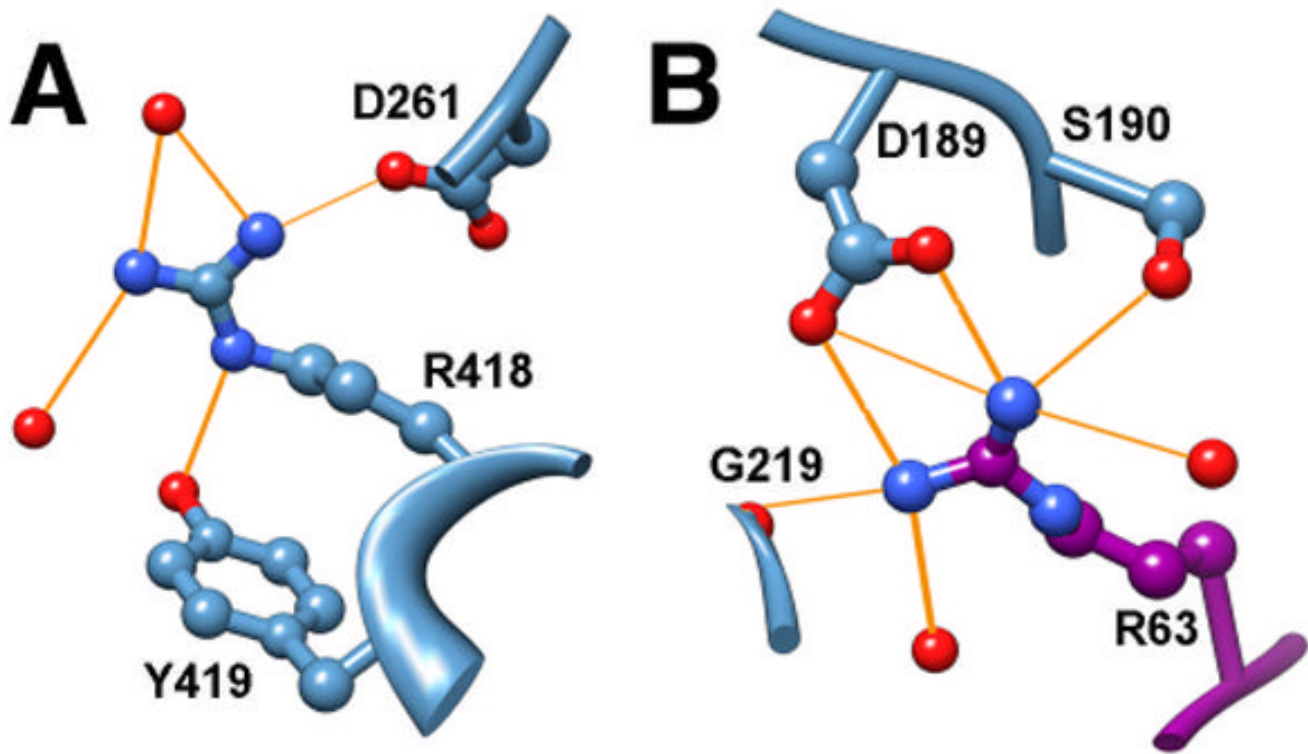
**Figure 10. Molecular dynamics simulation of the Arg Pathway**

(A) The hydrolysis of E-XMP\* with Arg418 acting as the general base catalyst. Red denotes atoms treated with QM; blue denotes atoms treated with MM. (B) The free energy landscape for the Arg418 pathway. R, reactant; TS, transition state; P, product. The x-axis denotes the difference between the distances of the migrating proton between the hydrolytic water and the NH group of Arg418, where 0.0 is the midpoint between the two acceptors; the y-axis specifies the progress of nucleophilic attack, where 0.0 is the midpoint between the original position of the nucleophilic oxygen and the final position. The transition state is the highest point in the energy landscape. Here, the proton has moved past the midpoint and is now associated with Arg418. In contrast, nucleophilic attack has yet to begin. (C) The transition state structure for the Arg418 pathway. Reprinted from reference <sup>137</sup> with permission.



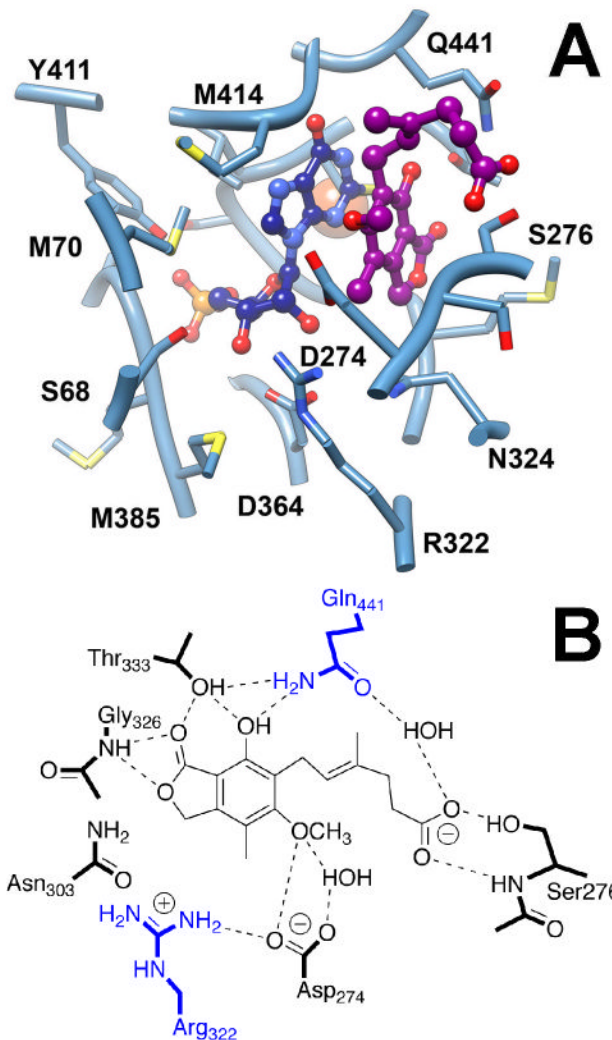
**Figure 11. Simulation of the Thr321 pathway**

(A) The hydrolysis of E-XMP\* with Thr321 acting as the general base catalyst. Color key as described above. (B) The free energy landscape of the Thr321 pathway, with axes as described above, except that the second proton acceptor is the OH of Thr321. As above, proton transfer is virtually complete at the transition state, while nucleophilic attack has just reached the reaction midpoint. (C) The corresponding transition state structure. (D) The correlation between proton transfer from water to Thr321 and proton transfer from Thr321 and Glu431. Atoms treated as described in Figure 1. The reaction coordinate for the proton transfer between water and Thr321 was set as the distance traversed by the proton as it moves between the oxygen of water to the oxygen of Thr321; the reaction coordinate for the proton transfer between Thr321 and Glu431 was set as the distance traversed by the proton that moves between the oxygen of Thr321 and the oxygen of Glu431. Reprinted from reference <sup>137</sup> with permission.



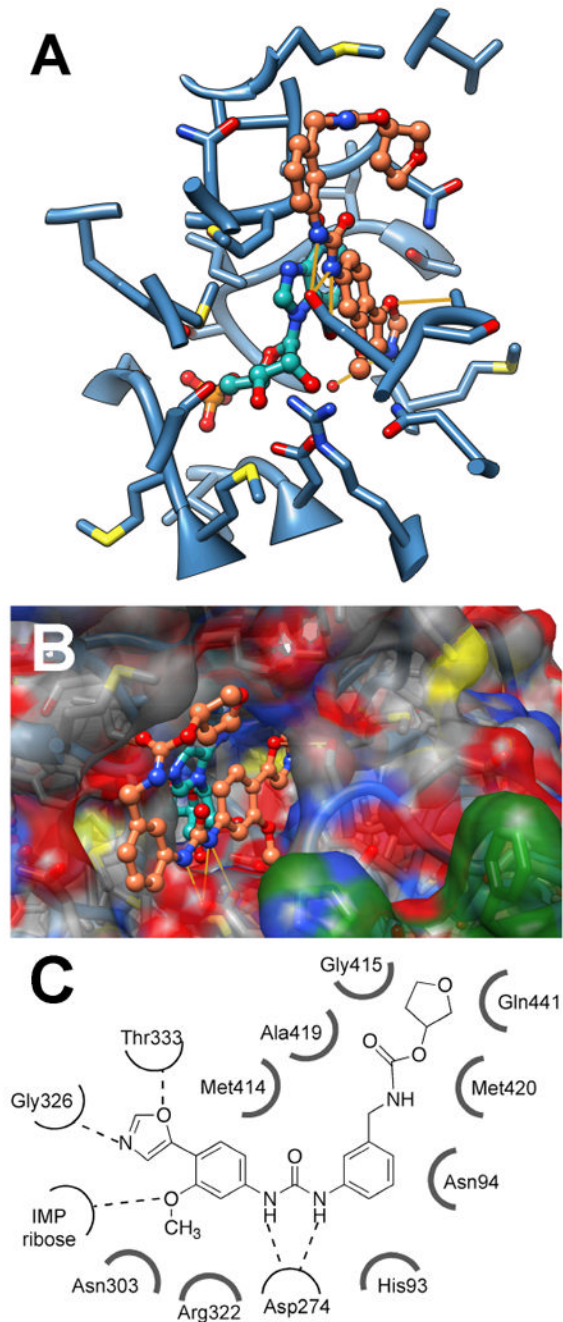
**Figure 12. Hydrogen bonding interactions of Arg residues**

A. The putative general base Arg418 in IMPDH; B. A positively charged Arg in the substrate binding site of trypsin. Note that the putative general base has fewer potential hydrogen bonding interactions.



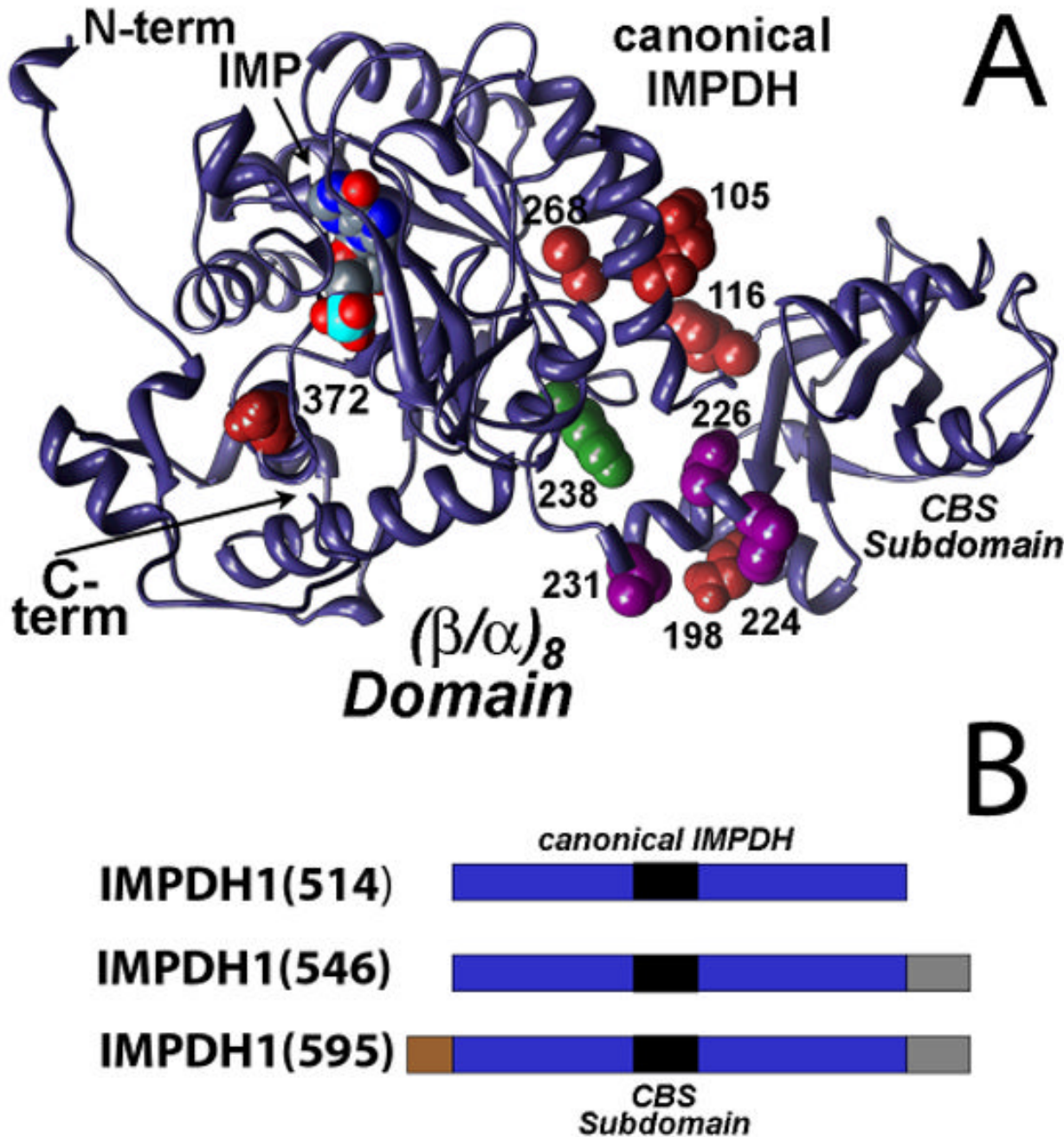
**Figure 13. The MPA binding site**

(1jr1). Enzyme is shown in slate blue. XMP\* is navy, MPA is dark magenta, potassium is orange. The residues within 4.0 Å of the XMP\* and MPA are shown. Chinese hamster IMPDH type 2 numbering is used (identical to human IMPDH type 2). Arg322 and Gln441 are analogous to Lys130 and Glu, respectively, in *T. foetus* IMPDH. B. Interactions of MPA. Modified from reference <sup>76</sup> with permission.



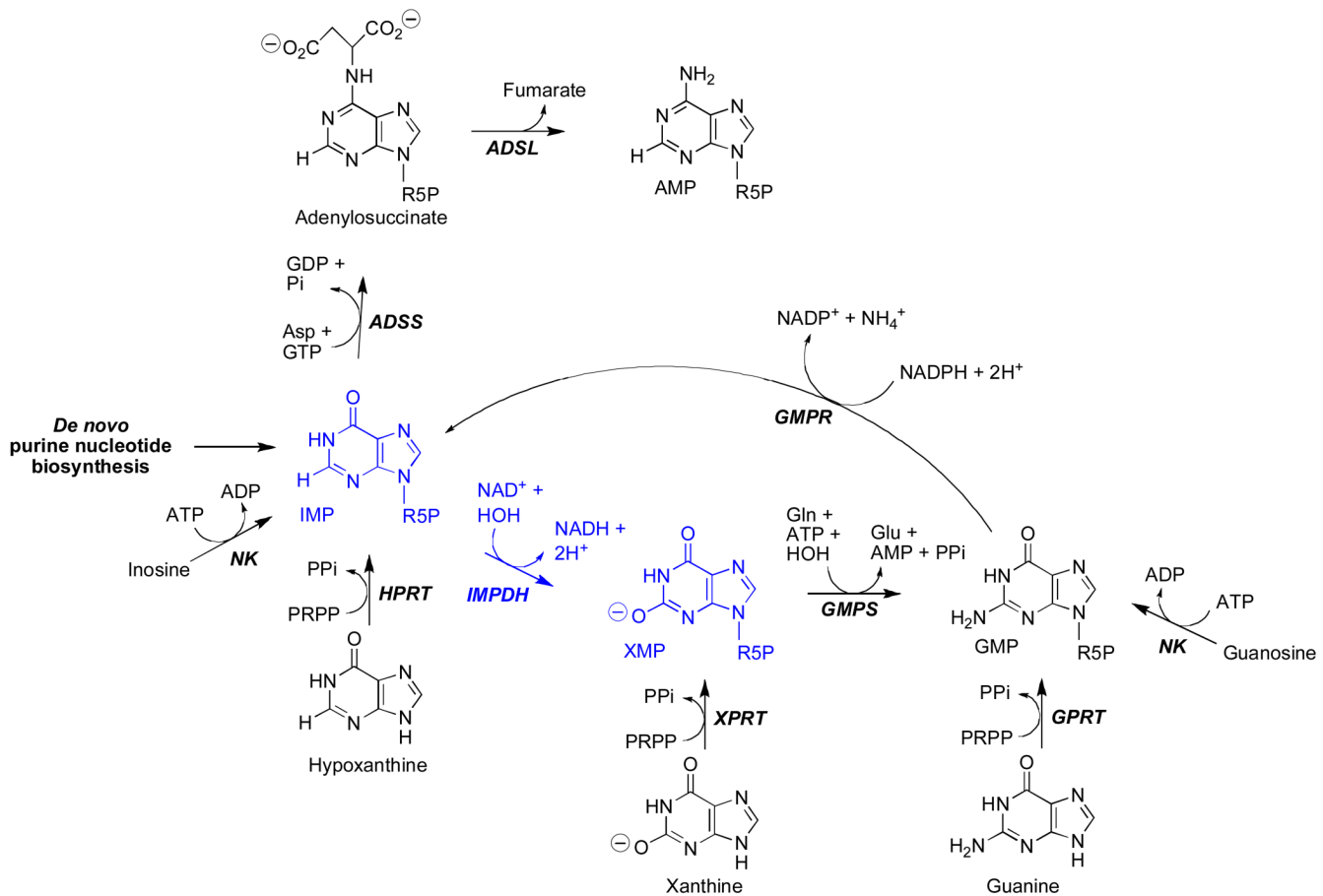
**Figure 14. The phenyl-oxazole urea binding site**

A. The structure of E-XMP\*•merimepodib is shown (coordinates courtesy of Marc Jacobs). Residues within 4 Å of the ligands are displayed. Merimepodib is depicted in coral, XMP\* in cyan. Gold lines indicate hydrogen bonds. Hydrogen bonds are shown in gold. B. Spacefill depiction of the drug binding site. The surfaces of His253 and Phe282, which sandwich the adenine ring of NAD<sup>+</sup>/NADH, are shown in green. C. Interactions of phenyl-oxazole urea. Modified from reference <sup>12</sup> with permission.

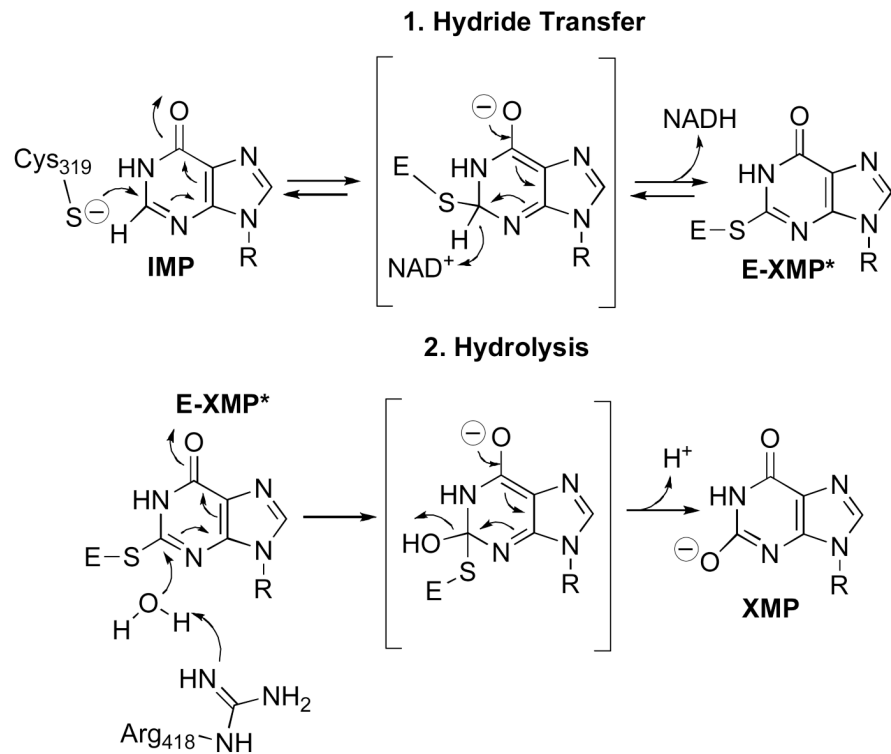


**Figure 15. The adRP/LCA-causing mutations of IMPDH**

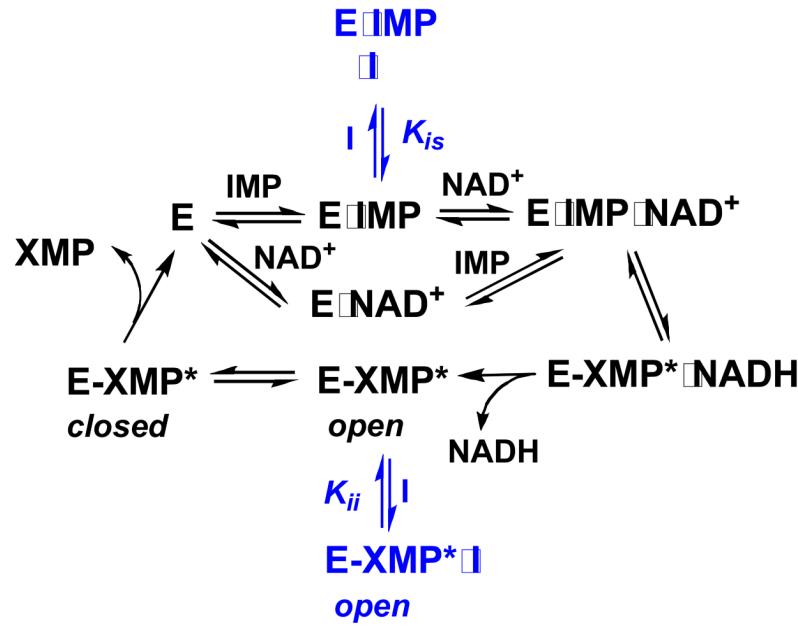
A. The positions of the disease associated mutations are depicted on a monomer of IMPDH from *S. pyogenes*, which corresponds to the canonical IMPDH1(514) (1ZFJ); note that the CBS domains are disordered in the structure of human IMPDH1 (1JCN), so that several of the positions of mutation are not observed). Magenta denotes mutations that are clearly pathogenic; red, likely pathogenic; green, possibly pathogenic<sup>9</sup>. B. Schematic of the hIMPDH2 variants produced by alternative splicing. Modified from reference<sup>6</sup> with permission.

**Scheme 1. Purine nucleotide biosynthesis**

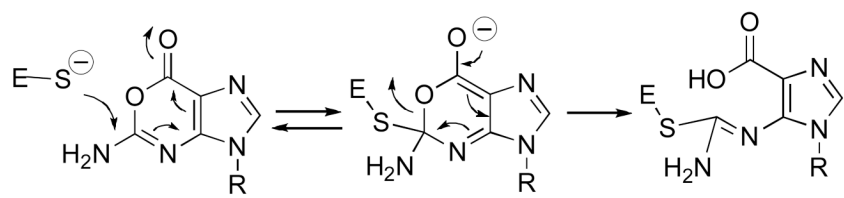
The commonly occurring guanine nucleotide biosynthetic and salvage reactions are shown, as is the adenine nucleotide biosynthetic pathway. The IMPDH reaction is depicted in blue. R5P, ribose 5'-monophosphate; NK, nucleoside kinase; HPRT, hypoxanthine phosphoribosyl transferase; XPRT, xanthine phosphoribosyl transferase; GPRT, guanine phosphoribosyl transferase; GMPR, guanosine 5'-monophosphate reductase; ADSS, adenylosuccinate synthetase; ADSL, adenylosuccinate lyase.



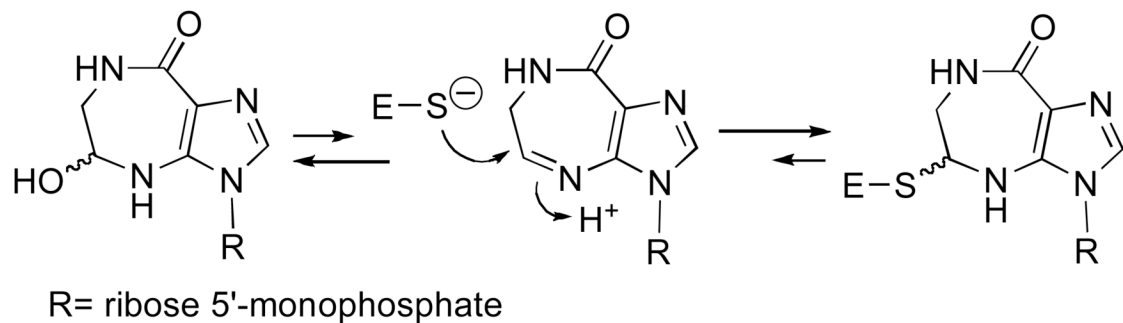
**Scheme 2. Mechanism of the IMPDH reaction. *T. foetus* IMPDH numbering is shown**

**Scheme 3. Kinetic mechanism of IMPDH and inhibition by NAD analogs**

Inhibitory complexes are shown in blue. Since most assays are performed at saturating concentrations of IMP, a NAD analog can bind to both E•IMP and E-XMP\*, and therefore will display noncompetitive inhibition.



Scheme 4. Potential mechanism of inactivation of IMPDH by oxanosine monophosphate



R= ribose 5'-monophosphate

Scheme 5. Proposed mechanism for inhibition of IMPDH by fat base nucleotide

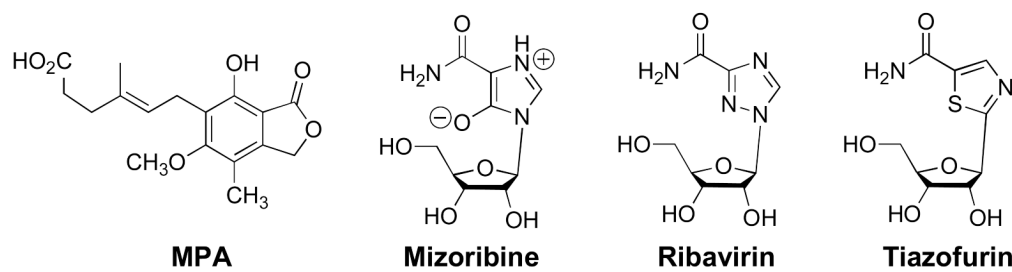
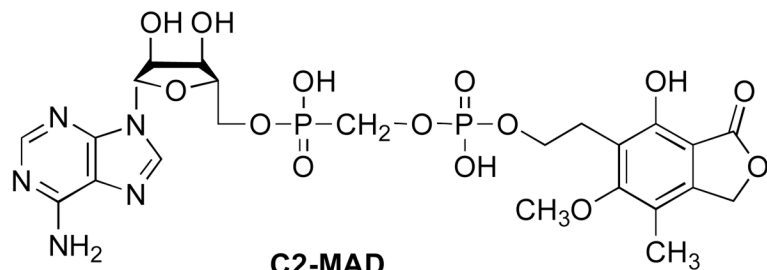


Chart 1. Drugs targeting human IMPDH



$K_i = 20 \text{ nM}$  for hIMPDH1,  $37 \text{ nM}$  for hIMPDH2

**Chart 2. C2-MAD**

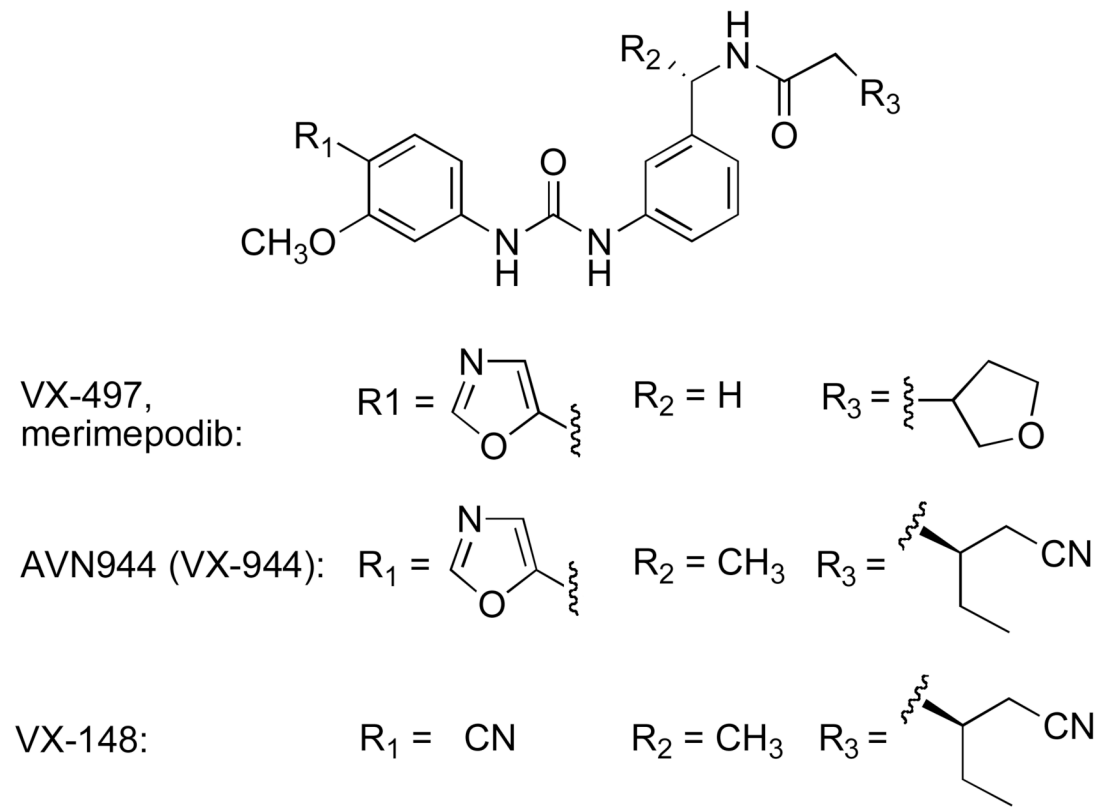
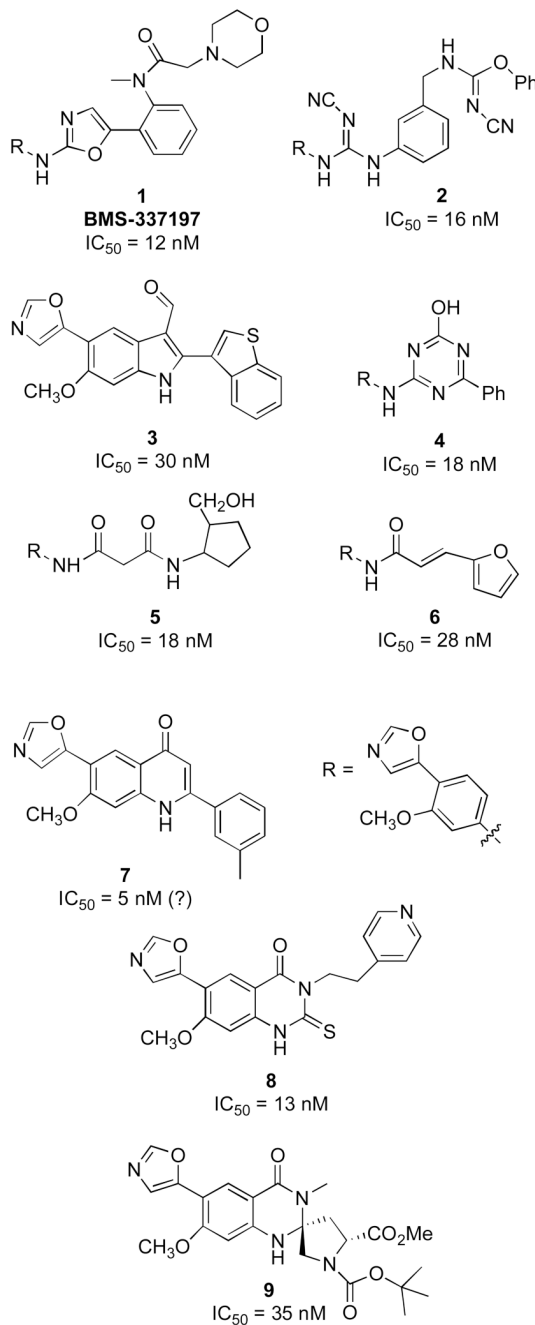
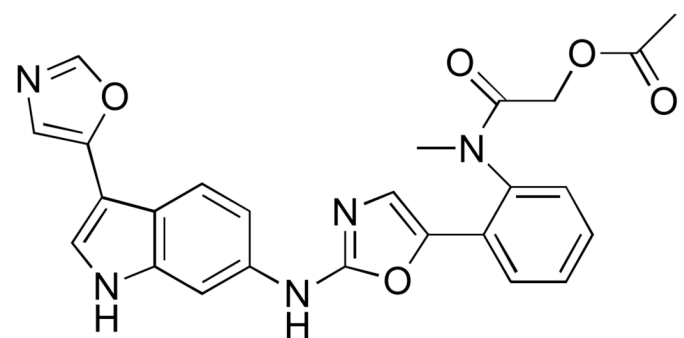


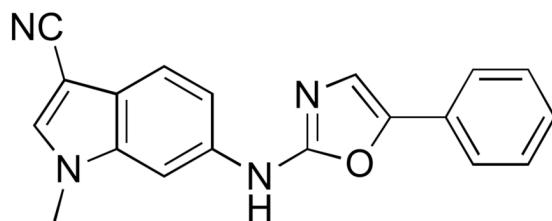
Chart 3. Phenyl-oxazole urea inhibitors



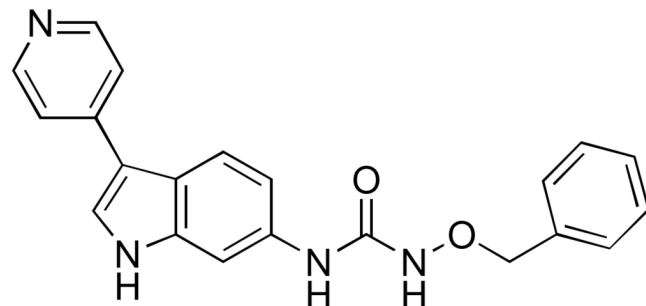
**Chart 4. Modifications of the phenyl-oxazole urea linker. IC<sub>50</sub>s versus hIMPDH2 are shown. (?) denotes IC<sub>50</sub> values that are below 50% of the enzyme concentration**



**10**  
 $IC_{50} = 7 \text{ nM (?)}$



**11**  
 $IC_{50} = 33 \text{ nM}$



**12**  
 $IC_{50} = 76 \text{ nM}$

**Chart 5. Indole derivatives.  $IC_{50}$ s versus hIMPDH2 are shown. (?) denotes  $IC_{50}$  values that are below 50% of the enzyme concentration**

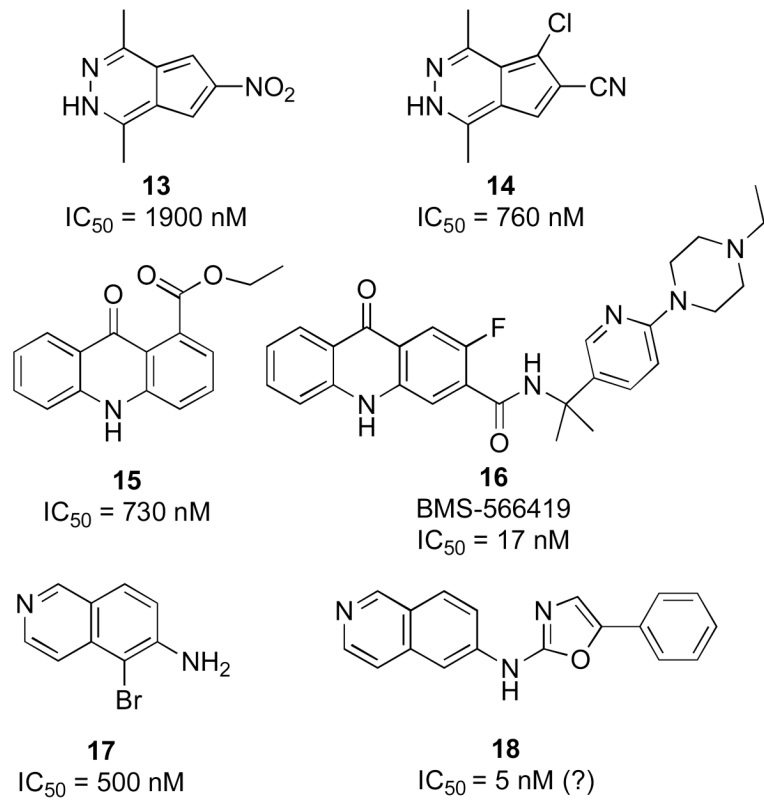


**Chart 6. Novel frameworks.  $IC_{50}$ s versus hIMPDH2 are shown. (?) denotes  $IC_{50}$  values that are below 50% of the enzyme concentration**

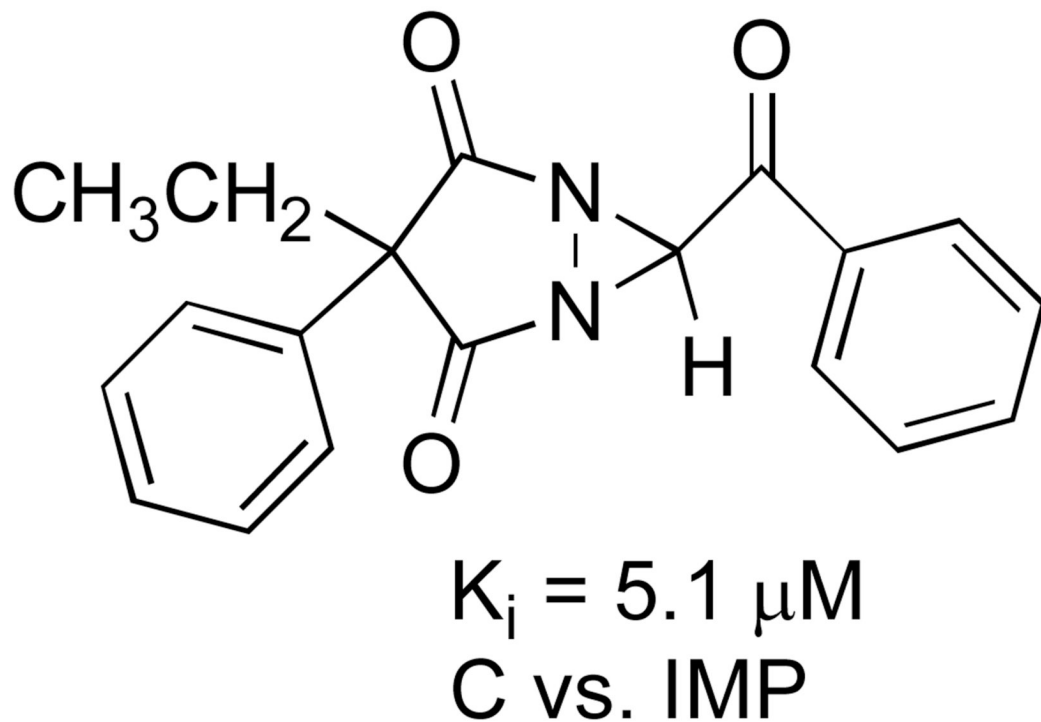
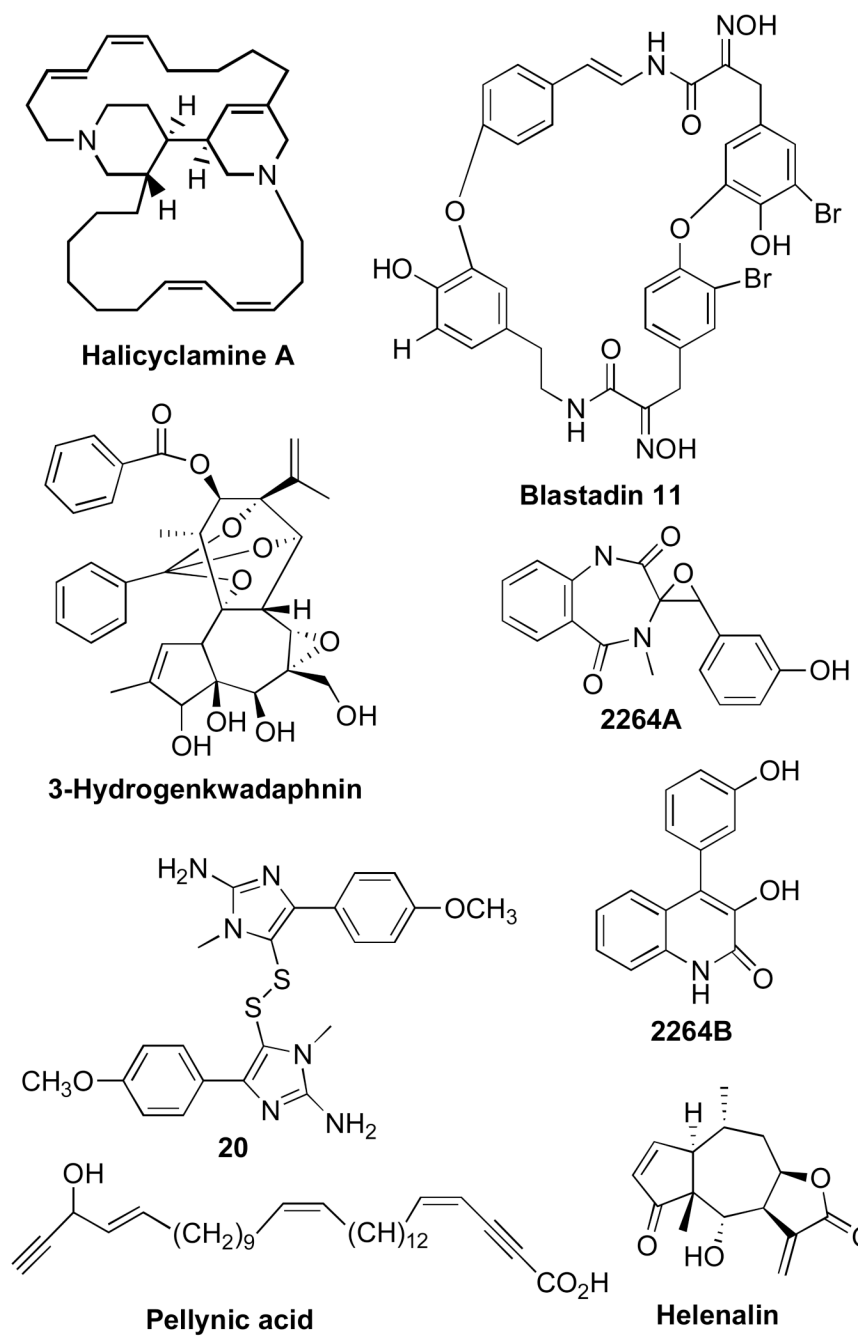
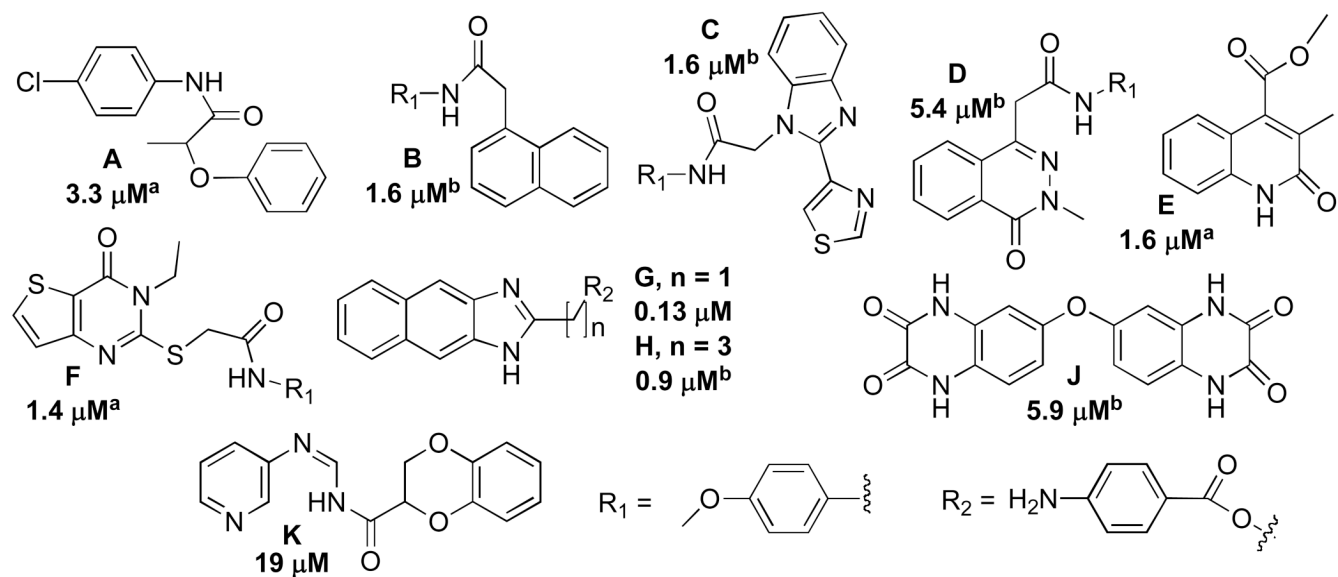


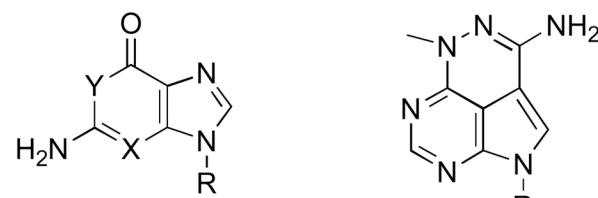
Chart 7. 1,5-Diazabicyclo[3.1.0]hexane-2,4-diones



**Chart 8. Natural product inhibitors of hIMPDH2**

**Chart 9. Inhibitors selective for *C. parvum* IMPDH**

a. antagonize ADP binding. b. bind in the nicotinamide subsite and do not interact with ADP.



**GMP:**  $\text{X} = \text{N}$ ,  $\text{Y} = \text{NH}$

**Oxanosine-MP:**  $\text{X} = \text{N}$ ,  $\text{Y} = \text{O}$

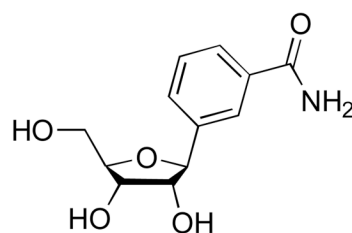
**1-AG-MP:**  $\text{X} = \text{N}$ ,  $\text{Y} = \text{NNH}_2$

**3-deaza-GMP:**  $\text{X} = \text{C}$ ,  $\text{Y} = \text{NH}$



**Triciridine phosphate**

$\text{R} = \text{ribose-5'-phosphate}$



**Benzamide  
riboside**

**Chart 10. Nucleoside inhibitors of IMPDH**

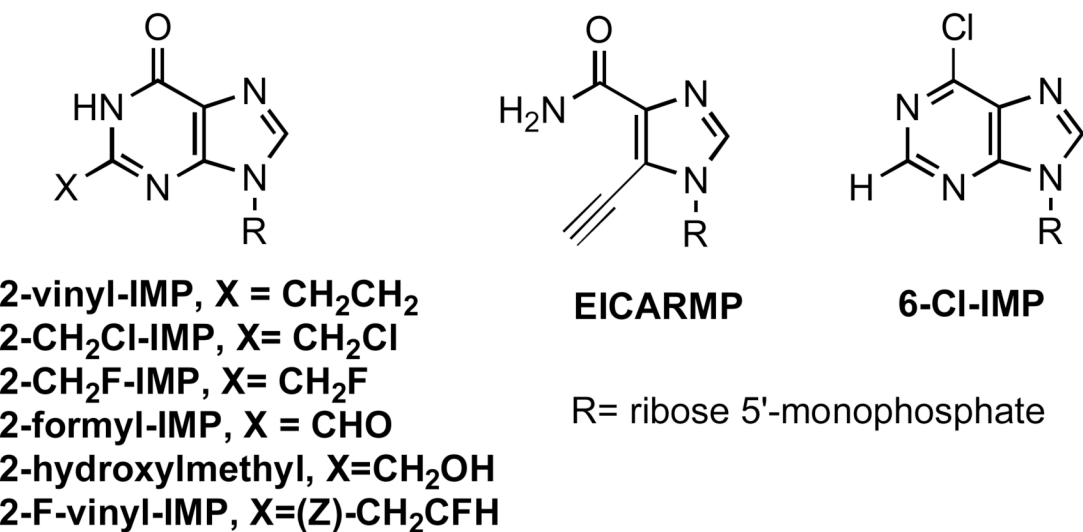


Chart 11. Mechanism-based inactivators. R= ribose 5'-monophosphate

**Table 1**  
**Intrinsic binding energy of ligands for the dinucleotide site<sup>a</sup>**

| Enzyme               | $K_c$ | NAD <sup>+</sup> (mM) |            | $\beta$ -Me-TAD ( $\mu$ M) |            | Tz (mM)   |            | ADP (mM)  |            |
|----------------------|-------|-----------------------|------------|----------------------------|------------|-----------|------------|-----------|------------|
|                      |       | $K_i$                 | $K_{intr}$ | $K_i$                      | $K_{intr}$ | $K_i$     | $K_{intr}$ | $K_i$     | $K_{intr}$ |
| TfMPDH <sup>b</sup>  | 150   | 6.8 ± 1.8             | 0.07       | 2.3 ± 0.4                  | 0.02       | 50 ± 10   | 0.3        | 31 ± 2    | 0.2        |
| CpIMPDH <sup>c</sup> | 4     | 4.9 ± 0.5             | 0.30       | 0.6 ± 0.04                 | 0.1        | 1.5 ± 0.1 | 0.3        | 42 ± 6    | 8          |
| hIMPDH2 <sup>d</sup> | ≤ 0.2 | 0.59 ± 0.02           | 0.59       | 0.06 ± 0.02                | 0.06       | 1.3 ± 0.1 | 1.3        | 8.8 ± 2.2 | 8.8        |

<sup>a</sup>The intrinsic binding constant for NAD<sup>+</sup> is derived from the global fits. The intrinsic binding constants for  $\beta$ -Me-TAD, tiazofurin (Tz) and ADP are calculated from  $K_{intr} = K_i(1/(1 + K_C))$ .  
<sup>b</sup>*74,272.*  
<sup>c</sup>*75.*  
<sup>d</sup>*77.*

The intrinsic binding constant for NAD<sup>+</sup> is derived from the global fits.

**Table 2****Mutational analysis of the residues that interact with water**

Rate constants are determined in global analysis using Dynafit<sup>273</sup>. Note that  $k_{cat}$  is a composite of all the steps after formation of E•IMP•NAD<sup>+</sup>. The value of  $K_c$  is determined using multiple inhibitor experiments as described in the text. a. 127; b. 133

| Enzyme                 | $k_{cat}$ (s <sup>-1</sup> ) | NADH              |   | $K_c$      | $k_{HOH}$ (s <sup>-1</sup> ) | $k_{HOH}$ (s <sup>-1</sup> ) |
|------------------------|------------------------------|-------------------|---|------------|------------------------------|------------------------------|
|                        |                              | E-XMP*            | Hydride transfer ( $k_7 + k_8$ ) (s <sup>-1</sup> ) |            |                              |                              |
| Wild-type <sup>a</sup> | 1.9                          | 93                | 8.5   |            | 140                          | 4                            |
| Thr321Ala <sup>b</sup> | 0.18                         | 1.7 ( $k_7$ only) | $\geq 8$  |            | $\geq 20$                    | 0.18                         |
| Arg418Ala <sup>a</sup> | 0.004                        | 42                | 11  | 1          | 0.008                        |                              |
| Arg418Gln <sup>b</sup> | 0.0069                       | $\geq 400$        | $\geq 4$  |            | 10-50                        | 0.007                        |
| Arg418Lys <sup>b</sup> | 0.15                         | 83                | 6.5   | $\leq 0.1$ | $\geq 1$                     |                              |
| Tyr419Phe <sup>a</sup> | 0.22                         | 70                | 10  | 20         | 0.22                         |                              |

**Table 3****Monovalent cation selectivity in IMPDH**

All IMPDHs are activated by K<sup>+</sup>, NH<sub>4</sub><sup>+</sup> and Rb<sup>+</sup>, but the effects of Na<sup>+</sup> vary among IMPDHs from different organisms. The sequences of the Cys319 loop (residues 312-331) and C-terminal helix (residues 480-487) are shown; residues that interact with K<sup>+</sup> are shown in bold. The % helix is calculated for the corresponding peptide using AGADIR<sup>274</sup>. conditions: ionic strength = 0.1, 278 degrees K, pH 7. a. <sup>84</sup>; b. <sup>147</sup>; c. <sup>143</sup>

| Source                             | Na <sup>+</sup> | Cys 319 loop                      | C-term helix | %helix |
|------------------------------------|-----------------|-----------------------------------|--------------|--------|
| <i>C. parvum</i>                   | no effect       | GIGPGSIC <sup>T</sup> TRIVAGVGVPQ | TTSGLRESH    | 0.54   |
| <i>B. burgdorferi</i> <sup>a</sup> | inhibits        | GIGPGSIC <sup>T</sup> TRIVAGVGVPQ | SHSSLKESH    | 0.40   |
| <i>S. pyogenes</i>                 | unknown         | GIGPGSIC <sup>T</sup> TRVVAGVGVPQ | SGAGLIESH    | 0.24   |
| <i>E. coli</i> <sup>b</sup>        | inhibits        | GIGPGSIC <sup>T</sup> TRVTGVGVPQ  | SGAGIQESH    | 0.30   |
| human type 2 <sup>c</sup>          | activates       | GNGSGSIC <sup>T</sup> QEVLACGRPQ  | TSSAQVEGG    | 0.27   |
| <i>T. foetus</i>                   | activates       | GIGGGSIC <sup>T</sup> REQKGIGRGQ  | SSVSIVEGG    | 0.16   |

**Table 4****TAD analogs. data from<sup>220</sup>**

a. Uncompetitive inhibition is observed with both IMP and NAD<sup>+</sup>; the value of K<sub>i</sub> with IMP as the variable substrate is shown. Note that experimental conditions were not described, so there is a concern that the concentration of SAD was not in excess of enzyme, so that the value of K<sub>i</sub> is an upper limit.

| Compound | X  | Y  | hIMPDH1 <sup>a</sup><br>K <sub>i</sub> μM | hIMPDH2 <sup>a</sup><br>K <sub>i</sub> μM |
|----------|----|----|---|---|
| TAD      | S  | N  | 0.7                                       | 0.43                                      |
| SAD      | Se | N  | 0.03                                      | 0.02                                      |
| TFAD     | S  | CH | 0.37                                      | 0.32                                      |
| SFAD     | Se | CH | 0.58                                      | 1.10                                      |
| FFAD     | O  | CH | 38  | 56  |